COMPLEX PERMITTIVITY OF GERMANIUM AT MICROWAVE FREQUENCIES

THE EFFECT OF FREQUENCY, DOPING AND TEMPERATURE ON THE COMPLEX PERMITTIVITY OF N-TYPE GERMANIUM

By

RIAZ HUSSAIN SHEIKH, B.SC. ENGG. (PUNJAB,PAKISTAN)
D.R.C. (GLASGOW); M. ENG. (McMASTER)

A Thesis
Submitted to the Faculty of Graduate Studies
in Partial Fulfilment of the Requirements
for the degree of
Ph. D.

McMaster University
March 1968

DOCTOR OF PHILOSOPHY (1968) McMaster University

(ELECTRICAL ENGINEERING) Hamilton, Ont

TITLE: The Effect of Frequency, Doping and Temperature on the Complex Permittivity of N-Type Germanium.

AUTHOR: Riaz Hussain Sheikh, B. Sc., (University of Punjab, Pakistan)
D.R.C. (Royal College of Science & Technology, Glasgow)
M. ENG. (McMaster University, Hamilton, Ont.)

SUPERVISOR: Professor M. W. Gunn

NUMBER OF PAGES: viii, 151

SCOPE AND CONTENTS: A number of microwave measuring techniques for the measurement of the complex permittivity of semi-conductors have been investigated and a new method of measurement is described. Also a study has been made of wave propagation and higher order mode effects in rectangular waveguides partially filled with a semi-conductor together with a theoretical and practical investigation of the dependence of the complex permittivity on temperature, frequency and doping.

ACKNOWLEDGEMENTS

The author expresses his sincere gratitude to Dr. M. W. GUNN for his continued advice and encouragement. Thanks are also due to the National Research Council of Canada for a grant for the equipment and to the Government of Canada for the award of a scholarship under the Colombo Plan. The author is grateful to Dr. C. K. CAMPBELL for the loan of the Delta Design chamber and to Dr. W. R. DATARS for the loan of a dewar. Special thanks are also due to Computer Centre Staff, especially Dr. D. J. KENWORTHY, for timely help in computations, and to the friends who have helped the author in any way in connection with the project. And last, but not least, the author expresses his very special thanks to his wife, who has held her patience during this period.

ABSTRACT

A number of microwave measuring techniques for the measurement of the complex permittivity ($\hat{\varepsilon} = \varepsilon_0 \varepsilon_r - j \frac{\sigma}{\omega}$) have been investigated and a new method based on the replacement of the narrow wall of a rectangular wave-guide by a block of semi-conductor has been developed. This technique is shown to be suitable for the measurement of σ when $\sigma >> \omega\varepsilon_0 \varepsilon_r$ and for the measurement of σ and ε_r for $\sigma \simeq \omega\varepsilon_0 \varepsilon_r$.

An investigation has been made of the propagation characteristics of a rectangular wave-guide containing a centrally placed slab of semi-conductor parallel to the narrow walls of the guide. A comparison of exact solutions for the propagation constant in such a structure with the approximate solutions normally used has shown that the conditions for the validity of the approximate solutions are much more stringent than has been reported previously. It is further shown that under certain conditions the structure offers a convenient method of measuring the conductivity of a semi-conductor. In addition, a theoretical and experimental investigation of the effects of the higher order modes excited at the interface of such a structure with an empty wave-guide has been made. The study has shown that under certain conditions, the effects of these modes can be significant.

A theoretical and experimental study has also been made of the effects of temperature, frequency and doping on the complex permittivity

of lightly doped n-type germanium. Measurements of these effects which have not been reported previously have been made over a temperature range 100° K - 500° K at frequencies 9.25 and 34.5 GHz and confirm the theoretical model used.

TABLE OF CONTENTS

CHAPTER 1

INTRODUCTION

In recent years an increasing interest has been shown in the microwave properties of semi-conductors [1-8]. Due to rapidly advancing technology, semi-conducting devices are finding growing application at microwave frequencies and also microwave measurement techniques provide a convenient means of studying charge transport phenomenon in semi-conducting materials. The electrical parameters such as conductivity σ and permittivity ϵ may be different at high frequencies from those at static fields, because at sufficiently high frequencies the inertia of the charge carriers becomes observable.

Thus at microwave frequencies σ and ϵ_r for a one carrier semi-conductor are given by [9]

$$\sigma = q^2 \frac{n}{m_c^*} \left\langle \frac{\tau}{1 + \omega^2\tau^2} \right\rangle = \sigma_o \left\langle \frac{\tau}{1 + \omega^2\tau^2} \right\rangle / \langle\tau\rangle \qquad - 1.1$$

$$\epsilon_r = \epsilon/\epsilon_o = \epsilon_\ell/\epsilon_o - \frac{q^2 n}{m_c^* \epsilon_o} \left\langle \frac{\tau^2}{1 + \omega^2\tau^2} \right\rangle \qquad - 1.2$$

q = magnitude of electronic charge

$\tau = \tau(\epsilon)$ = relaxation time of the charge carrier as a function of energy

n = concentration of the charge carriers

m_c^* = conductivity effective mass of the carriers

ω = radian frequency of the waves

σ_o = d.c. conductivity

$\langle\tau\rangle$ denotes the Maxwellian average of $\tau(\varepsilon)$.

$$= \int_o^\infty \tau(\varepsilon)\ \varepsilon^{3/2}\exp^{-\varepsilon/KT}\ d\varepsilon \Big/ \int_o^\infty \varepsilon^{3/2}\exp^{-\varepsilon/kT} d\varepsilon$$

From observations of the changes in σ and ε_r at high frequencies from their d.c. values, one can study the scattering phenomena. Further, the changes in σ and ε_r at mm wave length (or even at cm wave lengths) may be significant. As these parameters play an important role in the design of semi-conducting devices, accurate data on their frequency dependence is desirable.

The use of semi-conductors at microwaves is of interest from another point of view. The conductivity of semi-conductors can be varied over a wide range, comparatively easily. By changing the conductivity and hence the loss in a semi-conductor, one can vary the propagation characteristics of a given guided wave structure, which may be useful in the design of microwave devices [10-12].

The objects of this thesis are three-fold, as follows.

(i) Because of the wide range of conductivities possible in a semi-conductor, different methods of measurements of its electrical properties are required. Experiments involving the measurement of VSWR [5,13], reflection coefficient [14] and transmission coefficient [15] are reported in the literature. These methods are mostly useful when the conductivity of the semi-conductor is relatively low ($\tilde{<}$ 10 mho/m). At higher conductivities, the measurements are effected by the unavoidable gap present between the semi-conductor and the broad walls of the wave-guide when the completely filled wave-guide is used [16,17] (fig. 1.1).

For measuring high conductivities, cavity perturbation [18,19] or substitution methods [20] are used. These methods are most useful for $\sigma \gtrsim 1000$ mho/m.

Thus the development of a new method that could provide accurate results of ε_r and σ in the middle range of conductivities, is desirable. Such a method, based on the replacement of one narrow wall of a rectangular wave-guide by a semi-conductor block (fig. 1.2) has been developed and is described in this thesis. It is found that this method is accurate when $\sigma=\omega\varepsilon_0\varepsilon_r$. This method is free from the gap effect discussed in the previous paragraph and it is shown to be more accurate at high frequencies, where wave-guide dimensions become small. The theory of this "lossy wall" wave-guide structure is developed and exact and approximate methods of calculations of the propagation constants are discussed. Finally the results of measurements which confirm the theory at 9.25GHZ are presented.

(ii) The second object of this thesis is to study the propagation characteristic of the wave-guide structure shown in the fig 1.3. This configuration has not only been used for the measurement of ε_r and σ [21 - 23], but is also useful for devices such as attenuators or modulators [10]. In all of these reported measurements, the propagation constants have been calculated using approximate techniques based on perturbational or variational methods which are subject to errors.

A study of these methods and their errors has been made and calculations of the propagation constant of such a system have been carried out for t/a and σ ranges of $0.001 \lesssim t/a \lesssim 0.25$, $0.1 \lesssim \sigma(\mho/m)$

$\lesssim 10$ ℧/m, for 10, 34.5 and 70.5 GHz with ε_r = 12 and 16. The computations were made using the exact equations governing wave propagation in the structure and the results have been compared with those obtained from the approximate techniques reported in the literature. It is shown that there is considerable error in the approximate calculations, unless $t/a << 1$. It is further shown that in certain ranges of σ and t/a the attenuation constant varies linearly with σ and for small t/a, the phase constant varies very slowly with σ. It is proposed that these ranges are useful for measurements of σ.

In practical measurements the structure shown in fig. 1.3 forms a junction with an empty guide, in which the dominant mode TE_{10} is propagating. Higher order modes are excited at such a junction and an investigation of these modes has been carried out. It has been shown that unless $t/a \lesssim 0.08$ and $\sigma \tilde{<} 2.5$ ℧/m, the higher order modes are not negligible. Experiments which confirm the theory have been performed at 9.25GHz.

(iii) Finally, the microwave measurement techniques have been used to determine the conductivity and dielectric constant of lightly doped n type germanium. Benedict and Shockley [1,2] used such a technique to determine the conductivity effective mass m_c^* of electrons and holes in germanium. However, their results are not in good agreement with the values obtained from subsequent cyclotron resonance experiments. This disagreement is probably due to experimental errors. Further work on ntype germanium using microwave techniques has been reported by Druesne [24]. His work involved measurements on n and p type germanium

(20, 10 and 1/2 ohm-cm) at 61.3 and 92 GHz using VSWR technique. His results are also in disagreement with the theory. This is because the VSWR measurement technique is probably not very accurate at these frequencies and because the gap effect seems to have been neglected in these measurements, rather than the inadequacy of the mobility theory as he has concluded. Thus there is a need of fresh experimental and theoretical work.

This thesis gives the computations of the microwave conductivity and dielectric constant of n type germanium as functions of doping ($Nd \lesssim 10^{16}/_{cm^3}$), frequency ($10^9 \lesssim f \lesssim 10^{12}$ Hz) and temperature ($100 \lesssim T \lesssim 500°k$). This has not been reported in literature. The theoretical model used to compute σ and ε_r includes the scattering by ionized impurities and lattice vibrations. The latter included the low energy acoustical phonon and high energy optical phonons. Inter-valley scattering by acoustical and optical modes was considered but it was found that neglecting them probably does not cause a serious error. At high temperatures, the holes in n type germanium are not negligible. Their effect on both σ and ε_r has been taken into account in the computations.

Experiments have been performed with a reflection type microwave bridge on n type germanium samples ($\sigma \approx 10$ and 4.5 mhos/m) between the temperature range of about 100° - 500°K, at two frequencies 9.25 and 34.5 GHz. The measurements are compared with theory.

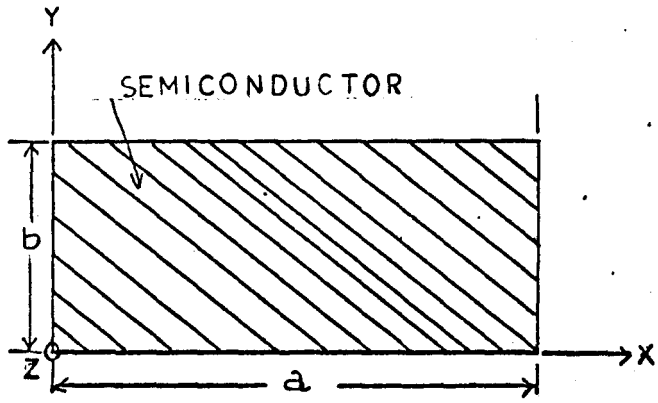

Figure 1.1 Completed Filled Wave-Guide

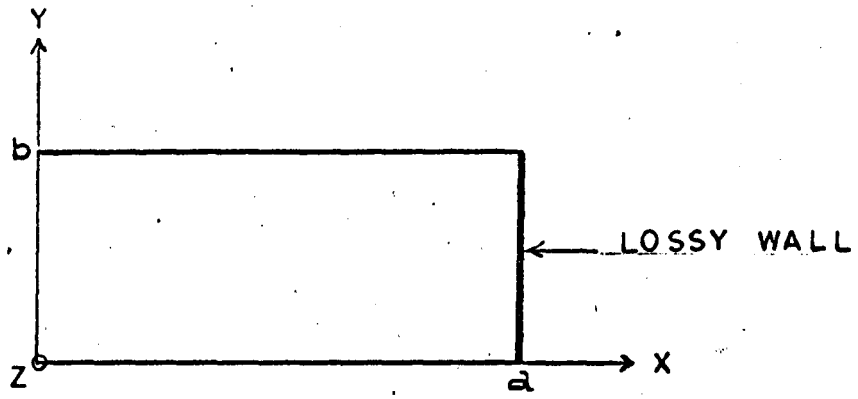

Figure 1.2 Lossy Wall Wave-Guide System

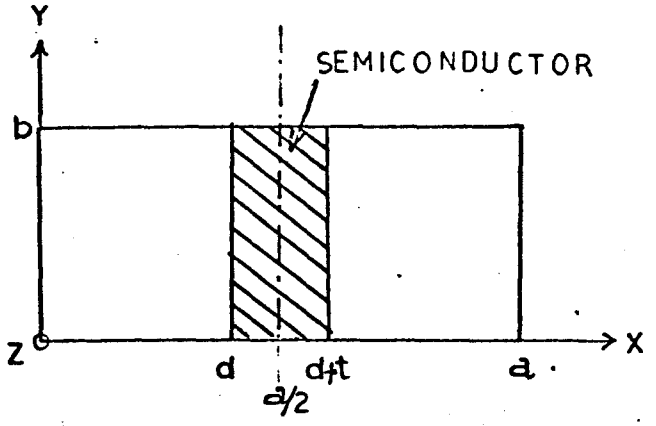

Figure 1.3 Partially Filled Wave-Guide Configuration

CHAPTER II

GENERAL THEORY OF WAVE PROPAGATION IN A WAVE-GUIDE CONTAINING SEMI-CONDUCTOR

2.1 INTRODUCTION

In this chapter the theory of electromagnetic waves in uniform rectangular wave guides containing an isotropic semi-conductor with relative permittivity $\hat{\varepsilon}_r(x,y) = \varepsilon_r(x,y) - j\,\frac{\sigma(x,y)}{w\varepsilon_0}$ and permeability μ_0 is developed. The longitudinal axis of the waveguide is along the direction of propagation which is assumed to be in z-direction. The walls of the wave guides are assumed to be perfectly conducting so that electric and magnetic fields satisfy the following boundary conditions,

$$\vec{n} \times \vec{E} = 0$$
$$\vec{n} \cdot \vec{H} = 0 \qquad (2.1)$$

$\vec{n}$ being normal to the wall, pointing outward from wall surface.

2.2 DERIVATION OF HERTZIAN POTENTIALS

The electromagnetic fields and the propagation constants in the system under consideration are obtained from the Maxwell's equations for the case of time variation according to $\exp(j\omega t)$ as given below,

$$\nabla \times \vec{E} = -j\omega\mu_0 \vec{H} \qquad (2.2a)$$
$$\nabla \times \vec{H} = j\omega\varepsilon_0 \hat{\varepsilon}_r \vec{E} \qquad (2.2b)$$
$$\nabla \cdot \vec{D} = \nabla \cdot \hat{\varepsilon}\, \vec{E} = \nabla \cdot \varepsilon_0 \hat{\varepsilon}_r \vec{E} = 0 \qquad (2.3a)$$
$$\nabla \cdot \vec{B} = \nabla \cdot \mu_0 \vec{H} = 0 \qquad (2.3b)$$

ε_o and μ_o are respectively the permittivity and permeability of free space. $\hat{\varepsilon}_r$ is the complex dielectric constant of the semi-conductor and will be assumed to be a function of x and y but not z.

The solution of fields may be obtained in terms of electric and magnetic Hertzian potentials $\vec{\Pi}_e$ and $\vec{\Pi}_h$ respectively. The special case for ε_r = constant has been dealt in the reference 27. In the following sections, the treatment is generalized to the case when $\hat{\varepsilon}_r$ is not a constant.

2.2.1 Magnetic Type Hertzian Potential Since from (2.3a)

$$\nabla \cdot \hat{\varepsilon}_r \vec{E} = 0$$

$\hat{\varepsilon}_r \vec{E}$ may be taken as the curl of a vector say $\vec{\Pi}_h \hat{\varepsilon}_r$ so that

$$\hat{\varepsilon}_r \vec{E} = -jw\mu_o \nabla \times \vec{\Pi}_h \hat{\varepsilon}_r$$

and

$$\vec{E} = -jw\mu_o \hat{\varepsilon}_r^{-1} \nabla \times \vec{\Pi}_h \hat{\varepsilon}_r \qquad (2.4)$$

where $\vec{\Pi}_h$ is called the magnetic type Hertzian potential [27].

Taking the curl of the preceding equation and substituting the result into 2.2a, one gets

$$\vec{H} = \nabla \times (\hat{\varepsilon}_r^{-1} \nabla \times \vec{\Pi}_h \hat{\varepsilon}_r)$$

$$= \nabla \times \{\hat{\varepsilon}_r^{-1} [\hat{\varepsilon}_r \nabla \times \vec{\Pi}_h + \nabla \hat{\varepsilon}_r \times \vec{\Pi}_h]$$

$$= \nabla \times \nabla \times \vec{\Pi}_h + \nabla \times (\nabla \log \hat{\varepsilon}_r \times \vec{\Pi}_h) \qquad (2.5)$$

where $\nabla \log \hat{\varepsilon}_r = \varepsilon_r^{-1} \nabla \hat{\varepsilon}_r = \nabla \Phi$

$$\Phi \equiv \log \hat{\varepsilon}_r$$

Now from 2.2b,

$$\nabla \times \vec{H} = jw\varepsilon_o \hat{\varepsilon}_r \vec{E}$$

$$= j\omega\varepsilon_o\,(-j\omega\mu_o)\,\nabla \times \vec{\Pi}_h \hat{\varepsilon}_r$$

$$= \nabla \times (k_o^2\,\vec{\Pi}_h\,\hat{\varepsilon}_r)$$

so that $$\vec{H} = k_o^2\,\vec{\Pi}_h\,\hat{\varepsilon}_r + \nabla\phi$$

where $k_o^2 = \omega^2\mu_o\varepsilon_o$ and ϕ is an arbitrary function ($\nabla \times \nabla\phi = 0$). Equating this to 2.5 yields

$$k_o^2\,\vec{\Pi}_h\,\hat{\varepsilon}_r + \nabla\phi = -\nabla^2\vec{\Pi}_h + \nabla\nabla\cdot\vec{\Pi}_h + \nabla \times (\nabla\phi \times \vec{\Pi}_h) \qquad (2.6)$$

So far ϕ and $\vec{\Pi}_h$ are arbitrary functions. If a condition is imposed on these so that

$$\nabla\phi = \nabla\nabla \cdot \vec{\Pi}_h$$

or $$\phi = \nabla \cdot \vec{\Pi}_h + \text{constant}$$

then 2.6 reduces to

$$\nabla^2\vec{\Pi}_h + k_o^2\hat{\varepsilon}_r\,\vec{\Pi}_h = \nabla \times (\nabla\phi \times \vec{\Pi}_h) \qquad (2.7)$$

2.2.2 Electric Type Hertzian Potentials

A similar set of equations as that in the previous section may be obtained from electric type Hertzian potential $\vec{\pi}_e$ [27]. One now starts from 2.3b and takes

$$\vec{H} = j\omega\varepsilon_o\nabla \times \vec{\Pi}_e \qquad (2.8)$$

so that $$\nabla\times\vec{H} = j\omega\varepsilon_o\nabla \times\nabla\times\vec{\Pi}_e = +j\omega\varepsilon_o\hat{\varepsilon}_r\,\vec{E}$$

and $$\vec{E} = \hat{\varepsilon}_r^{-1}\,\nabla\times\nabla\times\vec{\Pi}_e \qquad (2.9)$$

Now from 2.2a $$\nabla\times\vec{E} = -j\omega\mu_o\vec{H} = k_o^2\nabla \times\vec{\Pi}_e$$

This yields $$\vec{E} = k_o^2\,\vec{\Pi}_e + \nabla\phi$$

ϕ again being an arbitrary function ($\nabla\times\nabla\phi = 0$). Equating this to 2.9 gives

$$k_o^2 \hat{\epsilon}_r \vec{\Pi}_e + \hat{\epsilon}_r \nabla\phi = \nabla\times\nabla\times\vec{\Pi}_e$$
$$= \nabla\nabla.\vec{\Pi}_e - \nabla^2\vec{\Pi}_e \qquad (2.9a)$$

Again $\nabla\, \hat{\epsilon}_r\phi = \hat{\epsilon}_r\nabla\phi + \phi\nabla\hat{\epsilon}_r$

So that $\hat{\epsilon}_r\nabla\phi = \nabla\hat{\epsilon}_r\phi - \phi\nabla\hat{\epsilon}_r$

Substituting this into 2.9a and taking

$$\nabla\nabla.\vec{\Pi}_e = \nabla\hat{\epsilon}_r\phi$$

or $\nabla.\vec{\Pi}_e = \hat{\epsilon}_r\phi$ + constant

yields $\phi = \hat{\epsilon}_r^{-1}\, \nabla.\vec{\Pi}_e$

$$\nabla^2\vec{\Pi}_e - \hat{\epsilon}_r^{-1}\,(\nabla\epsilon_r)\,\nabla.\vec{\Pi}_e + k_o^2\,\hat{\epsilon}_r\,\vec{\Pi}_e = 0.$$

or $$\nabla^2\vec{\Pi}_e - \nabla.\vec{\Pi}_e\,\nabla\phi + k_o^2\epsilon_r\,\vec{\Pi}_e = 0 \qquad (2.10)$$

2.3 SPECIAL CASES

2.3.1 $\phi = \log_e \hat{\epsilon}_r$ = Constant

In this case $\nabla\phi = 0$ and the equations 2.7 and 2.10 reduce respectively to

$$\nabla^2\vec{\Pi}_h + k_o^2\hat{\epsilon}_r\,\vec{\Pi}_h = 0 \qquad (2.11a)$$

$$\nabla^2\vec{\Pi}_e + k_o^2\hat{\epsilon}_r\,\vec{\Pi}_e = 0 \qquad (2.11b)$$

and from 2.4 and 2.5

$$\vec{E} = -j\omega\mu_o\,\nabla\times\vec{\Pi}_h$$
$$\vec{H} = \nabla\times\nabla\times\vec{\Pi}_h \qquad (2.12)$$

and (2.8) and (2.9) give

$$\vec{H} = +j\omega\epsilon_o\nabla\times\vec{\Pi}_e$$
$$\vec{E} = \hat{\epsilon}_r^{-1}\nabla\times\nabla\times\vec{\Pi}_e \qquad (2.13)$$

The solution to these equations can be divided into two basic sets of solutions. One such mode is TE to z or simply TE or H mode and the

other is TM to z or TM or E mode. These modes can respectively be obtained from a single component of $\vec{\pi}_h$ or $\vec{\pi}_e$ directed in the z-direction and the equations 2.12 and 2.13.

The TE or H mode in the fig. 1.1 will be treated here for reference in later applications Thus let

$$\vec{\pi}_h = \vec{a}_z \, \psi(x,y) e^{-\gamma z} \tag{2.14}$$

where γ = propagation constant = $\alpha + j\beta$.

Substitution of 2.14 into (2.11a) gives

$$\nabla_t^2 \psi + (\gamma^2 + k_o^2 \hat{\varepsilon}_r) \psi = 0$$

where $$\nabla_t^2 = \frac{\partial^2}{\partial x^2} + \frac{\partial^2}{\partial y^2}$$

The solution for ψ and γ for the structure shown in the fig. 1.1 are given below (28).

$$\psi_{n,m} = \cos \frac{n\pi x}{a} \cos \frac{m\pi y}{b}$$

$$\gamma_{n,m}^2 = (n\pi/a)^2 + (m\pi/b)^2 - k_o^2 \varepsilon_r$$

The dominant mode in the structure is when m = 0 and n = 1. For the dominant mode, the above equations reduce to

$$\psi = \cos \frac{\pi x}{a}$$

$$\gamma^2 = (\pi/a)^2 - k_o^2 \hat{\varepsilon}_r \tag{2.15}$$

where the subscripts n and m have been omitted. From the form of $\psi_{n,m} = \psi_p$, it is obvious that

$$\int\int \psi_p \psi_{p'} \, dx \, dy = \delta_{pp'}$$

$\delta_{pp'} = 0$ if $p \neq p'$ $p' \rightarrow n', m'$.

2.3.2 $\hat{\varepsilon}_r = \hat{\varepsilon}_r(x)$

This case is applicable to the structures shown in the figs. 1.2 and 1.3. The solutions to the wave equations can again be divided into two basic sets, TE to X and TM to X. Here only TE to X will be considered. The solution to this mode can be obtained from equations 2.4, 2.5 and 2.7 with a single component of $\vec{\Pi}_h = \vec{a}_x \Pi_{hx}$. If it is assume that

$$\Pi_{hx} = \psi(x,y)e^{-\gamma z} \tag{2.16}$$

then 2.7 reduces to

$$\nabla t^2\psi + (\gamma^2 + k_o^2 \hat{\varepsilon}_r)\psi = 0 \tag{2.17}$$

The solution for γ and ψ may be obtained for a particular arrangement.

In a rectangular wave-guide, it is found that an infinite number of solutions for γ and ψ are possible. It will be shown here that these solutions are orthogonal to each other. Let ψ_i and ψ_j be two different solutions with propagation constants γ_i and γ_j respectively. Then

$$\nabla_t^2\psi_i + (\gamma_i^2 + k_o^2 \hat{\varepsilon}_r)\psi_i = 0$$

$$\nabla_t^2 \psi_j + (\gamma_j^2 + k_o^2 \hat{\varepsilon}_r)\psi_j = 0$$

Multiplying the first by ψ_j and the second by ψ_i and subtracting one obtains

$$\psi_j \nabla_t^2 \psi_i - \psi_i \nabla_t^2 \psi_j = (\gamma_j^2 - \gamma_i^2)\psi_i \psi_j$$

integrating this over the cross section of the wave guide, applying Green's second theorem and the boundary condition 2.1, yields

$$(\gamma_j^2 - \gamma_i^2)\iint_s \psi_i \psi_j ds = \iint_s (\psi_i \nabla_t^2\psi_j - \psi_j \nabla_t^2 \psi_i)ds$$

$$= \oint_c (\psi_i \nabla\psi_j - \psi_j \nabla\psi_i) dl$$

$$= 0$$

because of the boundary condition 2.1

where s denotes the surface of the Cross-section of the wave guide and c is the contour enclosing it. Thus if $\gamma_i \neq \gamma_j$

$$\iint_s \psi_i \psi_j \, ds = 0$$

ψ's may be normalized so that

$$\iint_s \psi_i \psi_j \, ds = \delta_{ij} = \begin{cases} 1 & i = j \\ 0 & i \neq j \end{cases} \qquad (2.18)$$

2.3.3 $\hat{\varepsilon}_r = \hat{\varepsilon}_r(y)$

The solution for fields and propagation constants can be obtained for TM to y mode from equations 2.8 through 2.10 by taking single component of $\vec{\pi}_e$ along y direction. If

$$\vec{\pi}_e = \vec{a}y \ \psi(x,y) e^{-\gamma z} \qquad (2.19)$$

then 2.10 reduces to

$$\nabla_t^2 \psi - \frac{\partial \Phi}{\partial y} \frac{\partial \psi}{\partial y} + (k_o^2 \hat{\varepsilon}_r + \gamma^2) \psi = 0 \qquad (2.20)$$

or $$\frac{\partial^2 \psi}{\partial^2} + \frac{\partial^2 \psi}{\partial y^2} - \frac{\partial \Phi}{\partial y} \frac{\partial \psi}{\partial y} + (k_o^2 \hat{\varepsilon}_r + \gamma^2) \psi = 0$$

multiplying throughout by $e^{-\Phi} = \hat{\varepsilon}_r^{-1}$, gives

$$\frac{\partial^2 \psi}{\partial x^2} e^{-\Phi} + \frac{\partial}{\partial y} (e^{-\Phi} \frac{\partial \psi}{\partial y}) + e^{-\Phi} (k_o^2 \hat{\varepsilon}_r + \gamma^2) \psi = 0$$

or $$\frac{\partial^2 \psi}{\partial x^2} + e^{\Phi} \frac{\partial}{\partial y} (e^{-\Phi} \frac{\partial \psi}{\partial y}) + (k_o^2 \hat{\varepsilon}_r + \gamma^2) \psi = 0$$

Again in a wave-guide, there are an infinite possible values of γ and ψ and again it can be shown that different ψ's are orthogonal to each other. However, the orthogonality relationship is now

$$\iint_S e^{-\Phi}\psi_i\psi_j ds = \iint_S ds\hat{\varepsilon}_r^{-1}\psi_i\psi_j = \delta_{ij} = \begin{cases} 1 & i=j \\ 0 & i\neq j \end{cases} \qquad (2.21)$$

CHAPTER III

WAVE PROPAGATION IN RECTANGULAR WAVE-GUIDE WITH A SEMI-CONDUCTOR WALL

3.1 INTRODUCTION

When a perfectly conducting wall of a wave guide is replaced by a semi-conducting one, a tangential electric field can be supported and losses occur in that guide. From measurements of the changes in the propagation constant in a guide when one of its wall is replaced by a semi-conductor, it is possible to deduce the properties of the semi-conducting material. This principle has been used to measure highly conducting semi-conductors from the observation of the changes in the resonant frequency and the Q-factor of a microwave cavity [19]. This method has been successful for conductivities greater than 1000 mhos/m approximately.

For materials of lower conductivity the method of measurement described in this chapter has been investigated and developed. An analysis has been made of the wave propagation of a rectangular guide with one of its narrow walls replaced by a thick semi-conducting slab as shown in the fig. 3.10. Computations of the dominant mode propagation constant have been made for $1 \leq \sigma \leq 1000$ mhos/m, $0 \leq \varepsilon_r \leq 16$ at three different frequencies of 9.25, 34.5 and 70.5 GHz. Exact and approximate methods of computations are discussed and experiments which confirm the theory at 9.25 GHz, have been made.

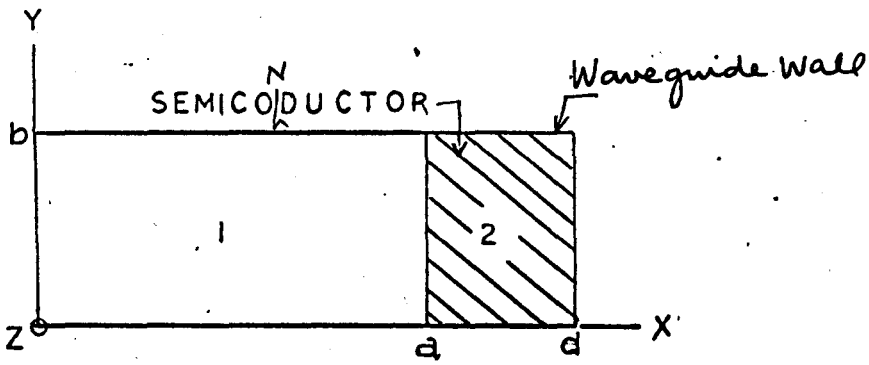

Figure 3.1 Wave-Guide System Analysed Theoretically

3.2 THEORY

The arrangement illustrated in the fig. 3.1 will be considered. The region (1) is empty and the region (2) consists of a semi-conducting material which is homogeneous and isotropic with complex permittivity $\epsilon_0\hat{\epsilon_r} = \epsilon_0\epsilon_r - j\frac{\sigma\epsilon_0}{w\epsilon_0}$. It will be assumed that the thickness of the semi-conductor is much larger than the skin depth in the material so that the fields vanish at x = d.

Because of the non-uniformity in the x-direction, in general a hybrid mode (a combination of E and H modes) will be propagating. One such set is an LSE mode with no electric field perpendicular to the air semi-conductor interface [29]. The fields and the propagation constants may be obtained from the solution of equations 2.4, 2.5 and 2.7. When Φ is a function of x alone and variation in z-direction as $e^{-\gamma z}$ is assumed, 2.7 reduces to

$$\nabla_t^2\Pi_x + (k_0^2\epsilon_r + \gamma^2)\,\Pi_x = \frac{\partial}{\partial y}\left(\Pi_y \frac{\partial\Phi}{\partial x}\right) + \frac{\partial}{\partial z}\left(\Pi_z \frac{\partial\Phi}{\partial x}\right)$$

$$\nabla_t^2\Pi_y + (k_0^2\epsilon_r + \gamma^2)\,\Pi_y = -\frac{\partial}{\partial x}\left(\Pi_y \frac{\partial\Phi}{\partial x}\right) \qquad (3.1)$$

$$\nabla_t^2\Pi_z + (k_0^2\epsilon_r + \gamma^2)\,\Pi_z = -\frac{\partial}{\partial x}\left(\Pi_z \frac{\partial\Phi}{\partial x}\right)$$

For an L.S.E. only one component of $\vec{\Pi}$ is required. This is obtained by taking $\Pi_y = \Pi_z = 0$ so that the above equation for $\Pi_x = \psi(x,y)e^{-\gamma z}$ reduces to

$$\frac{\partial^2\psi}{\partial x^2} + \frac{\partial^2\psi}{\partial y^2} + (k_0^2\hat{\epsilon_r} + \gamma^2)\,\psi = 0$$

$$\text{where } \hat{\epsilon}_r(x) = \begin{cases} 1 & 0 \leq x \leq a \\ \epsilon_r - j\frac{\sigma}{w\epsilon_0} & a \leq x \leq d \end{cases} \qquad (3.2)$$

Electric and magnetic field components are then obtained from 2.4 and 2.5 as follows

$$Ex = 0$$

$$Ey = + jw\mu_0 \gamma \psi e^{-\gamma z}; \quad Hx = \frac{-1}{jw\mu_0}\left(\frac{\partial Ez}{\partial y} - \frac{\partial Ey}{\partial z}\right)$$

$$Ez = + jw\mu_0 \frac{\partial \psi}{\partial y} e^{-\gamma z} \qquad Hy = \frac{1}{jw\mu_0}\left(\frac{\partial Ez}{\partial x}\right)$$

$$Hz = \frac{-1}{jw\mu_0}\frac{\partial Ey}{\partial x} \tag{3.3}$$

The boundary conditions on Ey and Ez at x = 0, d, and y = 0,b require that ψ be of the form

$$\begin{aligned} \psi &= A \sin k_1 x \cos \frac{m\pi y}{b} && 0 \leqslant x \leqslant a \\ \psi &= B e^{-k_2 x} \cos \frac{m\pi y}{b} && a \leqslant x \leqslant d \end{aligned} \tag{3.4}$$

where A and B are constants. k_1 and k_2 are wave vectors in the transverse direction (x direction) and m is the wave number in y direction. m = 0, 1, 2, 3, ..., k_1 and k_2 satisfy the following equations

$$\begin{aligned} \gamma^2 &= k_1^2 - k_0^2 + (m\pi/b)^2 \\ &= -k_2^2 - k_0^2 \hat{\epsilon}_r + (m\pi/b)^2 \end{aligned} \tag{3.5}$$

γ is the same in both the regions of fig. 3.1 so as to satisfy the boundary conditions for all values of z.

Now the continuity of E_z and Hy at x = a gives the following conditions

$$-\left(\frac{m\pi}{b}\right) A \sin k_1 a \sin \frac{m\pi y}{b} = -\left(\frac{m\pi}{b}\right) B e^{-k_2 a} \sin \frac{m\pi y}{b}$$

$$k_1 A \cos k_1 a \cos \frac{m\pi y}{b} = -k_2 B e^{-k_2 a} \cos \frac{m\pi y}{b}$$

so that $$k_1 \cot k_1 a = -k_2 \qquad (3.6)$$

Equations 3.5 and 3.6 give the eigenvalues $\gamma_{n,m}$, doubly infinite values. However, if m = 0, the structure can support only Hno modes. For Hno modes, Ez and Hy vanish and the fields and the propagation constants are as given below

$$Ex = 0 \qquad Hx = \frac{1}{j\omega\mu_0} \gamma^2 \psi e^{-\gamma z}$$

$$Ey = j\omega\mu_0 \gamma\psi e^{-\gamma z} \qquad = \frac{+1}{j\omega\mu_0} \frac{\partial Ey}{\partial z} \qquad (3.7)$$

$$Ez = 0 \qquad Hz = \frac{-1}{j\omega\mu_0} \frac{\partial Ey}{\partial x}$$

$$\gamma^2 = k_1^2 - k_0^2 = -k_2^2 - k_0^2 \hat{\epsilon}_r \qquad (3.8)$$

The lowest solution of 3.6 and 3.8 gives the dominant mode in the system and is H_{10}.

It may be seen from 3.6 and 3.8 that a complex transcendental equation must be solved to obtain γ. This is often a laborious task. Therefore, an approximate expression for γ^2 is desirable which can adequately give the value of γ. Methods based on perturbational and variational techniques are available for this purpose [30].

However, a simpler technique can be used in this case under certain assumptions. If it is assumed that the conductivity is sufficiently high so that the field distribution in the region $0 \leq x \leq a$ is approximate

the same as in an ideal empty guide of broad dimension a, then the wave vector k_1 will not be much different from its value of $(n\pi/a)$ in the ideal case. Under this condition the equation 3.6 can be expanded in Taylor's series about $K_{10} = n\pi/a$. Thus

$$f(k_1) = k_1 + k_2 \tan k_1 a = f(k_{10}) + (k_1 - k_{10}) \left.\frac{\partial f}{\partial k_1}\right|_{k_1=k_{10}} \qquad (3.8)$$

If it is further assumed that $|\gamma^2| \ll |k_0^2 \hat{\epsilon}_r|$, then the approximate expression for k_1 and γ are as follows

$$k_1 = (n\pi/a) \left[1 - j/\sqrt{a^2 k_0^2 \hat{\epsilon}_r}\right]^{-1} \qquad (3.9)$$

$$\text{and } \gamma^2 = (n\pi/a)^2 \left\{1 + \frac{2j}{a\sqrt{k_0^2 \hat{\epsilon}_r}}\right\} - k_0^2 \qquad (3.10)$$

3.3 THEORETICAL RESULTS

The equations3.6 and 3.8 were numerically solved for $0 \leq \epsilon_r \leq 16$ and $1 \leq \sigma \leq 1000$ mho/m with the help of a 7040 IBM computer using the Newton-Raphson technique. The computations were made for three different frequencies, namely, 9.25, 34.5 and 70.5GHz. The results in the form of $\gamma_1 - \gamma_0$, γ_0 being the propagation constant in an ideal empty wave-guide of broad dimension a, are shown in the figs. 3.2 through 3.4. The abscissa represents the change in attenuation constant $\delta\alpha = \alpha_1 - \alpha_0 = \alpha_1$ (as $\alpha_0 = 0$) nep/m and the ordinate represents the change in the phase constant $\delta\beta = \beta_1 - \beta_0$ rad/m. The ϵ_r and log σ are taken as parameters.

In all the three figures, it may be observed that, in the range of σ considered, as the conductivity is decreased (resistivity of the semi-conducting sample is increased), the attenuation constant

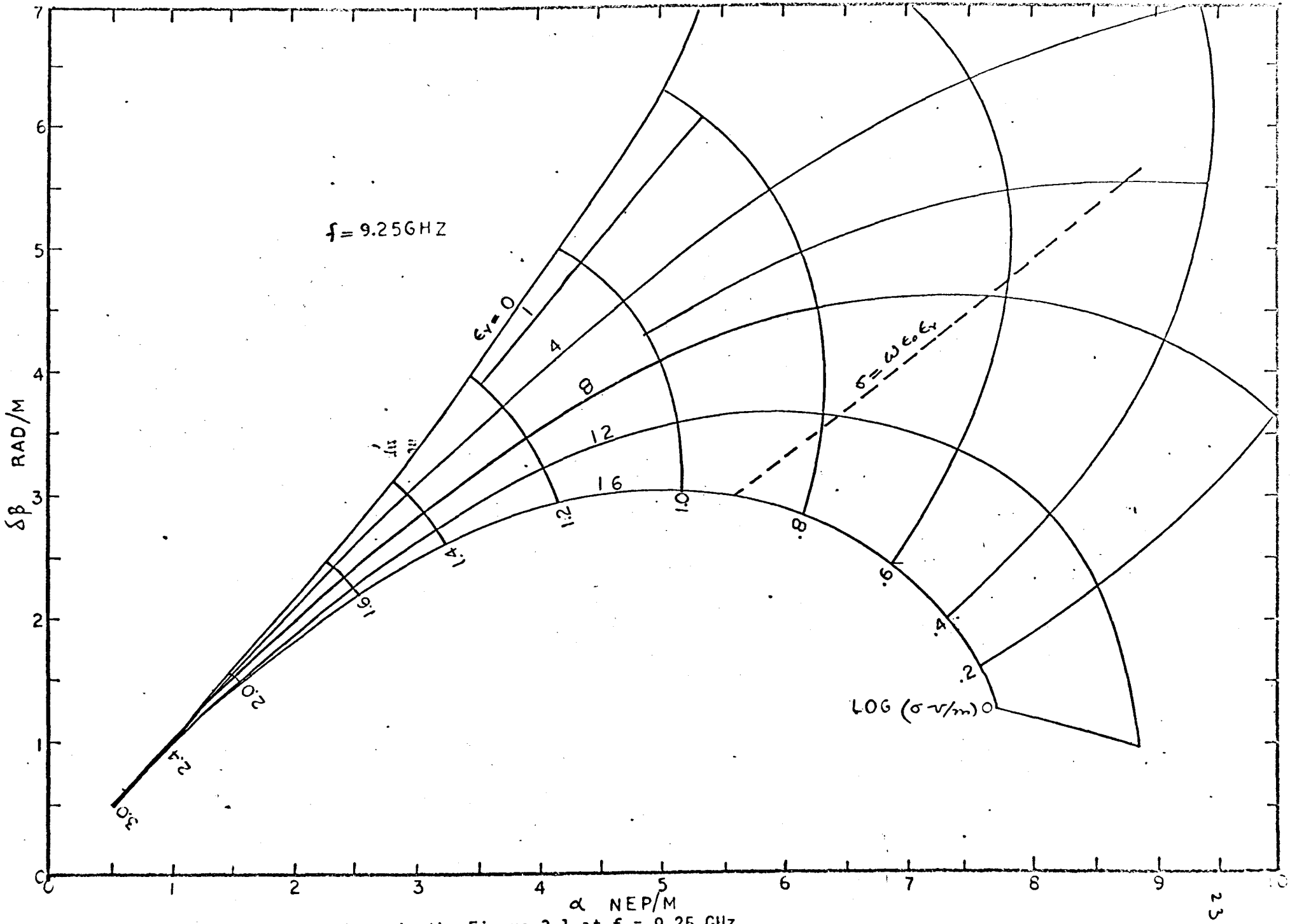

Figure 3.2 $\delta\gamma$ in the system shown in the Figure 3.1 at f = 9.25 GHz

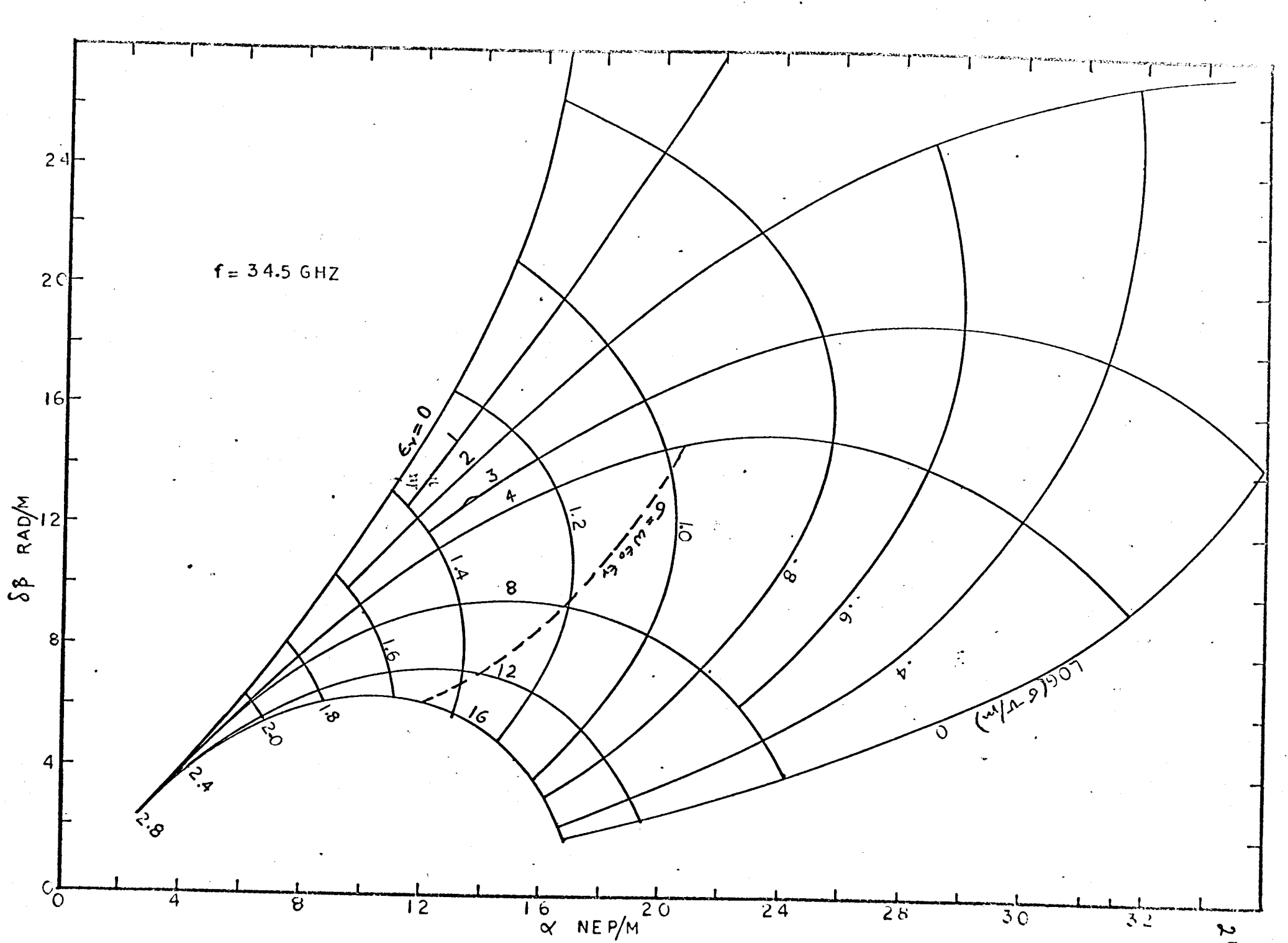

Figure 3.3 $\delta\gamma$ in the system shown in the Figure 3.1 at f = 34.5 GHz

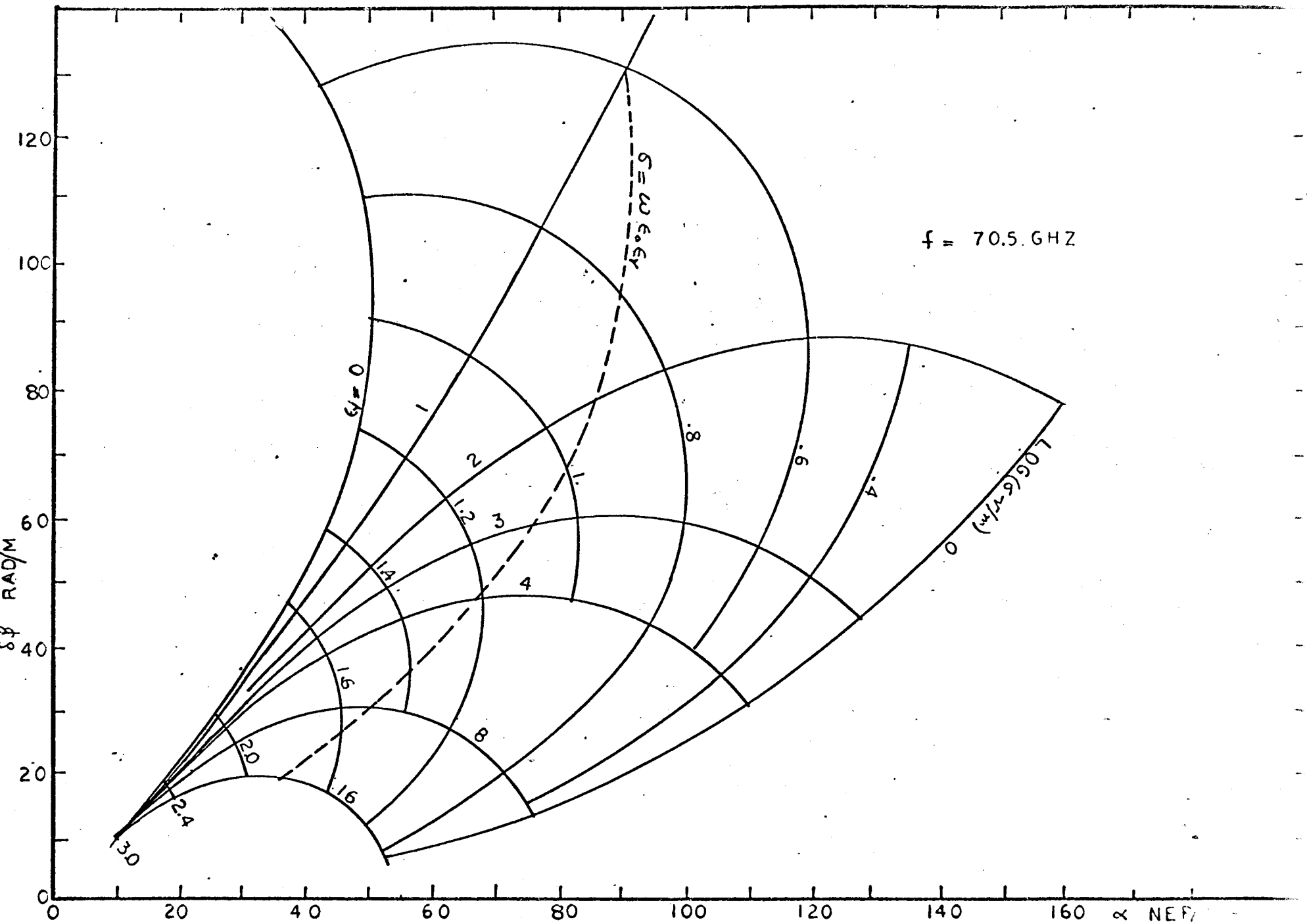

Figure 3.4 $\delta\gamma$ in the system shown in the Figure 3.1 at 70.5GHz

increases monotonically. The change in the phase constant, however, first increases with σ, attains a maximum and then decreases. This observation is true for $\epsilon_r \tilde{>} 1$. However, for $\epsilon_r < 1$, the things reverse and α attains a maxima and β increases monotonically as the resistivity is increased. It is further observed that maxima occur near, though not quite at $\sigma = w\epsilon_0\epsilon_r$. The locus of this condition is also plotted in the figures 3.2 to 3.4.

It may also be noted that at the higher end of the conductivity range considered, the curves for various values of ϵ_r are crowded and ultimately merge into each other. This is because as σ increases, $\sigma/w\epsilon_0 >> \epsilon_r$ and $\hat{\epsilon}_r \rightarrow \frac{-j\sigma}{w\epsilon_0}$, independent of ϵ_r.

The changes in the propagation constant γ were also computed from the expression 3.10. The results of computations are compared to those from exact equations in the fig. 3.5 for $\epsilon_r = 16$ and $\epsilon_r = 1$ and f = 9.25GHz. The solid and dotted lines give the values of α and $\delta\beta$ respectively as obtained from the exact equations as a function of σ. The circles and crosses give the corresponding values from equation 3.10. It may be observed that for high values of ϵ_r, the equation 3.10 is adequate to give α and $\delta\beta$ within $\pm$ 3% for the whole range of σ considered. However, as ϵ_r decreases the errors increase for $\sigma \lesssim 4.0$ mho/m. For $\sigma > 4$ mho/m, errors are negligible.

For semi-conductors, the value of dielectric constant is given by the contributions from the lattice and the free carriers. If it is

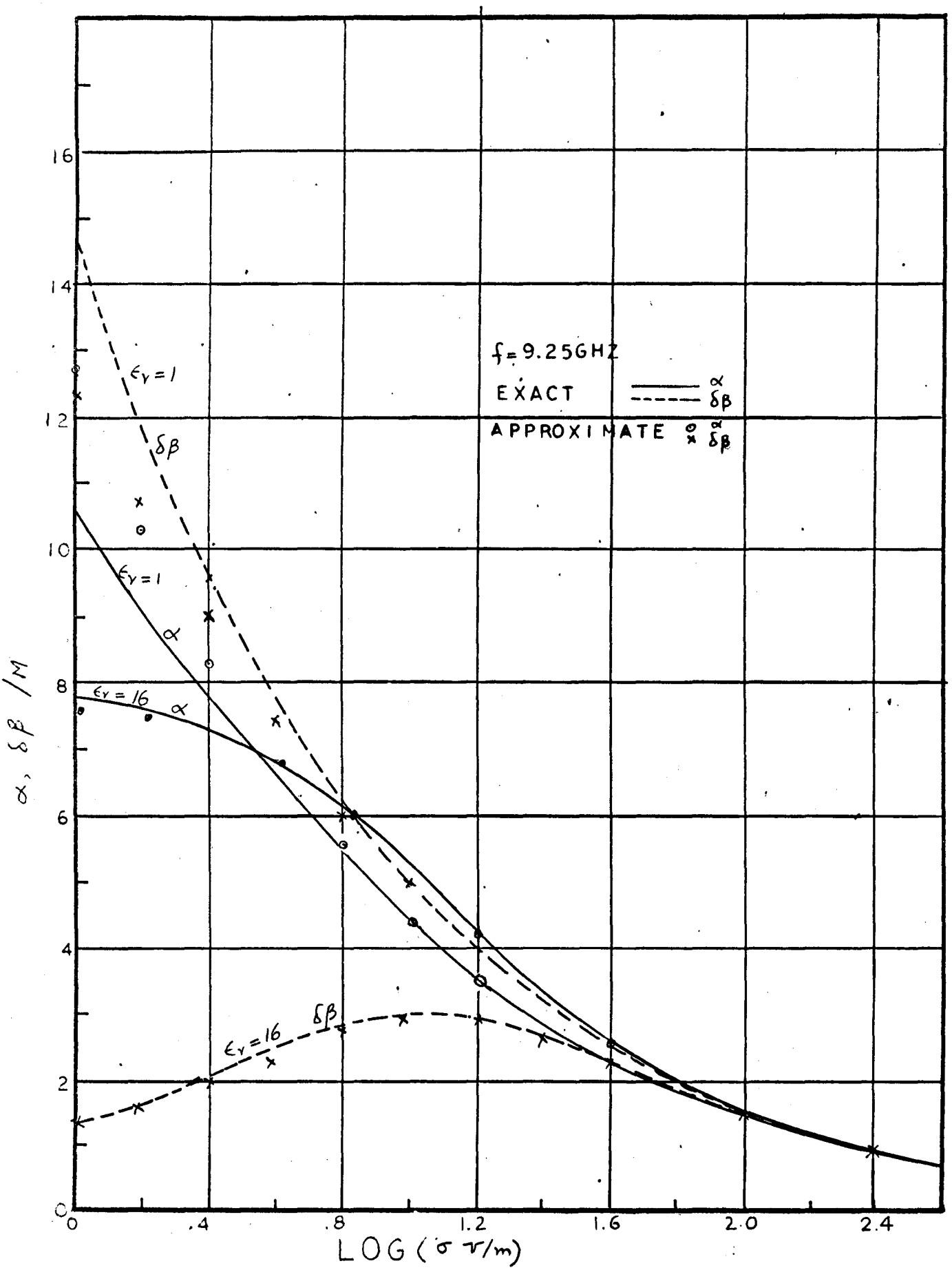

Figure 3.5 Comparison between exact and approximate values of $\delta\gamma$ as a function of ϵ_r and σ

assumed that there is only one type of carrier, say electrons, the conductivity and dielectric constant at frequency w are given by the equations 1.1 and 1.2. If, for the moment, it is assumed that τ = constant, i.e. does not change with energy, and further assumed that w is such that $(w\tau)^2 << 1$ then these expressions reduce to

$$\sigma = q^2 n\tau / m^* c = \sigma_o \qquad (3.11)$$

$$\varepsilon_r = \varepsilon/\varepsilon_o = \varepsilon_\ell/\varepsilon_o - \sigma_o\tau/\varepsilon_o \qquad (3.12)$$

$$\varepsilon_\ell/\varepsilon_0 = 16.0$$

A plot of ε_r with σ for various values of τ is given in the fig. 3.6. The propagation constant at f = 9.25GHz for $0 \leq \log \sigma \leq 3.0$ ($1.0 < \sigma < 1000$ ℧/m) and for values of τ and ε_r (given by 3.12) is shown in the fig. 3.7.

The values of k_1 and k_2 for various values of σ and $\tau = 3.0 \times 10^{-13}$ (approximate value for n type Ge at room temperature) are plotted in the fig. 3.8a and b. It may be observed that magnitude of k_1 is not very different from that for empty guide over the whole range of σ considered and that its angle does not vary more than a few degrees.

The magnitude of the electric field in y-direction as a function of x/a is plotted in the fig. 3.9 for $2 < \sigma \leq \infty$ mho/m.

3.4 MEASURING TECHNIQUE

For the measurement of the propagation constant a section of a wave-guide was milled as shown in the fig. 3.10. Into this milled out section could be clamped either a polished brass block or the semi-

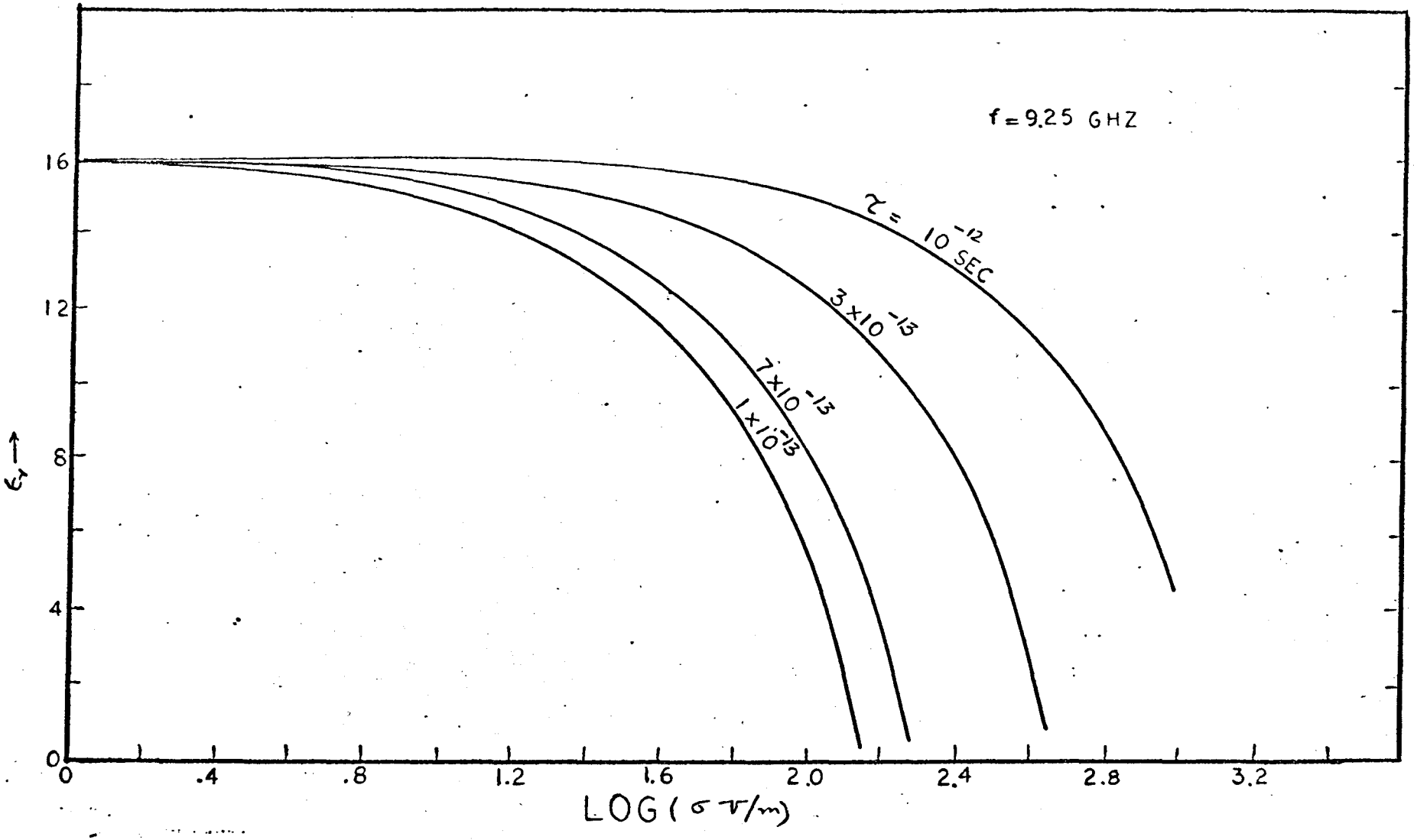

Figure 3.6 ε_r as a function of σ and τ

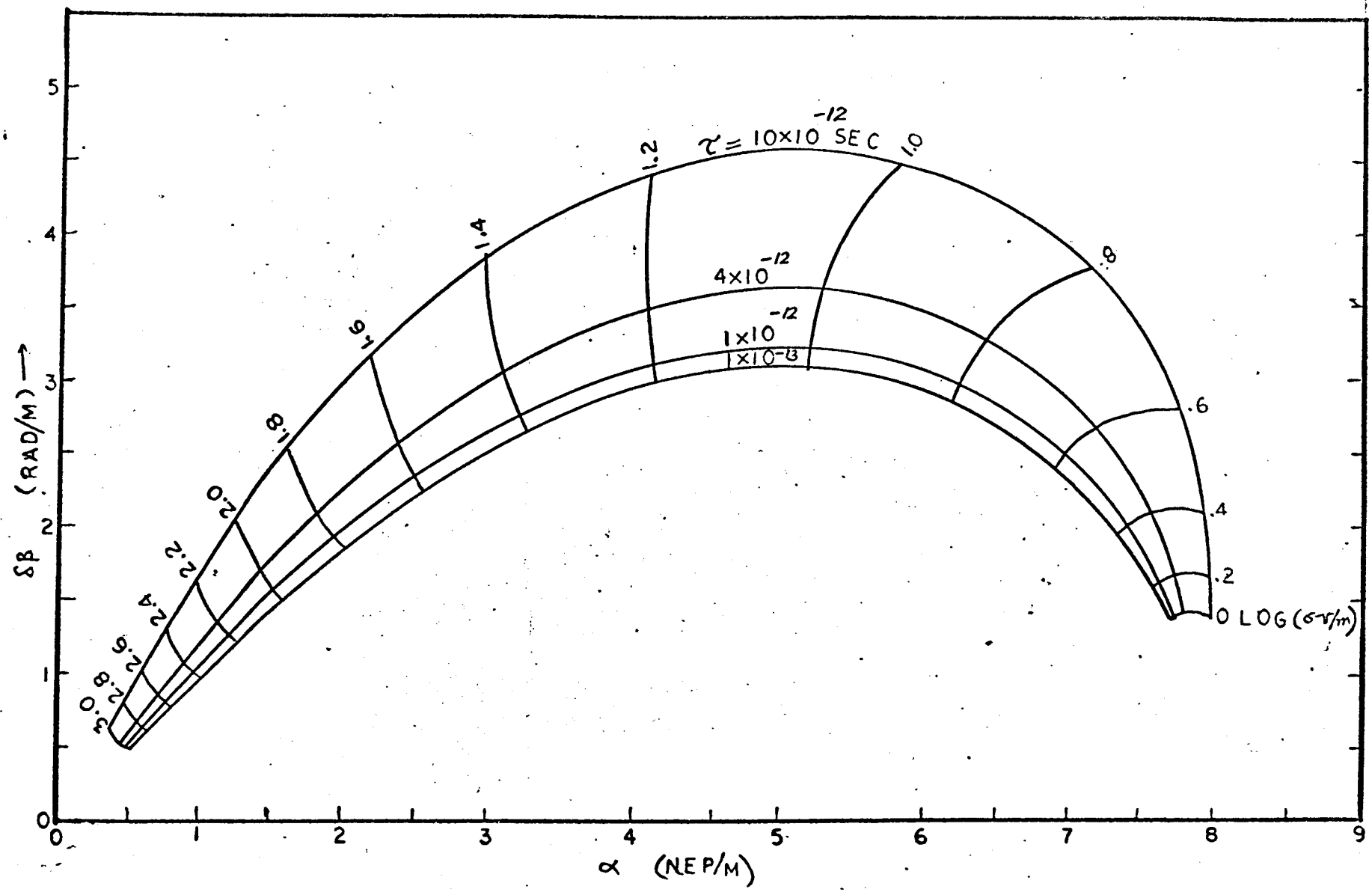

Figure 3.7 $\delta\gamma$ in the system of Figure 3.1 as a function of σ and τ

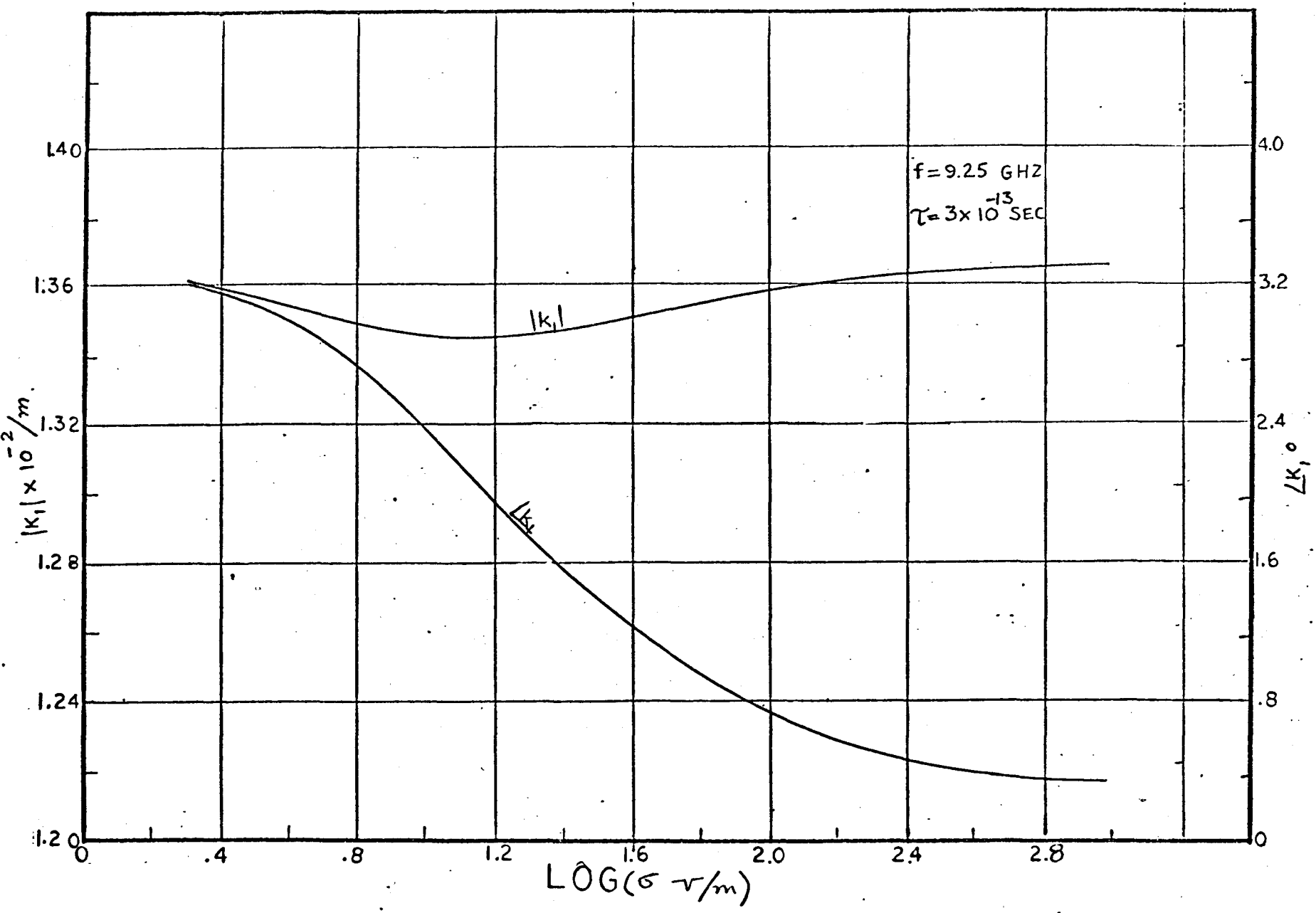

Figure 3.8 (a) $|k_1|$ and $\angle k_1$ as functions of σ

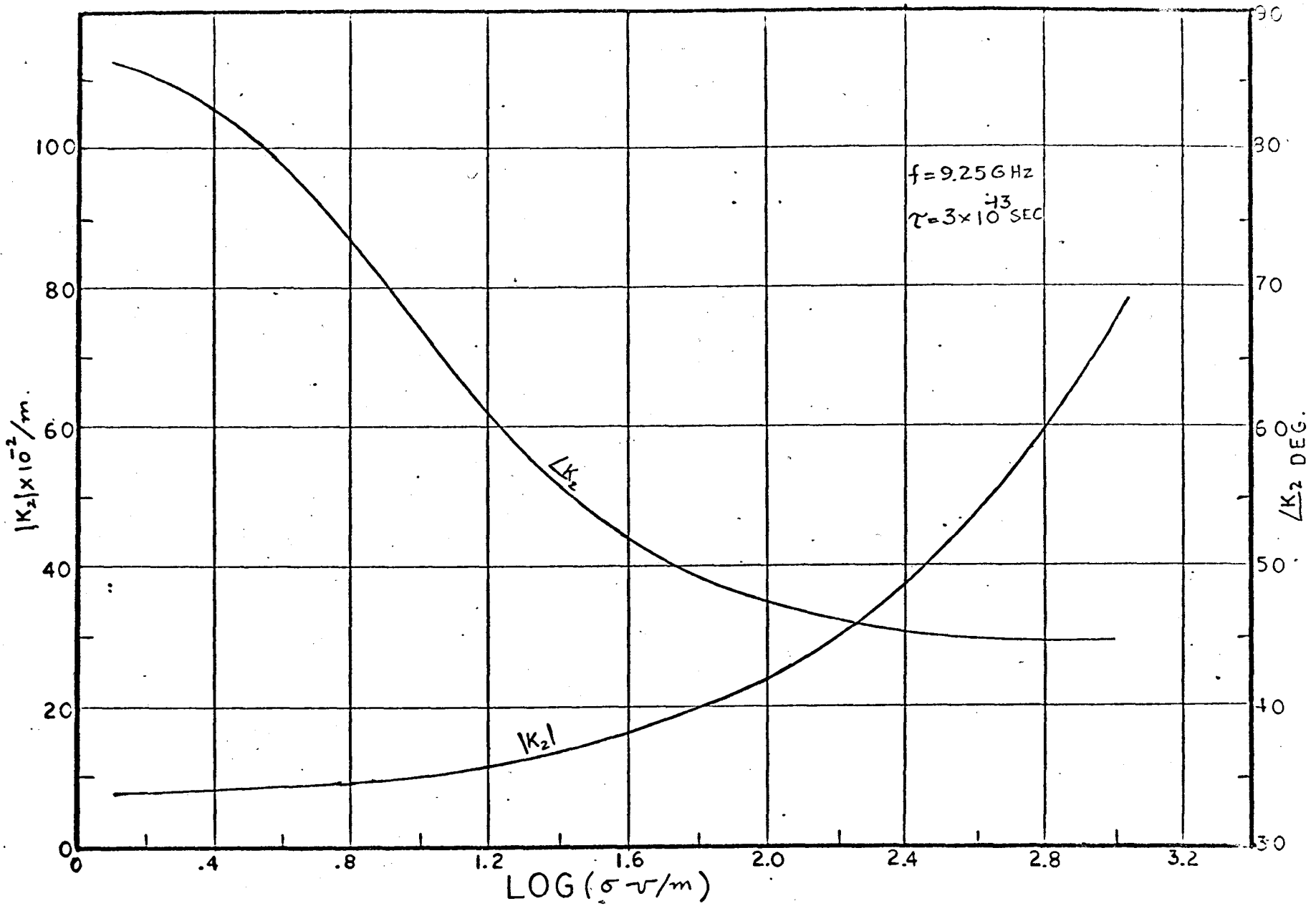

Figure 3.8 (b) $|K_2|$ and $\angle K_2$ as functions of σ

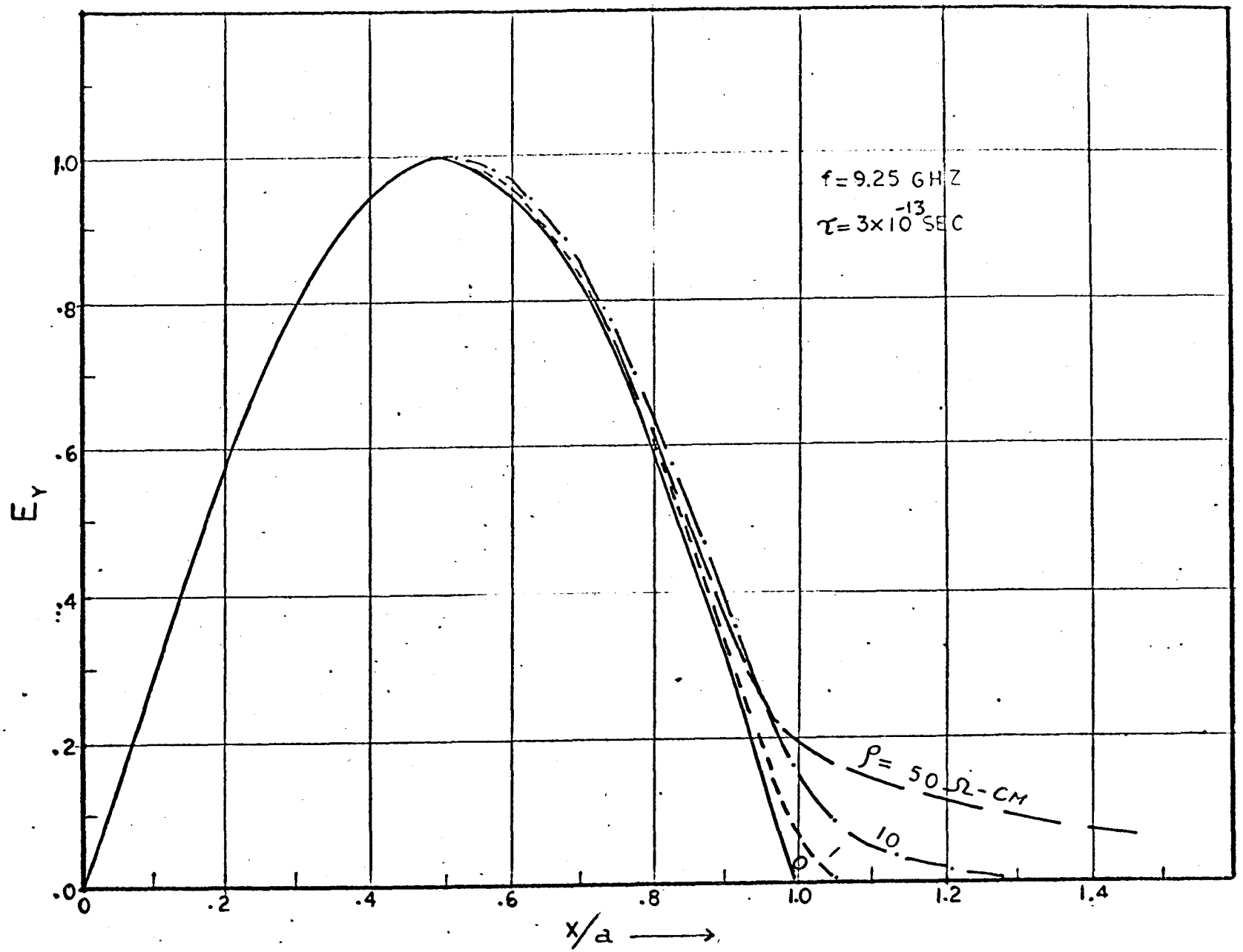

Figure 3.9 Distribution of Normalized Magnitude of Electric Field Intensity Ey as a Function of x/a

conductor block. This section of the wave guide was placed in one arm of a transmission bridge described by Montgomery [31]. The second arm of the bridge contained a precision attenuator and a phase shifter.

The zero balance of the bridge was first carried out with a brass block clamped into the milled section. A second balance was obtained when the brass block was replaced by a semi-conductor block. Both the readings were taken when the bridge balance was independent of the clamping pressure. If A_0 and Φ_0 are the readings of the atten-uator and the phase shifter in dbs and degrees respectively with brass block and A_1 and Φ_1 are corresponding readings with semi-conductor block, then neglecting the internal reflections and reflections at the interfaces at z = 0 and z = ℓ, the propagation constant in the lossy wall guide is given by

$$\alpha = (A_1 - A_0)/(8.686\ell) \quad \text{nep/m}$$

$$\beta = (\phi_1 - \phi_0)/57.296\ell \quad \text{rad/m}$$

where ℓ = length of the sample in meters.

The neglecting of the internal reflections and those at z = 0 and z = 1 was justified because these reflections were observed to be small (< .03). Theoretically if Z_0 and Z are wave impedances in the empty guide and the guide containg the semi-conductor, the reflection coefficient at z = 1 is given by

$$R = \left[\frac{Z-Z_0}{Z+Z_0}\right]$$

It is assumed here that in the empty guide section ($z \geq 1$) there is no reflected wave travelling and that the higher order modes which may be

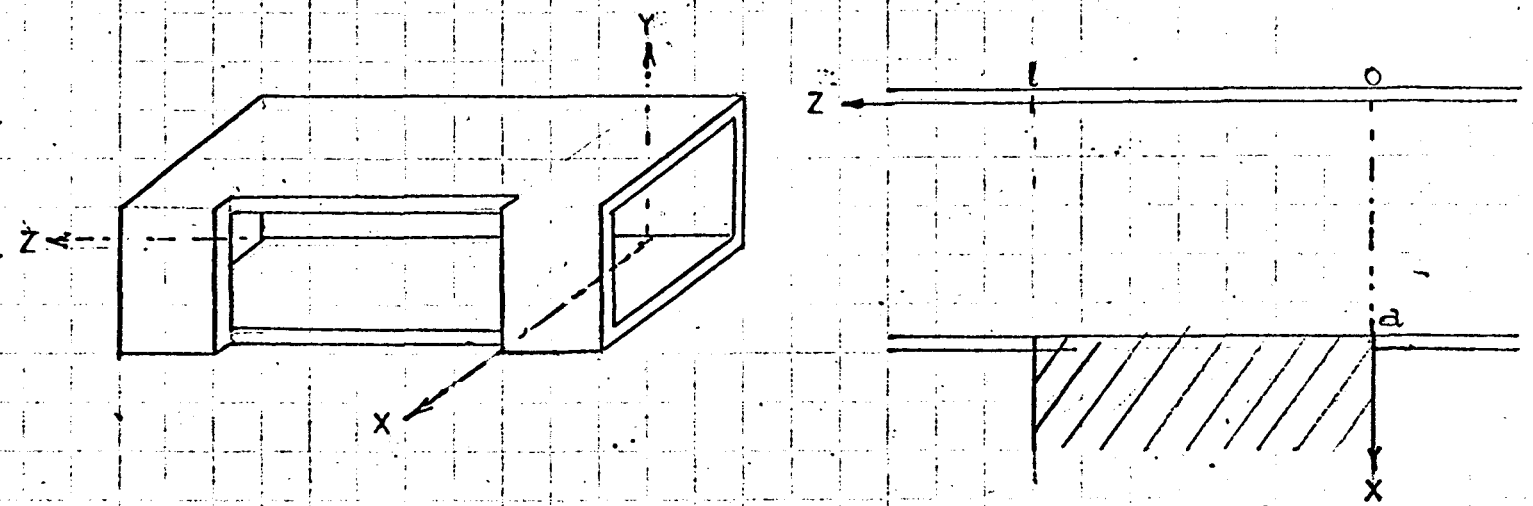

Figure 3.10 Milled out Section of the Wave-Guide used in the Experiments

excited at the junction are negligible. Now for TE_{10} wave

$$\frac{Z_0}{Z} = \frac{j\omega\mu_0}{\gamma_0} \quad \frac{\gamma_1}{j\omega\mu_0} = \frac{\gamma_1}{\gamma_0} = \frac{(\alpha_1+j\beta_1)}{j\beta_0} \simeq (1 - j\frac{\alpha}{\beta_0})$$

as $\beta_1 \simeq \beta_0$

$$|R| = \left|\frac{j\alpha_1/\beta_0}{2+j\alpha_1/\beta_0}\right| \simeq \frac{\alpha_1}{2\beta_0}$$

for $\alpha_1 << \beta_0$

At 9.25 GHz, for σ = 2℧/m and ε_r = 16, this evaluates to 0.03 approximately to give VSWR ≃ 1.05. This agreed well with the experiment.

3.5 EXPERIMENTAL RESULTS AND DISCUSSION

The measurements were carried out at 9.25 GHz on 6 samples, one of intrinsic germanium ($\sigma \simeq 2$ mho/m) and five of n type germanium having d.c. conductivities ranging from about 4 mho/m to 400 mho/m. The results of measurements are given in the table, 3.1.

Inspection of the results shows that over the resistivity range $5 \lesssim \rho \lesssim 25\Omega$-cm($20 \gtrsim \sigma \gtrsim 4$ ℧/m) both ε_r and σ can be measured accurately. The microwave measurement of ρ agreed well with the d.c. measurements and it was found that the measurements were repeatable with the limits of 3%. For $\rho < 5\Omega$-cm ($\sigma > 20$ mho/m, $\log\sigma > 1.3$) agreement between microwave and d.c. values of ρ is also very good but accurate measurement of ε_r is not possible. This is because as σ increases $\varepsilon_r << \frac{\sigma}{\omega\varepsilon_0}$ and the contribution of ε_r to the propagation constant becomes small as compared to that due to σ. From fig. 3.2 it may be observed that the

TABLE 3.1

MEASURED VALUES OF ε_r AND ρ

SAMPLE RESISTIVITY (nominal)	SAMPLE LENGTH ℓ(cms)	ATTENUATION CHANGE A_1-A_0(dB)	PHASE CHANGE $\phi_1-\phi_0$(o)	MEASURED ρ_0(d.c.) (Ω-cm)	MICROWAVE MEASUREMENTS ρ(Ω-cm)	ε_r
50	4.27	2.85	3.35	50.7	99.4	16.1
25	2.79	1.66	4.00	24.2	23.8	15.9
10	5.10	2.47	9.10	11.4	11.8	15.3
5	2.79	0.890	4.54	5.00	5.00	15.7
1	5.10	0.632	4.82	0.99	1.01	-19.0
0.25	2.79	0.176	1.29	0.258	0.244	-67.0

curves of α and β for various values of ε_r merge into each other for $\sigma \gtrsim 50$ mho/m. An extremely accurate method indeed would be required to measure ε_r at high conductivities at X-band; such a method is unknown at the present time. However, fig. 3.3 and 3.4 suggest that at higher frequencies it may be possible to measure ε_r at higher values of σ. This assumes, of course that at high frequencies apparatus of the same accuracy as at X-band is available.

At higher end of resistivity range (25-50 Ω-cm) measured values of ε_r are in good agreement with the theoretical values (fig. 3.6) but there is a large discrepancy between d.c. and microwave measurements of ρ. This can be attributed to two reasons. Firstly, the measurement accuracy is small. It is found that errors of $\pm$ 0.5% and $\pm$ 3% in the measurement of $(A_1 - A_0)$ and $(\phi_1 - \phi_0)$ respectively caused an error of $\sim\pm$14% in ρ and $\pm$0.7% in ε_r. Secondly as the resistivity goes higher the perturbations in field distribution in the system become greater and the higher order modes excited at the junctions at z = 0 and 1 may not be negligible.

CHAPTER IV

WAVE PROPAGATION IN A RECTANGULAR WAVE-GUIDE CONTAINING A CENTRALLY PLACED SEMI-CONDUCTOR

4.1 INTRODUCTION

The wave-guide system shown in the fig. 4.1 has been used by a number of workers to determine the semi-conductors properties such as σ and ϵ_r [32], magneto-resistance [33], hot electron effect [23]. It has also been proposed foruse as a microwave modulator [10].

The theory of the fields present and the propagation constants in such a system may be obtained from the solution of the equations 2.4, 2.5 and 2.17. It is shown in section 4.2 that the propagation constant is given by the simultaneous solution of the equations

$$\gamma^2 = k_1^2 - k_o^2 = k_2^2 - k_o^2\,\hat{\epsilon}_\gamma$$

$$k_2 \tan k_2 t/2 = k_1 \cot k_1 d \qquad (4.1)$$

where k_1 and k_2 are the transverse wave numbers in the regions (1) and (2) respectively

$\gamma = \alpha + j\beta$ = propagation constant

α = attenuation constant $\qquad \beta$ = phase constant

$k_o^2 = \omega^2\mu_o\epsilon_o \qquad \hat{\epsilon}_\gamma = \epsilon_r - j\,\frac{\sigma}{\omega\epsilon_o}$ = complex permittivity

The solution of these equations for the case when the displacement current is negligible ($\omega\epsilon << \sigma$) with t/a of the order of 10^{-6} and

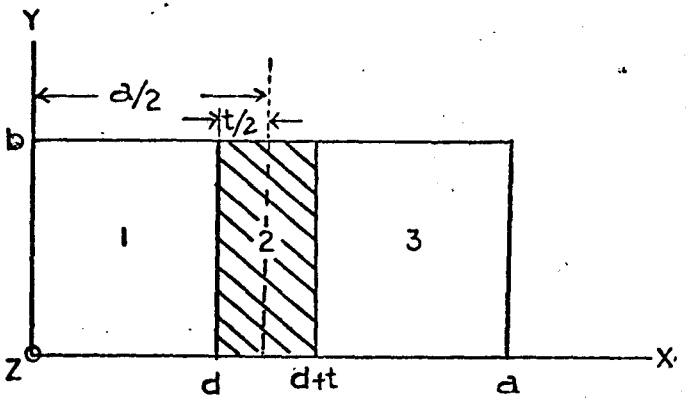

(a) Infinite Structure

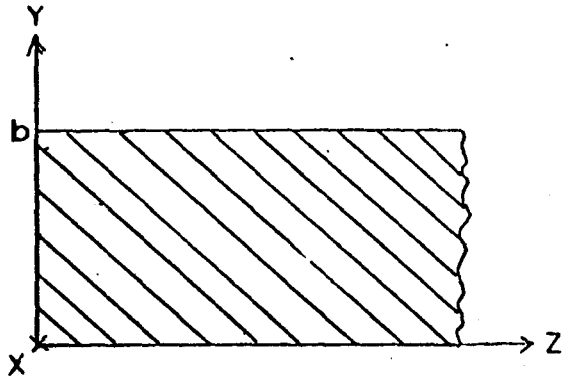

(b) Junction of Empty and Partially Filled Wave-Guides

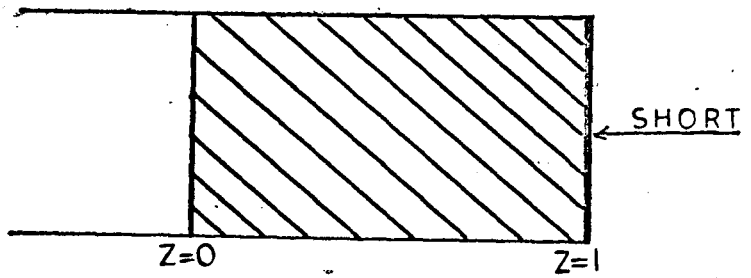

Figure 4.1 Partially Filled Rectangular Wave-Guide with Semi-Conductor Specimen in the Region (2). The regions (1) and (3) are empty.

for the lossless case ($\sigma = 0$) have been reported in literature[33,34]. The solution in both of these cases is comparatively easily obtained. However, for the case when the value of σ lies in the semiconducting range and the displacement and conduction currents are comparable, the computations of the propagation constant from equations 4.1 become very laborious. Because of this, in almost all of the measurements referred to above, recourse has been made to some sort of approximation. In particular, Nag et al[32] and Lilja and Stubb[35] used the following expression for γ:

$$\gamma^2 = (\pi/a)^2 - k_o^2 - k_o^2 (\hat{\epsilon}_\gamma - 1)(t/a + \frac{1}{\pi} \sin \frac{\pi t}{a}) \qquad (4.2)$$

where $k_o^2 = \omega^2 \mu_o \epsilon_o$

This equation can be obtained either by variational theory using the Rayleigh-Ritz technique with single mode approximation[36,37] or by the first order perturbation theory[35,38,39]. For $\sigma = 0$ it was first obtained by Berk[36] and was found to give the propagation constant with an accuracy of a few percent for $\epsilon_r = 2.45$. For complex permittivity values applicable to semiconductors, however, doubts have been expressed about the validity of (4.2) unless t/a is negligibly small[40,41].

The computations of the propagation constant in the configuration shown in Figure (4.1) are discussed in this chapter. Numerical solutions of equation 4.1 are given for dielectric constant, conductivity and t/a ranges of $12 \leq \epsilon_r \leq 16$, $0.1 \leq \sigma \leq 10$ mhos/m and $.001 \leq t/a \leq 0.25$ respectively, for the three frequencies 10.0, 34.5 and 70.5 GHz. These results are compared with the approximate values obtained from equation

(4.2) and also with those obtained using the two mode approximation in the Rayleigh-Ritz technique.

Further for practical measurements, the structure shown in the fig. 1.3 forms a junction with an empty guide supporting H_{10} mode. In all earlier measurements, the effect of the higher order modes at the junction has been assumed to be negligible. However, it is shown that this assumption may not be valid in view of the high values of dielectric constant and conductivity applicable to semiconductors. An analysis of these higher order modes has been carried out and the computations show that unless $t/a < .08$ and $\sigma \tilde{<} 2.5$ mho/m, the effect of the higher order modes is not negligible.

Experiments have been performed for three values of t/a at 9.25 GHz and the results of the measurements verify the above observations.

4.2 THEORETICAL CONSIDERATIONS

4.2.1 Exact Solution

The solutions to the Maxwell's equations in the system shown in the fig. 1.3 may be divided into two basic sets, TE to x and TM to x. The dominant mode in the system for lossless case ($\sigma = 0$) is given by TE to x mode. For the lossy case it will be the same and only this mode will, therefore, be considered.

The solution for the TE to x modes may be obtained from equations 2.4, 2.5 and 2.17 by taking a single component of $\vec{\pi}_h$. Thus if

$$\vec{\pi}_h = \vec{a}_x \psi\,(x,y)\, e^{-\gamma z} \qquad (4.3)$$

so that $$\nabla t^2 \psi + (k_o^2\, \hat{\varepsilon}_r(x) + \gamma^2)\psi = 0 \qquad (4.4)$$

where $\hat{\varepsilon}_r(x) = \varepsilon_r - j\frac{\sigma}{\omega\varepsilon_0}$ $(d \leq x \leq d+t)$

$= 1$ $(0 \leq x \leq d;\ d+t \leq x \leq d)$

then in order to satisfy the boundary conditions 2.1 at $x = 0, a$; $y = 0$, b and $x = d, d + t$ must be of the form

$$\psi = A \cos\frac{m\pi y}{b} \begin{cases} \sin k_1 x & 0 \leq x \leq d \\ \frac{\sin k_1 d}{\sin k_2 t}\left[\sin k_2(x-d) - \sin k_2 (x-t-d)\right] & d < x < d + t \\ \sin k_1(a-x) & d + t \leq x \leq a \end{cases} \quad (4.5)$$

where A = constant

$m = 0, 1, 2, 3, \ldots$

k_1 and k_2 are wave vectors in x-direction in regions (1), (3) and (2) respectively and satisfy the following equations

$$\gamma^2 = k_1^2 + (m\pi/b)^2 - k_o^2 = k_2^2 + (m\pi/b)^2 - k_o^2\,\hat{\varepsilon}_r \quad (4.6)$$

γ is the same in the three regions so that the boundary conditions are satisfied for all z.

A further condition on k_1 and k_2 may be obtained from the transverse resonance condition. Thus for symmetrical modes it is required that there be an open circuit at $x = a/2$. This condition gives the following relation

$$k_1 \cot k_1 d = k_2 \tan k_2 t/2 \quad (4.7)$$

The equation 4.7 gives infinite possible values of k_1 and k_2 and hence there are doubly infinite possible values of γ. If, however, $m = 0$, these reduce to singly infinite values. When $m = 0$, the TE to x modes reduce to TE_{n0} modes. The dominant mode propagation constant is given by the lowest order solution of 4.7 and is designated with $n = 1$. Thus for TE_{n0} modes,

$$\gamma_n^2 = k_{1n}^2 - k_o^2$$

$$= k_{2n}^2 - k_o^2 \hat{\varepsilon}_r \qquad (4.8)$$

and $k_{1n} \cot k_{1n} d = k_{2n} \tan k_{2n} t/2$.

For given values of ω, t/a and $\hat{\varepsilon}$, the values of the propagation constants may be obtained by solving 4.8 numerically. In the present work, this was done by using the Newton-Raphson iteration technique[42], in which the (M+1) th iteration of the unknown root of a transcendental equation $f(x) = 0$ is given by:

$$x_{m+1} = x_m - \frac{f(x_m)}{f'(x_m)}$$

The convergence of the method is good provided $f' = \frac{df}{dx}$ is not too small and the initial guess of the root x_o is not too far off. Equation 4.8 was accordingly put into the form:

$$f(k_1) = k_1 \cot k_1 d - k_2 \tan \frac{k_2 t}{2} = 0$$

with $k_2^2 = k_1^2 + k_o^2 (\hat{\varepsilon}_r - 1)$

and the value of k_1 determined accurately, which then enabled k_2 and γ to be calculated. The functions involved are periodic in nature and hence an infinite number of roots of the equation exist. The particular root obtained depends on the initial guess. In the present case, the initial value of the root was obtained from an approximate method, for example, the two mode approximation in the Rayleigh-Ritz technique discussed in the next section.

4.2.2 Approximate Solution

There are two approximate methods of solution that are commonly used, namely, variational and perturbational methods. The former method has been used for determining γ in a wave-guide system containing pure dielectrics and ferrites[36] and is known to give good results. Perturbational techniques have also been developed for such calculations[38,39]. It is found that the first order perturbational technique gives the same formula for γ as obtained from the variational method using a single mode approximation[35]. For higher accuracy either a two or higher mode approximation or a second or higher order perturbation theory may be employed. It should be pointed out, however, that unless t/a is negligibly small, the high value of complex permittivity of semiconductors alters a system so much that the perturbations are too large to be consistent with the accuracy requirement of the perturbation theory. In view of this, the use of two mode approximations with the Rayleigh-Ritz technique was preferred for these calculations.

The application of the Rayleigh-Ritz theory to inhomogeneously filled wave-guides has been discussed by Collin[29], and the salient steps

in the present analysis are as follows:

The one dimensional Helmholtz equation

$$\frac{d^2\phi}{dx^2} + \left[\gamma^2 + k_o^2\, \hat{\varepsilon}_r(x)\right]\phi = 0$$

$$\text{where } \hat{\varepsilon}_r(x) = 1 \quad 0 < x \leq d;\ d + t \leq x \leq a \qquad (4.9)$$

$$= \hat{\varepsilon}_r \quad d \leq x \leq d + t$$

can be obtained from equation 4.4 by taking m = 0 so that $\psi(x,y) = \phi(x)$ The function ϕ is to satisfy the condition that $\phi = 0$ at $x = 0$ and $x = a$, to make the tangential component of the electric field E_y vanish at the wave-guide walls.

The variational integral is obtained by multiplying 4.9 by ϕ and integrating with respect to x from $x = 0$ to $x = a$. The resulting expression is:

$$\gamma^2 \int_o^a \phi^2\, dx = \int_o^a \left[\left[\frac{d\phi}{dx}\right]^2 - k_o^2\, \hat{\varepsilon}_r(x)\phi^2 \right] dx \qquad (4.10)$$

The next step consists of expanding ϕ as a Fourier series and terminating the series at a finite number of terms. Thus one may obtain for the nth eigen-function:

$$\phi_n \simeq \sum_{r=1,3}^{N} a_{rn}\, f_r(x) \qquad (4.11)$$

where $f_r(x) = \sqrt{\frac{2}{a}} \sin \frac{r\pi x}{a}$ (eigen-functions for the empty guide). The symmetry of the system permits only odd values of r. The function ϕ_n may be normalized to give:

$$\int_o^a \phi_n^2\, dx = 1 = \sum_{r=1,3}^{N} a_{rn}^2$$

and substitution of equation 4.11 into 4.10 gives:

$$\gamma_n^2 \sum_{r=1}^{N} \sum_{s=1}^{N} a_{rn}\, a_{sn}\, \delta_{rs}$$

$$= \sum_{r=1,3}^{N} \sum_{s=1,3}^{N} a_{rn} a_{sn} \left[\int_0^a \left[\frac{df_r}{dx} \frac{df_s}{dx} - k_o^2\, \hat{\epsilon}(x)\, f_r f_s \right] dx \right]$$

where $\delta_{rs} = \begin{cases} 0 & r \neq s \\ 1 & r = s \end{cases}$ is the Kronecker delta function

Now it is required that:

$$\sum_{r=1}^{N} \sum_{s=1}^{N} a_{rn}\, a_{sn}\, (T_{rs} - \gamma_n^2\, \delta_{rs}) = \text{a stationary quantity}$$

where $T_{rs} = \int_0^a \left[\frac{df_r}{dx} \frac{df_s}{dx} - k_o^2\, \hat{\epsilon}(x)\, f_r f_s \right] dx = T_{sr}$ (4.11a)

For this equation to represent a stationary value of γ^2, the partial derivatives $\frac{\partial}{\partial a_{in}}$ for i = 1 to N must vanish. When this is done the following set of N homogeneous equations is obtained.

$$\sum_{r=1}^{N} a_{rn} (T_{rs} - \gamma_n^2\, \delta_{rs}) = 0 \quad s = 1 \text{ to } N \qquad (4.12)$$

Recalling that the modes being considered are symmetrical about the point x = a/2, the indices r and s should take only odd values, that is

$$r = 1, 3, 5, \ldots\ldots, N \text{ (odd)}$$

$$s = 1, 3, 5, \ldots\ldots, N \text{ (odd)}$$

For a non-trivial solution of (12), the determinant of the coefficients must vanish. Therefore, for the single mode approximation (N=1) one has:

$$\gamma_1^2 = T_{11} \qquad (4.13)$$

For the two mode approximation, N = 3, and γ_1^2 is given by the solution of:

$$(\gamma_1^2 - T_{11})(\gamma_1^2 - T_{33}) - T_{31}\, T_{13} = 0 \qquad (4.14)$$

Integration of equation (4.11a) over the wave-guide cross-section shown in the Figure (4.1) gives

$$T_{rr} = (r\pi/a)^2 - k_o^2 - k_o^2\,(\hat{\varepsilon}_\gamma - 1)\,(t/a + 1/r\pi \sin r\pi\, t/a) \qquad (4.15)$$

$$T_{rs} = T_{sr} = k_o^2\,(\hat{\varepsilon}_\gamma - 1)\left[(-1)^p \frac{\sin p\pi t/a}{p\pi} + (-1)^q \frac{\sin q\pi t/a}{q\pi}\right] \quad r \neq s$$

where $p = \dfrac{r+s}{2}$, $q = \dfrac{r-s}{2}$

In the present study, the dominant mode propagation constant was computed from both equations (4.13) and (4.14) and the results compared with those obtained from (4.8).

4.2.3 DISCUSSION ON EXACT AND APPROXIMATE SOLUTION

The dominant mode propagation constant $\gamma = \alpha + j\beta$ was computed from equations 4.8 as a function of t/a and σ at three different frequencies of 10.0, 34.5 and 70.5 GHz for ε_r = 12 and 16. The variations of t/a and σ were over the ranges $0.001 \lesssim t/a \lesssim 0.25$ and $0.1 \lesssim \sigma \lesssim 10$ mho/m, respectively and the results of the calculations are presented in the form of curves shown in Figures 4.2 through 4.4.

It may be observed from these figures that the phase constant β varies very slowly with conductivity σ for small values of t/a and σ. In fact the variations in the phase constant β are practically negligible for t/a < 0.1 and log σ = 0.50 (σ = 3.16 mhos/m) at 10 GHz. This also

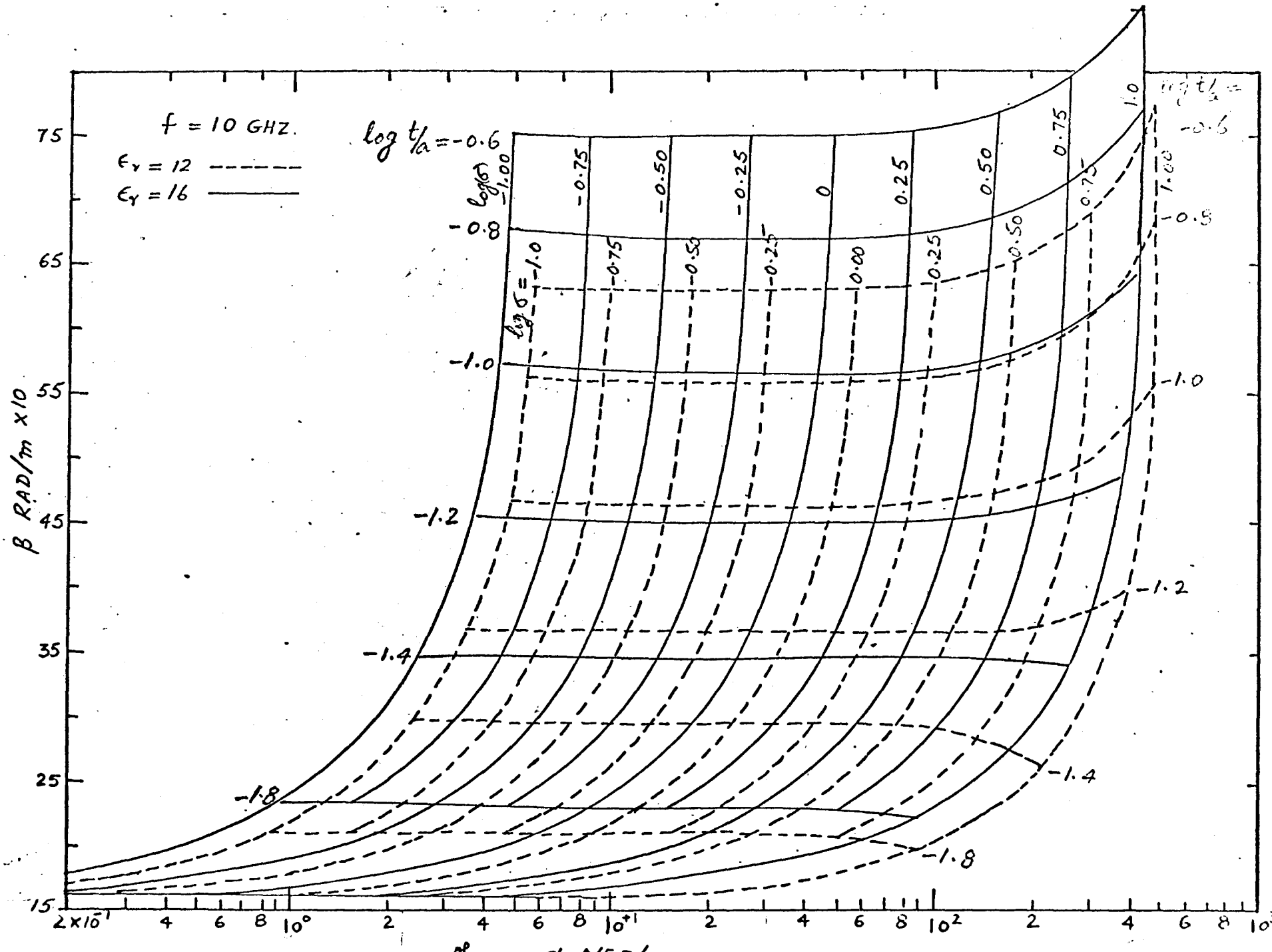

Figure 4.2 (a) The exact values of dominant mode Propagation constant $\gamma = \alpha + j\beta$ at 10 GHz

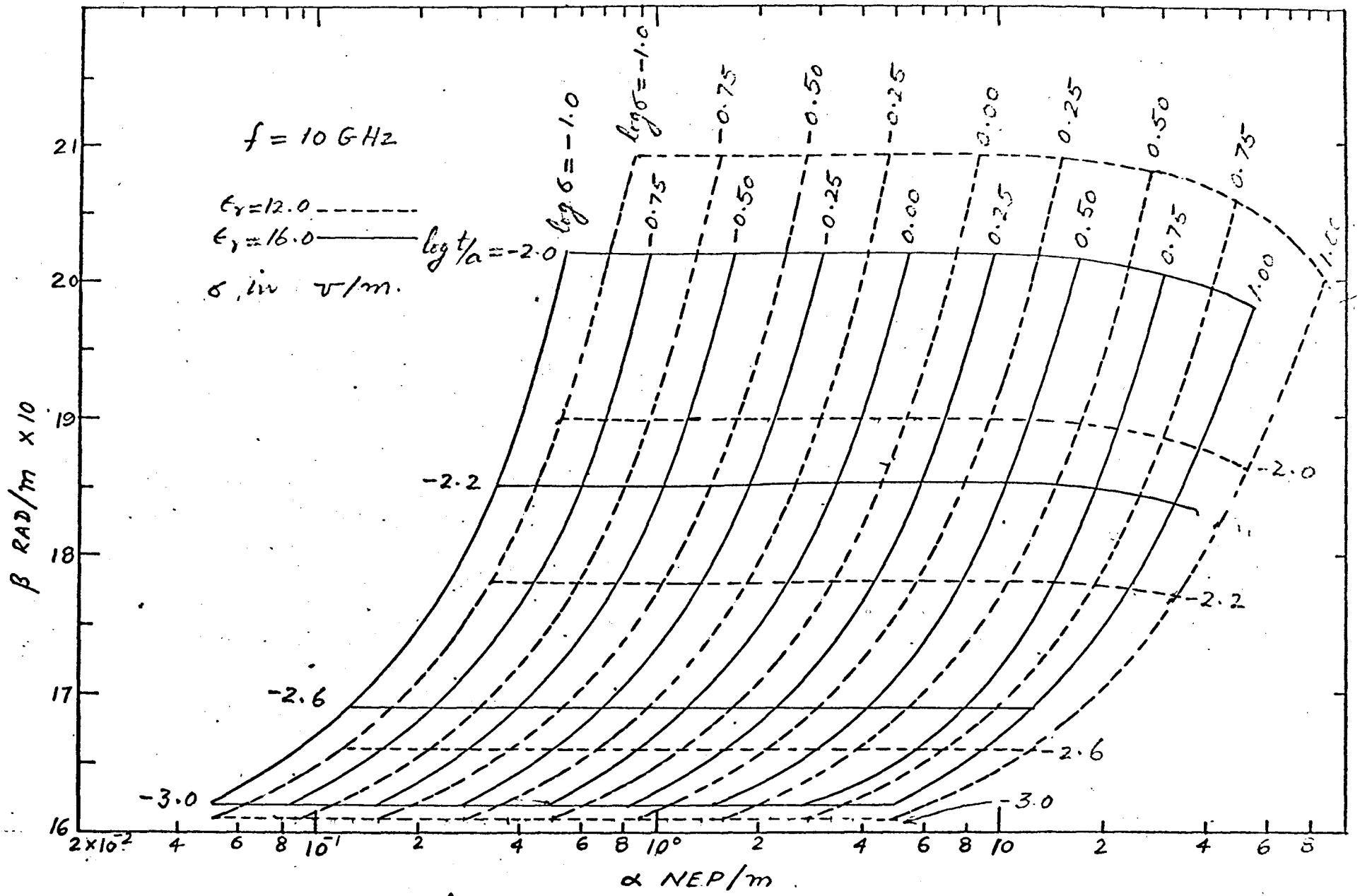

Figure 4.2 (b) The exact values dominant mode propagation constant $\gamma = \alpha + j\beta$ at 10 GHz

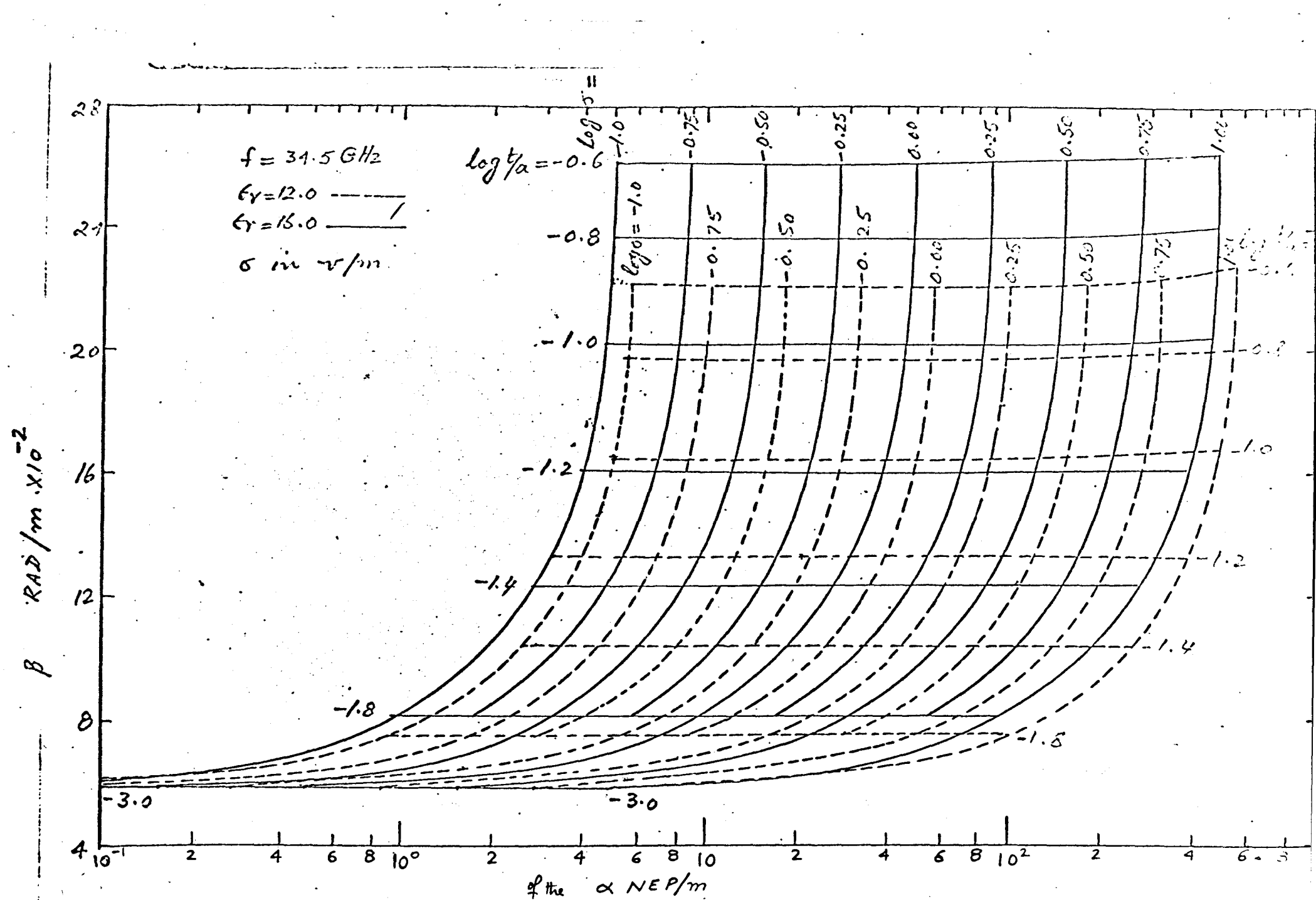

Figure 4.3 (a) The exact values of the dominant mode propagation constant $\gamma = \alpha + j\beta$ at 34.5 GHz

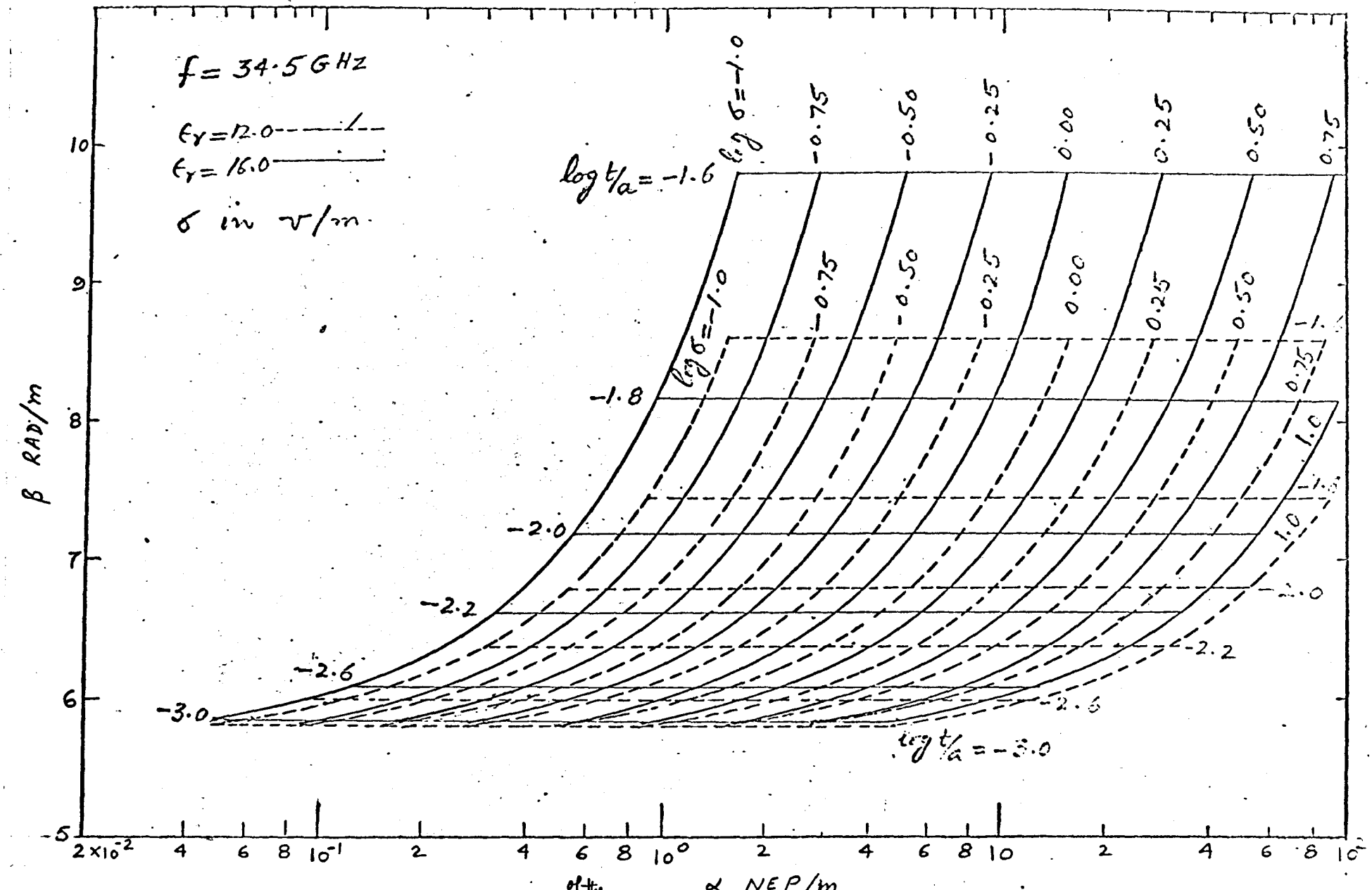

Figure 4.3 (b) The exact values of the dominant mode propagation constant $\gamma = \alpha + j\beta$ at 34.5 GHz

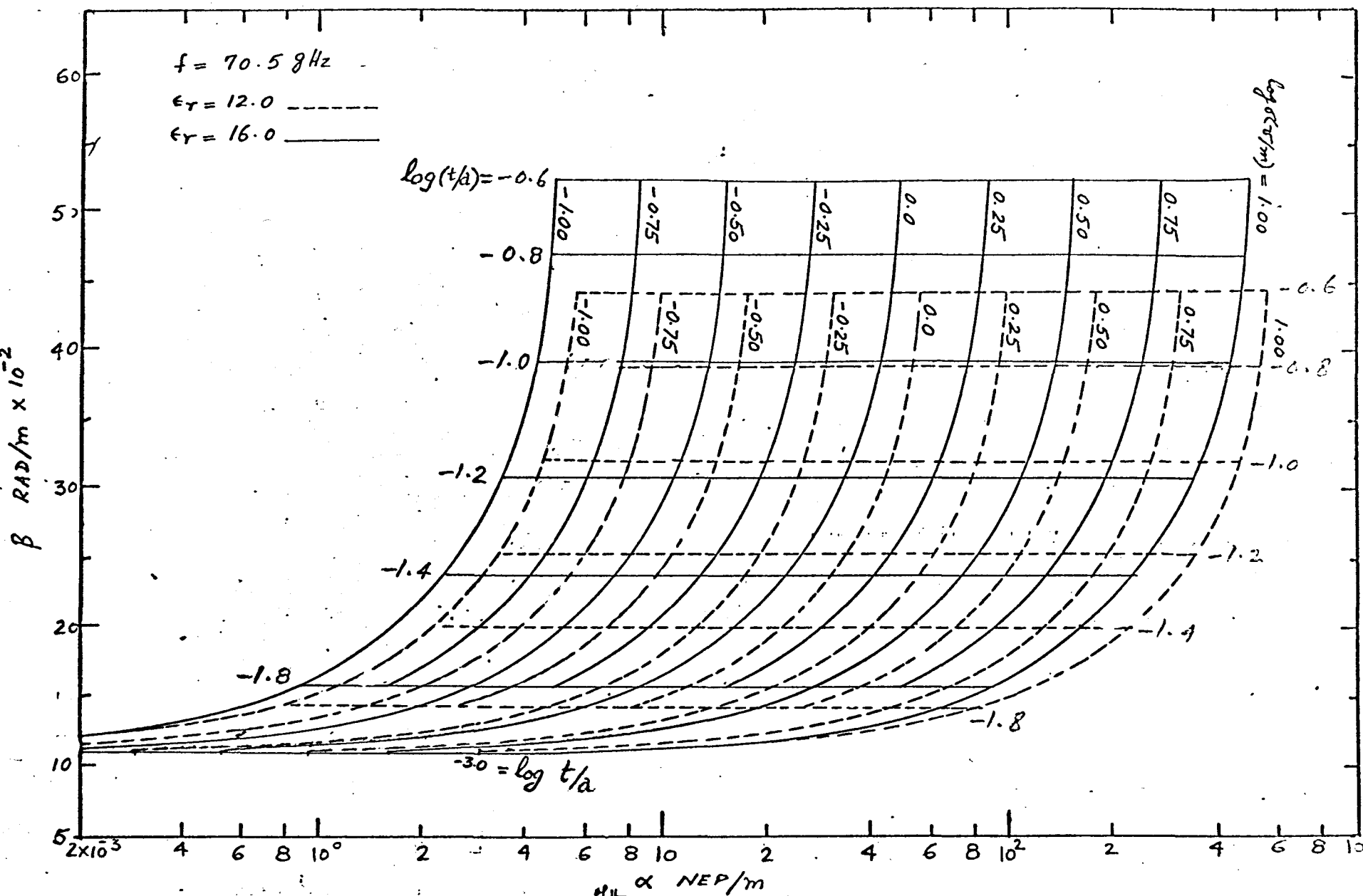

Figure 4.4 (a) The exact values dominant mode propagation constant $\gamma = \alpha + j\beta$ at 70.5 GHz

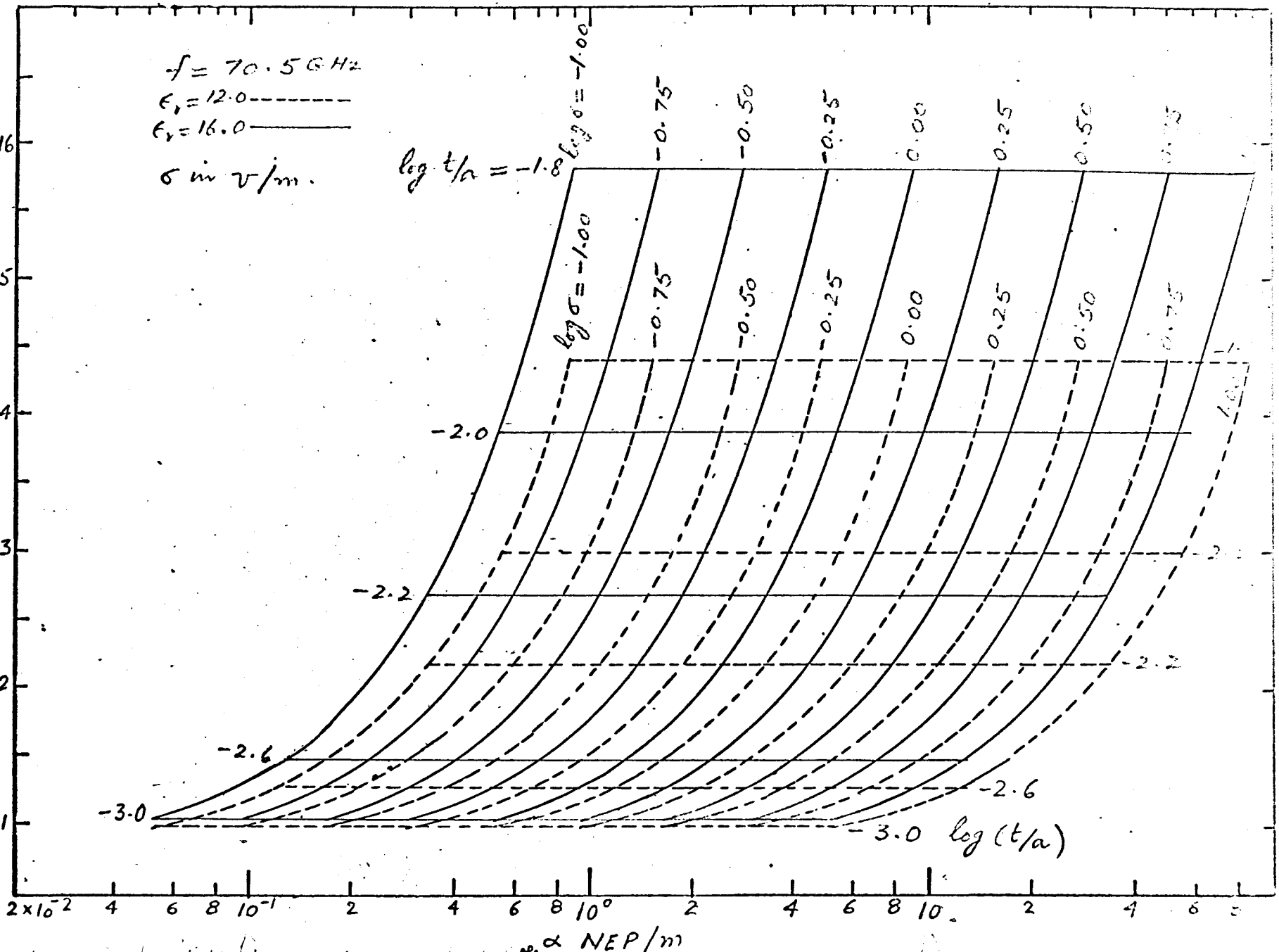

Figure 4.4 (b) The exact values of dominant mode propagation constant $\gamma = \alpha + j\beta$ at 70.5 GHz

applies for all the values of t/a and σ considered at the higher frequencies 34.5, 70 GHz. At 10 GHz, the variations in β with σ for $\log \sigma \gtrsim 0.5$ and $\log$ t/a $\gtrsim$ - 1.8 (t/a $\simeq$ .0158) become significant as can be seen from Figure (4.2a).

It may be observed from Figures (4.3) and (4.4) that for the ranges of σ and t/a chosen, the relationship between $\log \alpha$ and $\log \sigma$ is a linear one. In these ranges, one may write:

$$\log \alpha = \log M + n \log \sigma \qquad (4.16)$$

where n is the slope of the curves and M is the intercept with $\log \sigma = 0$. This relationship is more clearly shown in Figures (4.5a) and (4.5b), and examination of the curves shows that n = 1.00 which means that the attenuation constant α varies linearly with σ, i.e.

$$\alpha = M\sigma \qquad (4.17)$$

At 10 GHz (see Figure 4.2a) the relationship (4.17) also holds for t/a $\lesssim$ 0.05 and $0.1 \lesssim \sigma \lesssim 10$ mhos/m. For higher values of t/a, the value of n departs from unity. At t/a = 0.05 its value is 1.01 and increases as t/a is increased. At this frequency, equation (4.17) holds over the whole range of t/a considered but only up to $\sigma \simeq$ 1.0 mhos/m. For higher values of t/a, the slope of the $\log \alpha \sim \log$ t/a curve changes and equation (4.17) no longer holds. For values of t/a $\simeq$ 0.25 the slope is very small and practically equals that for t/a = 1. That is, the attenuation is very close to that of a completely filled guide.

It is interesting to note that a similar relationship between α and σ holds for very thin films of considerably higher conductivity than has been considered in the present work. Gunn[44] has carried out

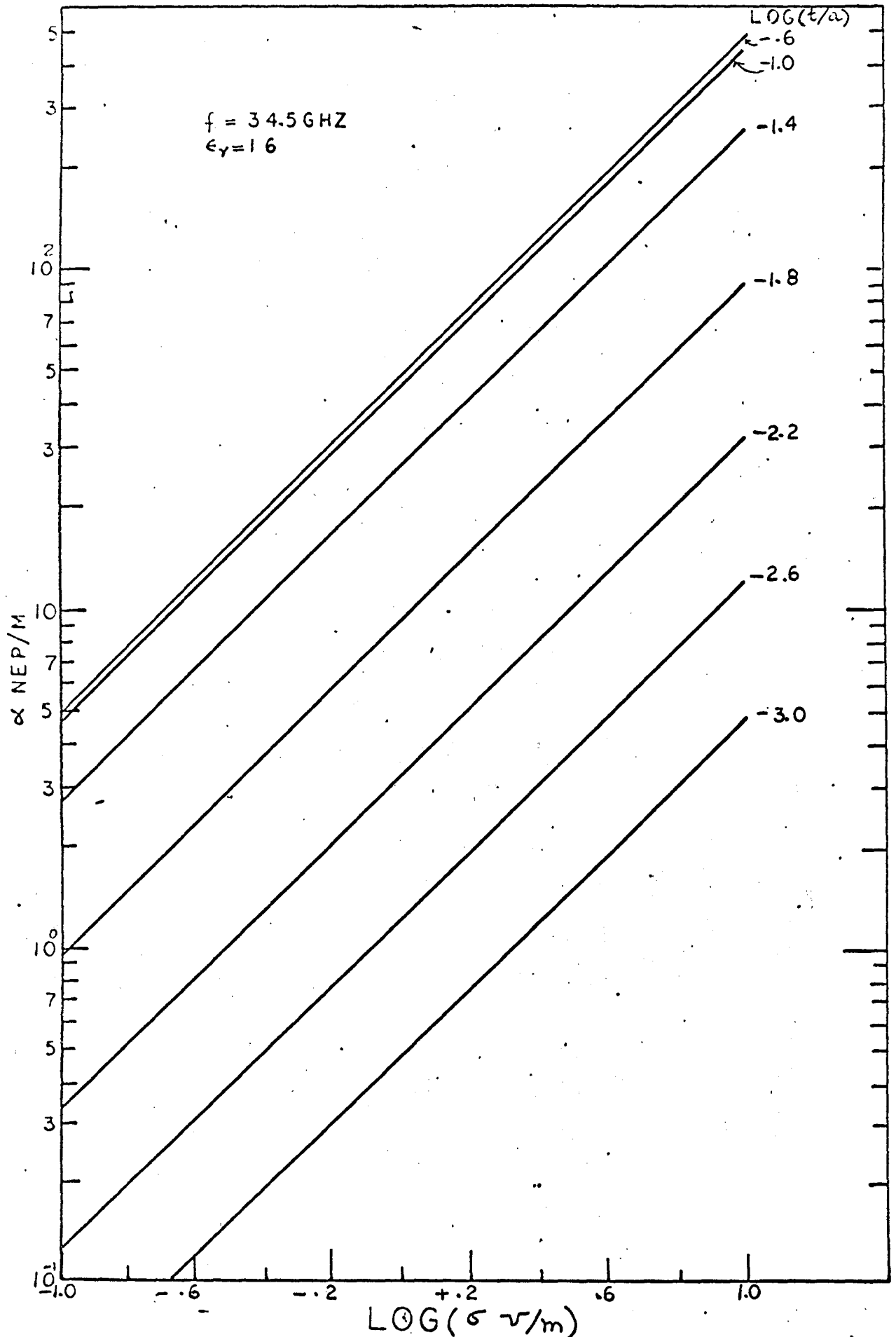

Figure 4.5 (a) The attenuation constant α as a function of t/a and σ

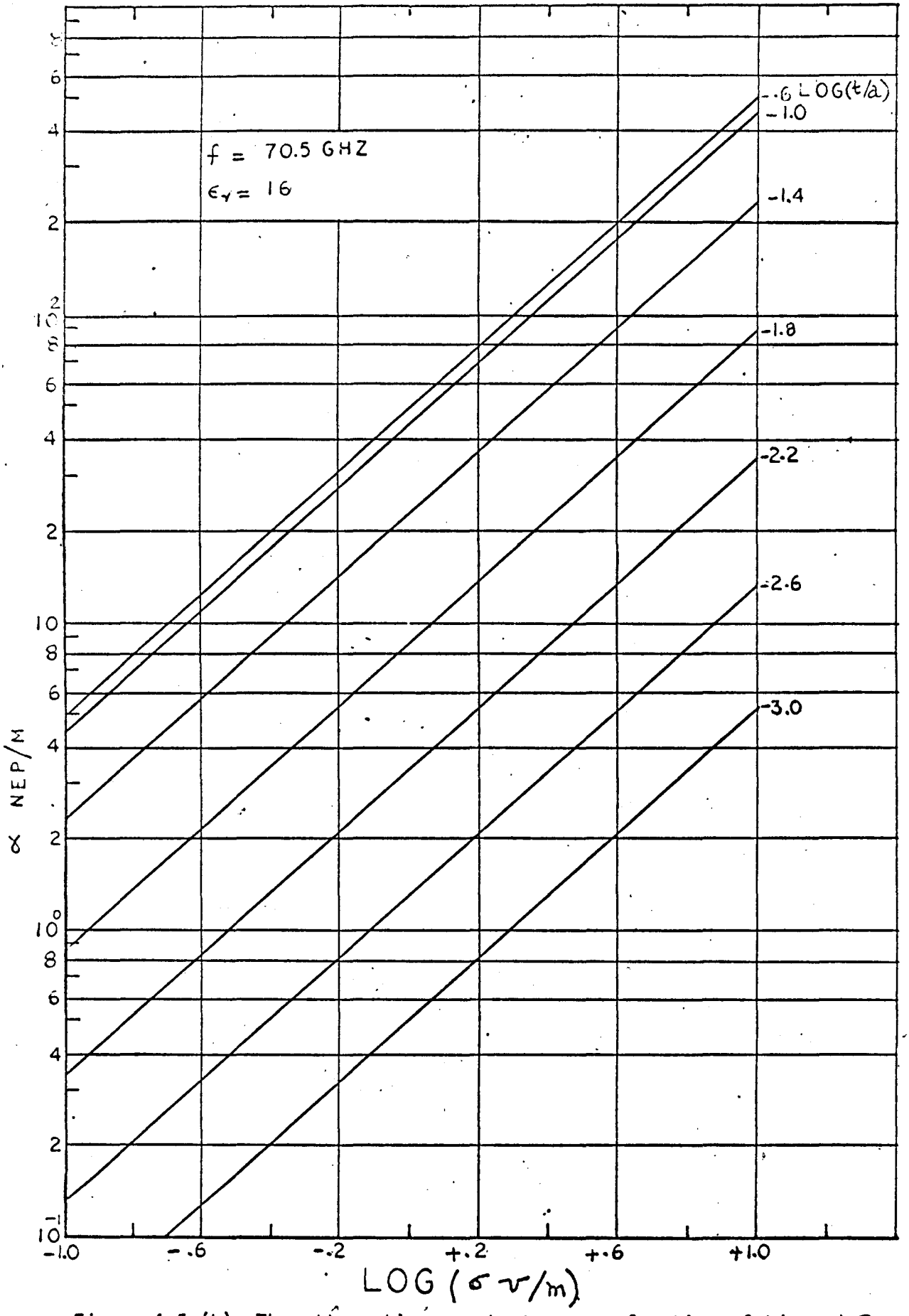

Figure 4.5 (b) The attenuation constant α as a function of t/a and σ

computations for thin films of semi-conducting materials, and found that theoretically and experimentally the relation (4.17) holds for $R = 1/\sigma t \gtrsim 400\Omega$/square. However in the present work it is found that equation (4.17) is

$$(\sigma \lesssim 1.0 \text{ v/m}, \; t/a \lesssim 0.25)$$

valid for $R \gtrsim 175\Omega$/square at 9.25 GHz and to at least 55Ω/square and 130Ω/square at 34.5 and 70 GHz respectively ($\sigma \lesssim 10$ v/m, $t/a \lesssim 0.25$).

To the extent that the phase constant β is nearly independent of σ, the propagation constant as a function of conductivity σ may be written as:

$$\gamma(\sigma) = \gamma(0) + \sigma \frac{\partial \gamma}{\partial \sigma} \Big|_{\sigma = 0} \qquad (4.18)$$

where $\frac{\partial \gamma}{\partial \sigma} = M$ is evaluated from equations (1) and (2) with $\sigma = 0$, and is:

$$M = \frac{1}{\gamma_0} \frac{j\omega\mu_{o/2}}{1 + \frac{k_{20}}{k_{10}} \left[\frac{k_{10} d \operatorname{cosec}^2(k_{10}d) - \cot(k_{10}d)}{\frac{k_{20}t}{2} \sec^2(k_{20}t/2) - \tan(k_{20}t/2)} \right]}$$

where the subscript 0 denotes that quantities are evaluated with $\sigma = 0$.

Equation (4.18) for $\gamma(\sigma)$ reduces much of the computation work as the numerical solution of (1) and (2) with $\sigma = 0$ is much easier and as a matter of fact may be done with a desk calculator. The calculation of M is then straightforward. This linear relationship between α and σ may prove useful in the measurement of magneto-conductivity, high field carrier mobility, the temperature dependence of conductivity, etc., of the semi-conductor bulk material.

The propagation constant was computed for two values only of dielectric constant (ϵ_r), namely 12, and 16. It may be observed from Figures 4.2 to 4.3 that the variations in α and β with ϵ_r are significant

only at the higher end of ranges of t/a and σ considered. For lower values of σ and t/a, the changes in ε_r do not cause appreciable changes in either α or β.

Figures 4.6 and 4.7 show the percentage differences between the exact values of the dominant mode propagation constant as obtained from equation 4.8 and those obtained from the single mode and two mode approximations given by equations 4.13 and 4.14 respectively. The errors shown are for σ = 10 mhos/m and f = 10.0 and 70.5 GHz. For lower values of σ in the range $0.1 \lesssim \sigma \lesssim 10$ mhos/m, the errors are not very different from the ones shown, for example in the range $0.03 \lesssim$ t/a $\lesssim 0.1$, this difference is not more than 3%. The errors in γ at 34.5 GHz are not shown here as these are found to be of the same nature and order as those at 70.5 GHz.

It may be observed from Figure 4.6 that the single mode approximation gives errors in α that are greater than 5% when t/a is as small as 0.0025. For t/a > 0.0025, the errors increase rapidly and then decrease at t/a $\approx$ 0.06 but are not less than 33% at t/a = 0.25. The two mode approximation gives better results, but the errors in α are significant unless t/a < 0.003 when these are about 5%. The error in α is reduced with a decrease in the dielectric constant.

Figure 4.7 shows that the approximate methods, both single mode and two mode, appear to give better results for β than for α. It may be seen that the errors are less than 5% for t/a < 0.015. For higher values of t/a, the errors become large but the maximum error in β is about one half of that in α. As t/a is increased beyond 0.1, the

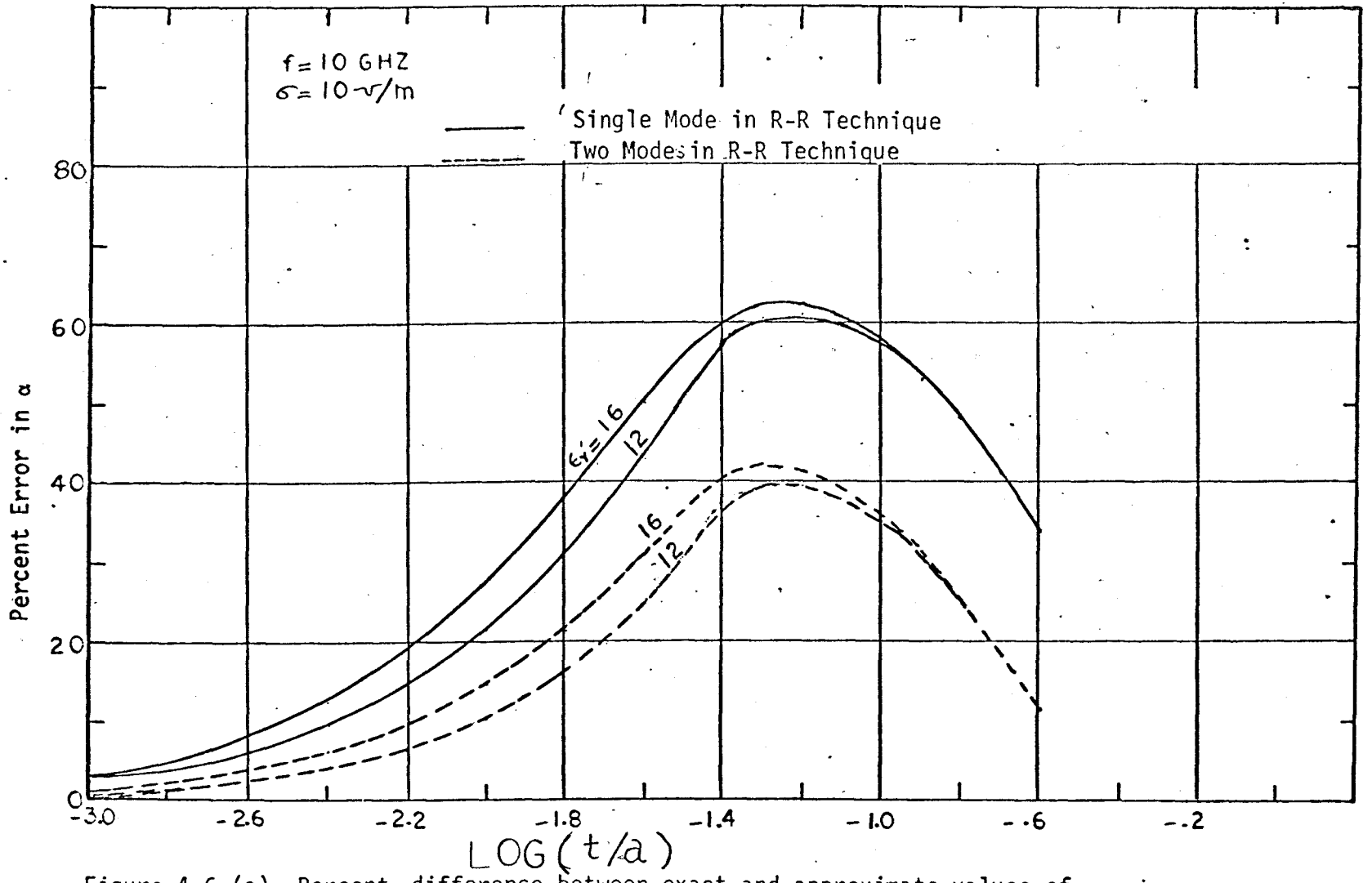

Figure 4.6 (a) Percent difference between exact and approximate values of α

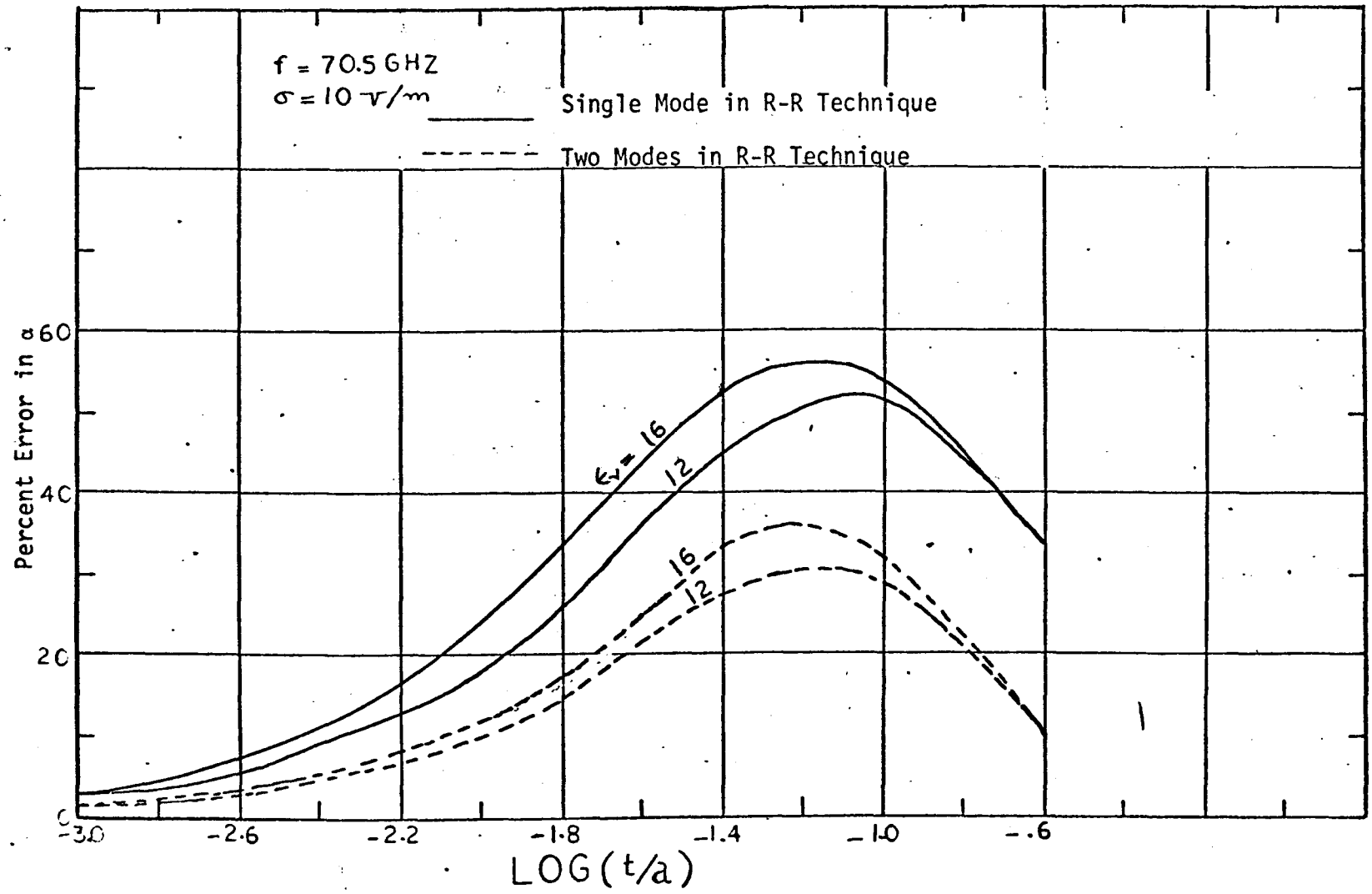

Figure 4.6 (b) Percent difference between exact and approximate values of α

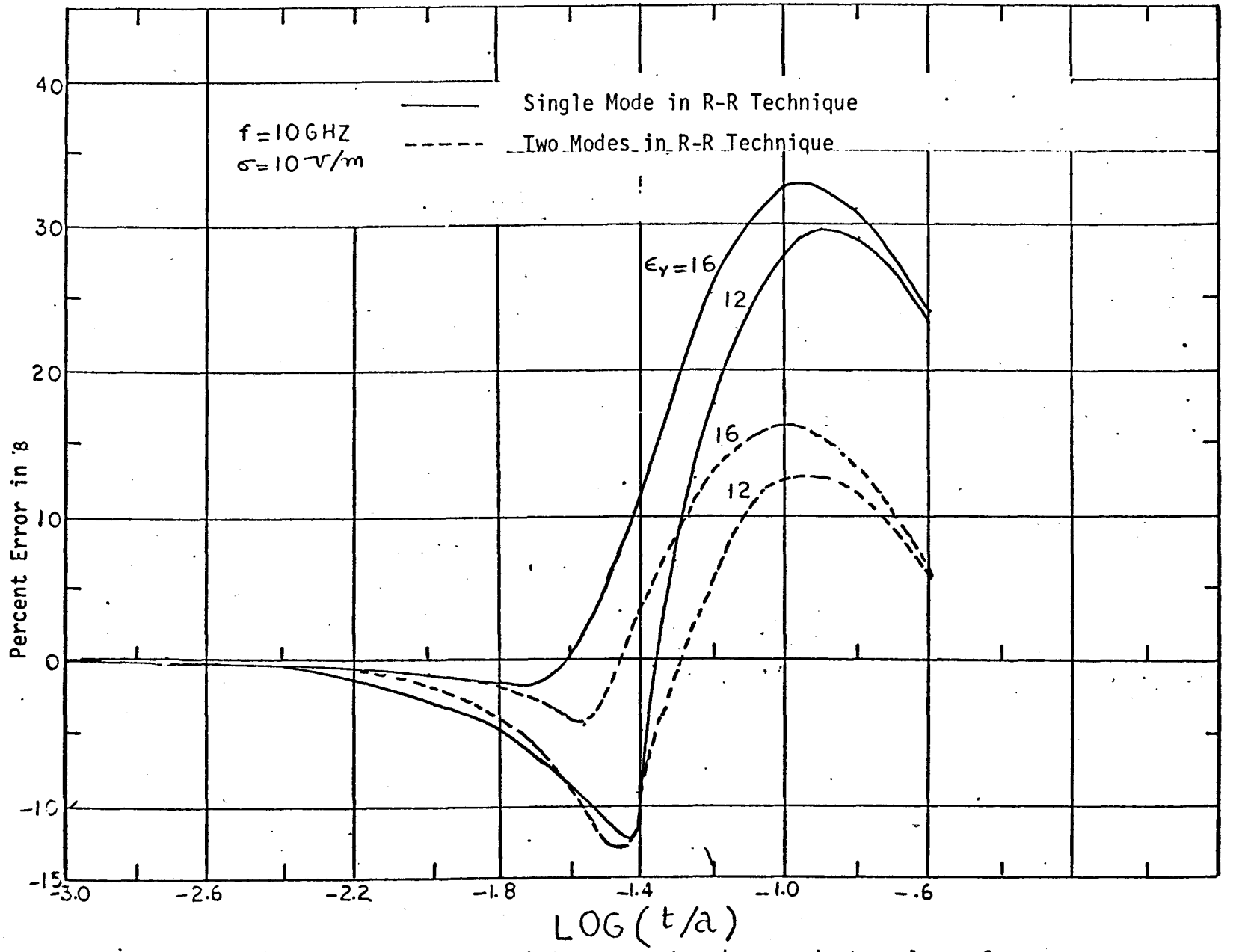

Figure 4.7 (a) Percent difference between exact and approximate values of β

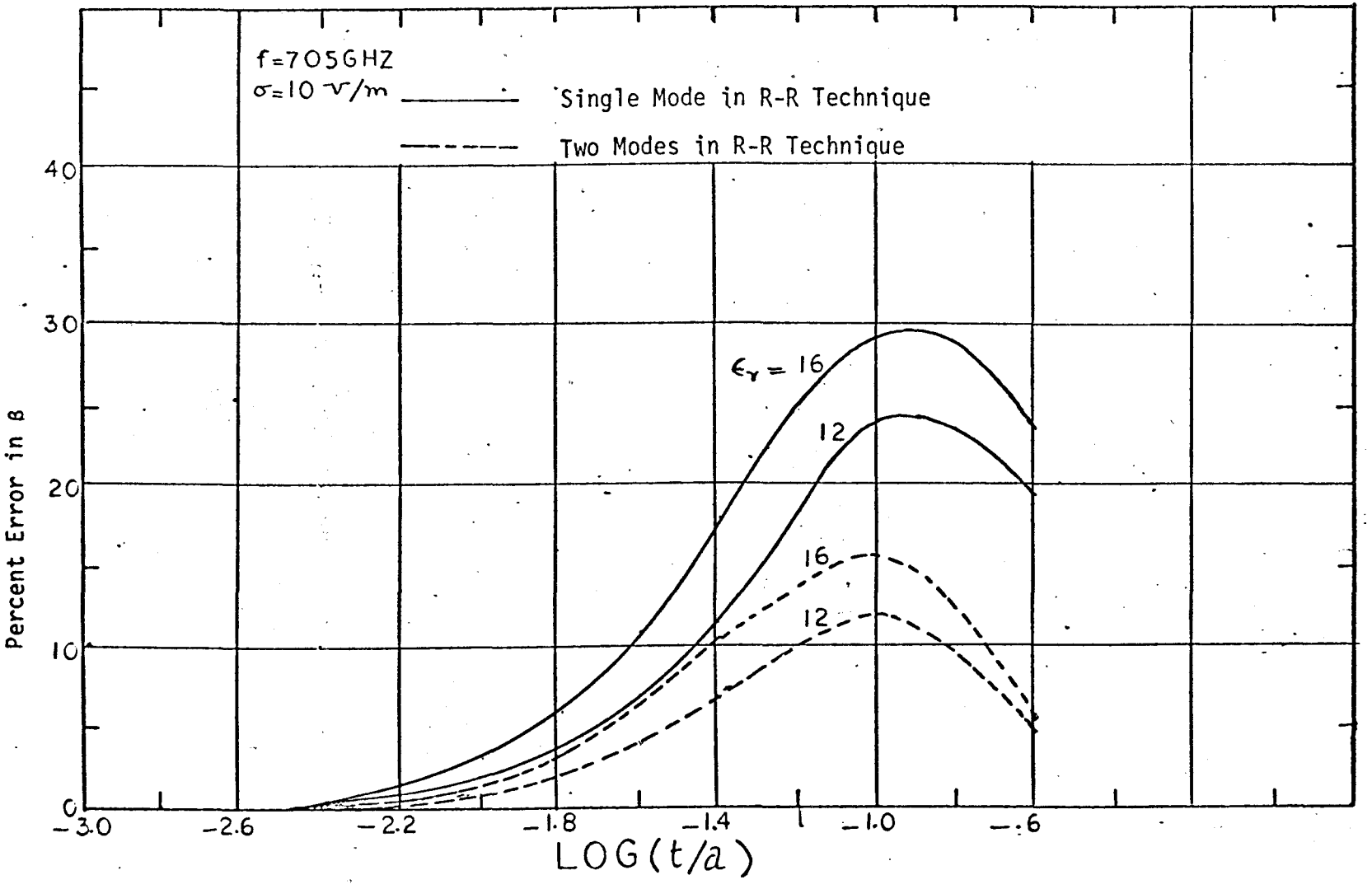

Figure 4.7 (b) Percent difference between exact and approximate values of β

errors reduce. This is because as t/a is increased, the condition approaches that of a completely filled guide in which case the errors should vanish.

4.2.4 Calculation of Junction Impedance

In this section the expression for the input impedance Zin at z = 0 of the system shown in the fig. 4.1 which has a short circuit at z = 1 will be derived.

In the analysis, it will be assumed that the input guide is supporting an H_{10} mode while in the output guide ($0 \leq z \leq 1$) H_{no} modes are present. If ϕ_n and ψ_n are the functions representing the H_{no} th mode in the input and output guides respectively and Γ_n and γ_n are their respective propagation constants, then the electric field Ey and the magnetic field Hx are given by the following expressions[43].

For $z \leq 0$

$$Ey = a_1(e^{-\Gamma_1 z} + R\, e^{\Gamma_1 z})\, \phi_1 + \sum_{n=3,5} a_n\, \phi_n e^{\Gamma_n z}$$

$$Hx = -a_1 y_{o1}(e^{-\Gamma_1 z} - R\, e^{\Gamma_1 z}) + \sum a_n\, \phi_n\, y_{on}\, e^{\Gamma_n z}$$

For $0 \leq z \leq 1$

$$Ey = \sum_{m=1,3,} b_m\, \psi_m \sinh \gamma_m (1-z)$$

$$Hx = \sum - b_m\, \gamma_m\, \psi_m \cosh \gamma_m (1-z)$$

where a's and b's are constants

R = reflection coefficient of the dominant mode in the input guide

$Y_{on} = \frac{1}{Z_{on}} = \frac{n}{j\omega\mu_o}$ = wave admittance for H_{no} modes in the empty guide

$Y_n = \frac{1}{Z_n} = \frac{n}{j\omega\mu_o}$ = wave admittance for H_{no} modes in the output guide

Now at z = 0 Ey and Hx must be continuous and these boundary conditions give

$$Ey = a_1(1+R)\phi_1 + \sum_{n=3,5} a_n\phi_n = \sum_{m=1,3} b_m \sinh(\gamma_m l)\psi_m$$

$$Hx = -a_1(1-R)Y_{o1}\phi_1 + \sum_{n=3,5} a_n Y_{on}\phi_n = - \sum_{m-1,3} b_m\psi_m Y_m \cosh(\gamma_m l)$$

These two equations can be solved either simultaneously or by the use of variational techniques. The latter method is easier and has been discussed by Collin[43]. Following his arguments, one obtains the expression for the input impedance $Z_{in} = (1+R)/(1-R)$ as follows:

$$Z_{in} = \frac{1}{Z_{o1}} \iint_o^a G(x;x')H_x(x)\, H_x(x')dxdx' / \left[\int_o^a H_x(x)\phi_1 dx\right]^2$$

where $G(x;x') = \sum_{n=3,5} Z_{on}\phi_n(x)\phi_n(x')$

$$+ \sum_{m=1,3,5} Z_m\psi_m(x)\, \psi_m(x')\tanh\gamma_m l$$

Now assuming that

$$Hx(x) = \sum_{n=1,3,5}^{N} a_n \phi_n(x)$$

and substituting this into 4.12, one gets

$$Z_{in} Z_{o1} a_1^2 - \sum_{r}^{N} \sum_{s}^{N} a_r a_s g_{rs} = 0$$

where $$g_{rs} = \sum_{n=3,5}^{\infty} Z_{on} \delta_{nr} \delta_{ns} + \sum_{m=1,3,5}^{\infty} Z_m \tanh\gamma_m l \, P_{rm} P_{sm}$$

where $$\delta_{nm} = \begin{cases} 1 & n=m \\ 0 & n \neq m \end{cases}$$

and $$P_{nm} = \int_0^a \phi_n(x) \, \psi_m(x) dx$$

$$= 2\sqrt{\frac{2}{a}} N_m \sin\frac{n\pi}{2} \left[\left(\frac{n\pi}{a}\right) \sin\frac{n\pi t}{2a} \sin k_{1m} d - k_{1m} \cos\frac{n\pi t}{2a} \cos k_{1m} d \right] x \frac{k_{2m}^2 - k_{1m}^2}{\left[k_{2m}^2 - \left(\frac{n\pi}{a}\right)^2\right]\left[k_{1m}^2 - \left(\frac{n\pi}{a}\right)^2\right]}$$

$$N_m^{-2} = \left[d - \frac{\sin k_{1m} d \cos k_{1m} d}{k_{1m}} + \frac{\sin^2 k_{1m} d}{\sin^2 k_{2m} t} (1 - \cos k_{2m} t) \right.$$

$$\left. x \left(t + \frac{\sin k_{2m} t}{k_{2m}}\right) \right]$$

Now equating the partial derivatives w.r.t. a_s to zero so as to render Z_{in} a stationary quantity, one gets the sets of equations

$$Z_{in} Z_{o1} a_1 - \sum_{r=1,3}^{N} a_r g_{1r} = 0$$

$$\sum_{r=1}^{N} a_r g_{rs} = 0 \qquad S = 3,5,7\ldots$$

whose determinant must be zero for non-vanishing values of a's. Therefore,

$$Z_{in} = \frac{1}{Z_{01}} \begin{vmatrix} g_{11} & g_{13} & & g_{1N} \\ \vdots & & & \\ g_{N1} & g_{N3} & \cdots & g_{NN} \end{vmatrix} \qquad (4.19)$$

$$\div \begin{vmatrix} g_{33} & g_{35} & & g_{3N} \\ \vdots & & & \\ g_{N3} & & \cdots & g_{NN} \end{vmatrix}$$

4.2.5 Calculation of Reflection Coefficient

The computations of the junction impedance were done with the help of a 7040 IBM computer, the equation 4.19 being solved for different values of t/a, σ and N at 9.25 GHz. The results are plotted for N = 7* in fig. 4.8 in the form of the reflection coefficient R,

$$R = (Z_{in} - 1)/(Z_{in} + 1)$$

which is a directly measurable quantity. The length of the sample was assumed to be one quarter wave length ($=\pi/2\beta$) at each point. The figure indicates the extent to which the reflection coefficient may vary.

In fig. 4.9 the magnitude of the reflection coefficient is plotted as a function of σ, for various values of t/a and N. It may be observed that as σ increases, the higher modes which are excited considerably change the reflection coefficient at z = 0. It may further be observed from the computational results that unless t/a

* The reason for the choice of N=7 in the fig. 4.8 is that in the range considered, this value gives good agreement with the experimental results. This agreement may be better with N=9 but the numerical computations are then too cumbersome to handle.

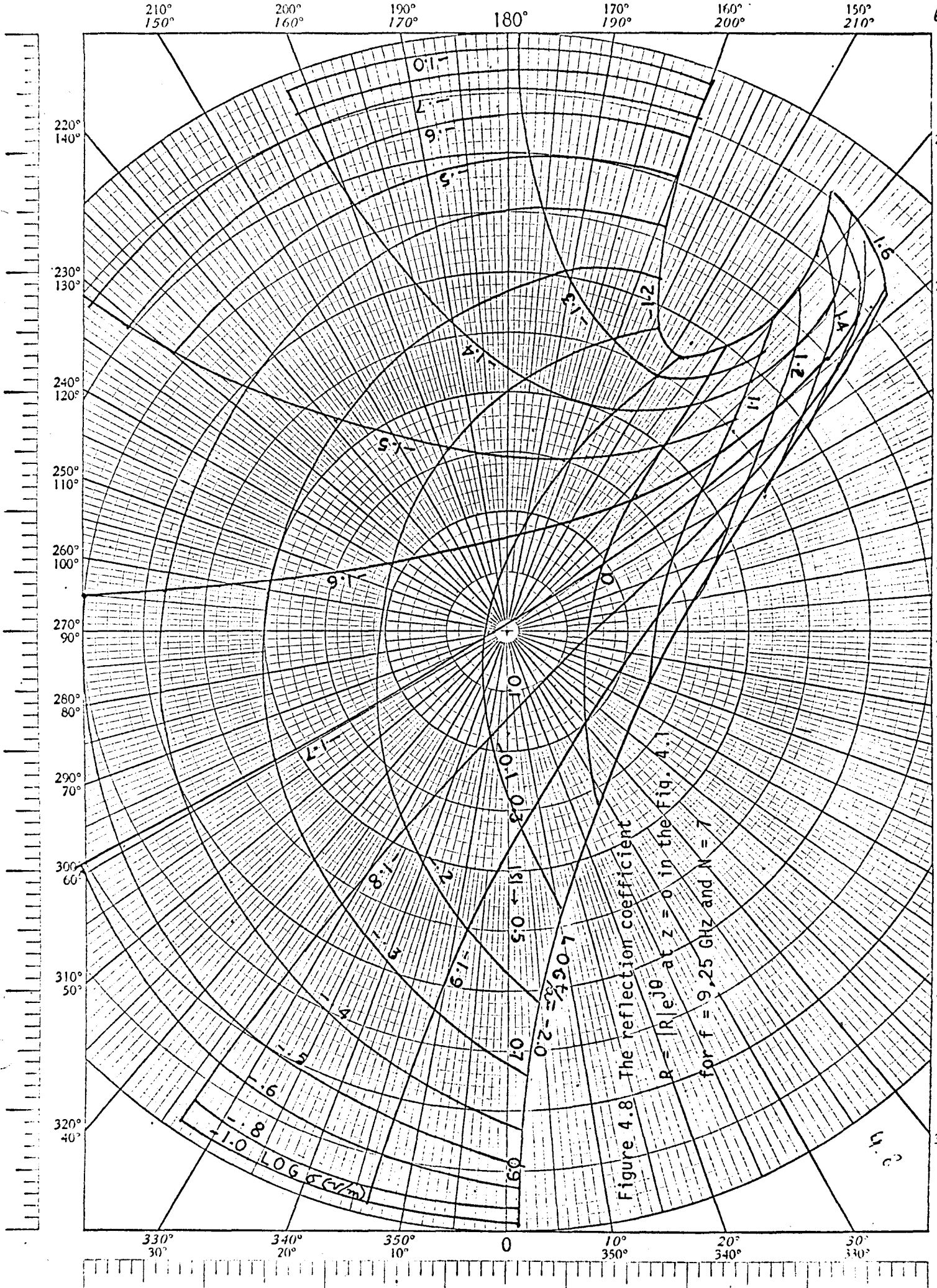

Figure 4.8 The reflection coefficient $R = |R|e^{j\theta}$ at $z = 0$ in the Fig. 4.1 for $f = 9.25$ GHz and $N = 7$

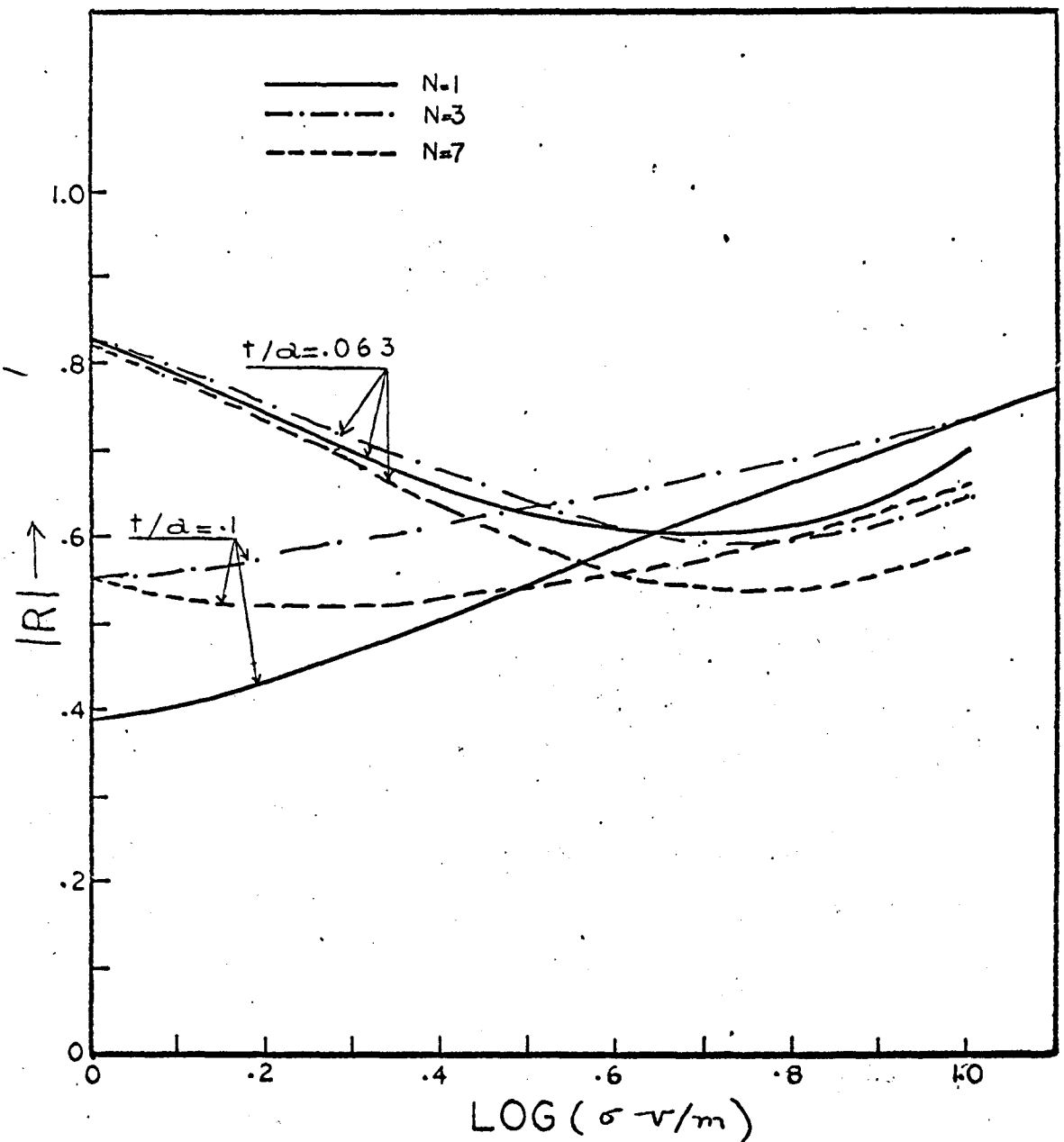

Figure 4.9 The reflection coefficient at z=o (Fig. 4.1) as a function of σ, t/a and N.

$\gtrsim$ 0.08 and $\sigma \gtrsim$ 2.5 ν/m, the effect of the higher order modes is not negligible.

4.3 MEASUREMENT OF REFLECTION COEFFICIENT

The reflection coefficient at the junction of an empty guide and the semi-conductor loaded guide as shown in the fig. 4.1, was measured by means of the reflection bridge as described in the Appendix A. This bridge directly measures the reflection coefficient $R = |R|e^{j\theta}$.

The short circuited wave-guide section containing the semi-conductor sample formed part of one of the side armsof the bridge and placed in a Delta Design oven. The arrangement is shown in the fig. 4.10 The zero balance of the bridge was carried out at each temperature with and without sample.

For practical convenience a slot of desired t and l was milled in the centre of the broad wall of a wave-guide section to assist in centrally locating the sample. At z = l, the guide was terminated with a solid short circuit plate. The samples used were of intrinsic germanium whose conductivity was varied with temperature which was varied from about 80°F. to 300°F.

4.4 RESULTS AND DISCUSSION

The experimental verification of equation 4.19 was carried out on three samples of intrinsic germanium with t/a ratios of .0133, .026 and .0515, at 9.25 GHz. The conductivity of the sample was varied from about 2 mho/m to over 100 mho/m by the variation of the temperature of the sample.

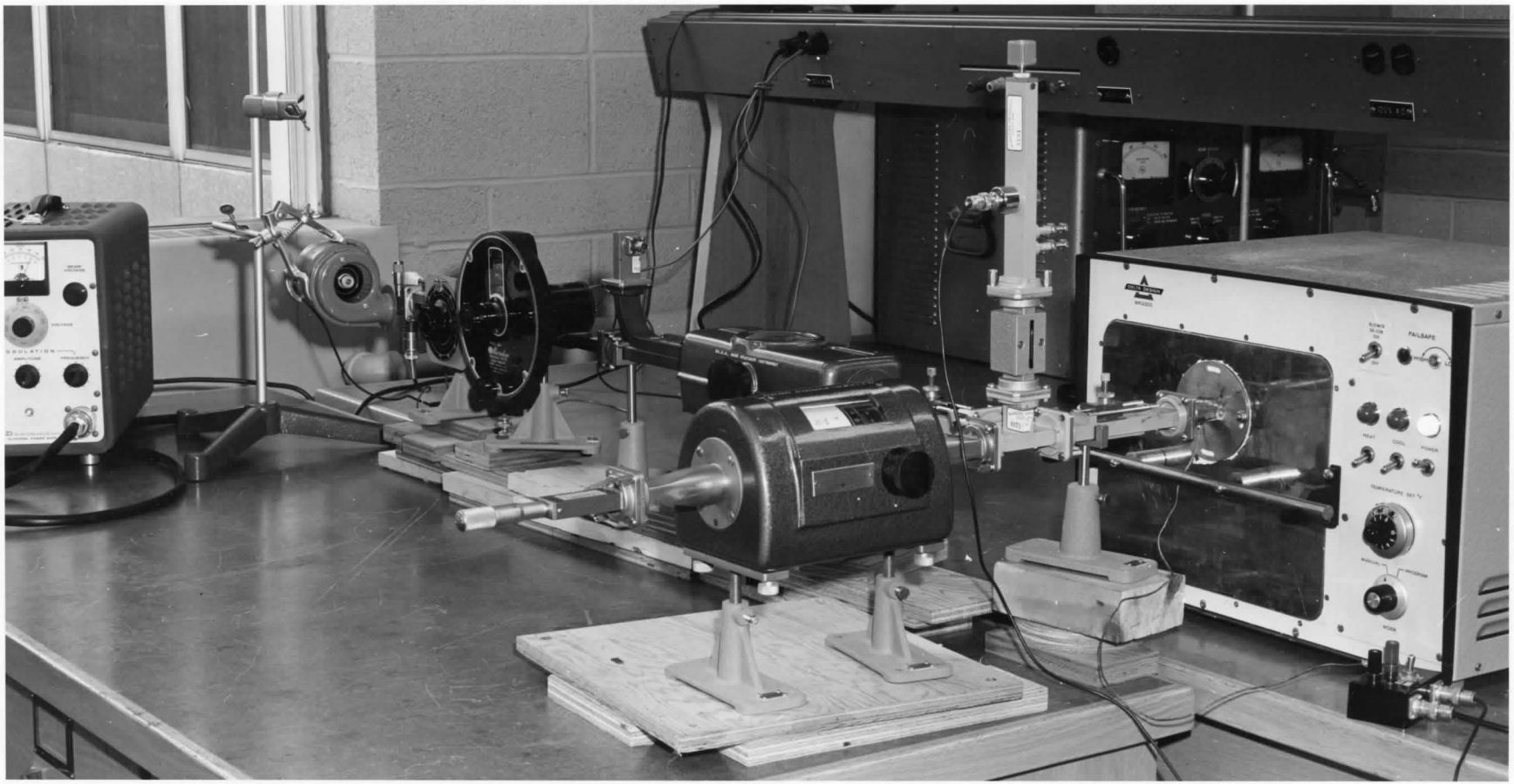

Figure 4.10 The photograph showing the microwave reflection bridge.
The sample is in the Delta Design oven on the right hand side.

The theoretical value of conductivity at the temperature T°k was calculated from the following relationships (45)

$$\sigma(T) = n_i(T)q\ \{\mu_n(T) + \mu_p(T)\}$$

where q = electronic charge = $(1.6 \times 10^{-19}$ coul)

$n_i(T)$ = intrinsic carrier density = $1.76 \times 10^{22} e^{-4550/T}\ T^{3/2}/m^3$

$\mu_n(T)$ = mobility of electrons = $.38\ (300/T)^{+1.66}$ m^2/volt-sec

$\mu_p(T)$ = mobility of holes = $0.18\ (300/T)^{+2.33}$ m^2/volt-sec

In the computations, it was assumed that over the temperature range used in these experiments, the dielectric constant remained constant.

The results of the measurements are shown in the figs. 4.11a and b. The solid curves show the quantity computed from 4.19 with N=7 and the dotted ones with N=1. The crosses are experimental points.

It may be observed that for $\sigma \gtrsim 10$ mho/m ($\log\sigma = 1.0$), the results agree well with N=7 curve. As the conductivity decreases, the solid curves and dotted curve approach each other and remain close to each other except in the case of t/a = .0515. In the latter case, the experimental points are close to the solid curve but lie above it. At the lower end of the conductivity range, the experimental points do not lie on these curves and there appears to be a small discrepancy between the theoretical curves and the experimental points.

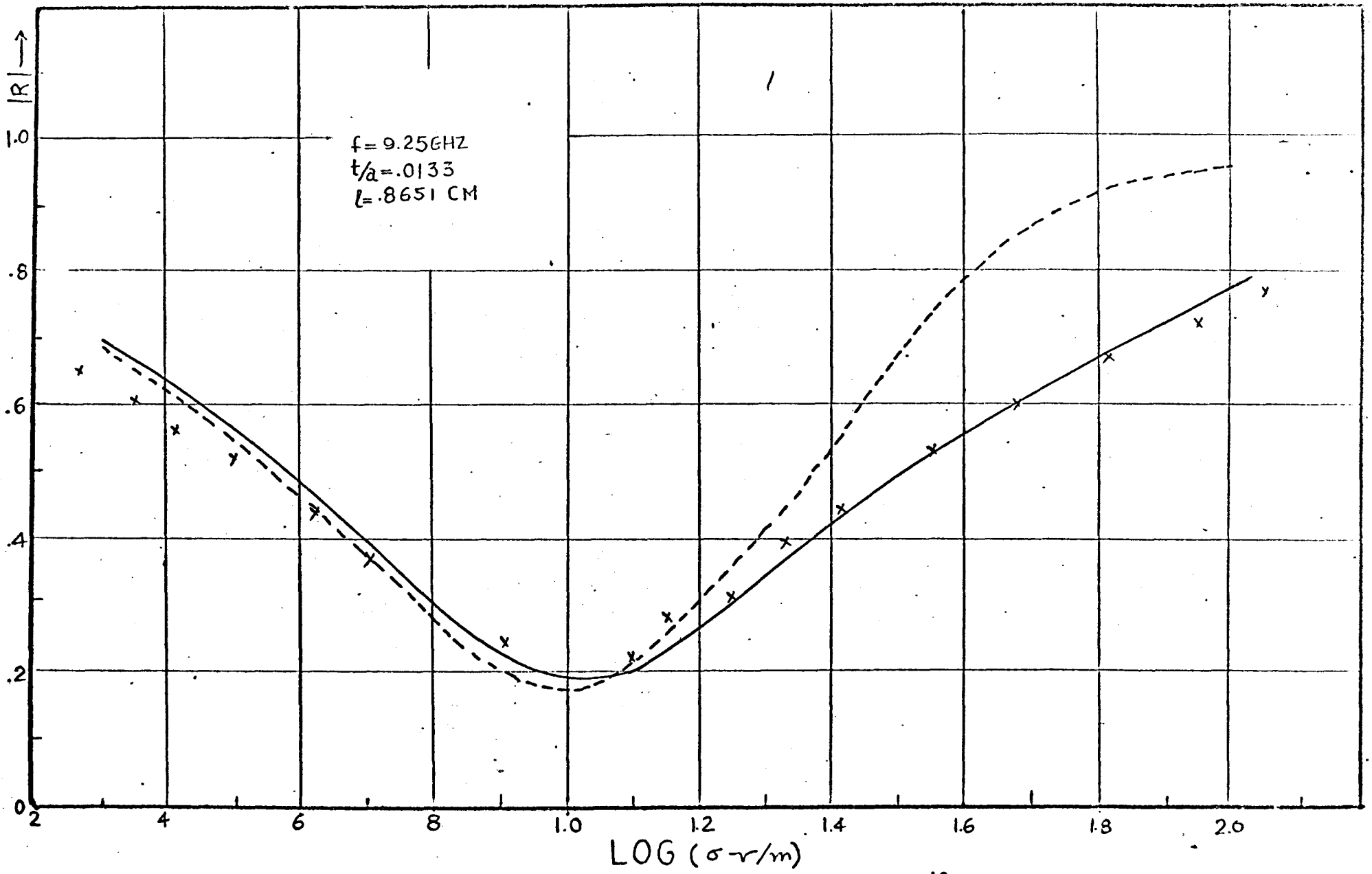

Figure 4.11 a-1 The Practical and Theoretical Values of $|R|$ in $R = |R|e^{j\theta}$ for $t/a = .0133$

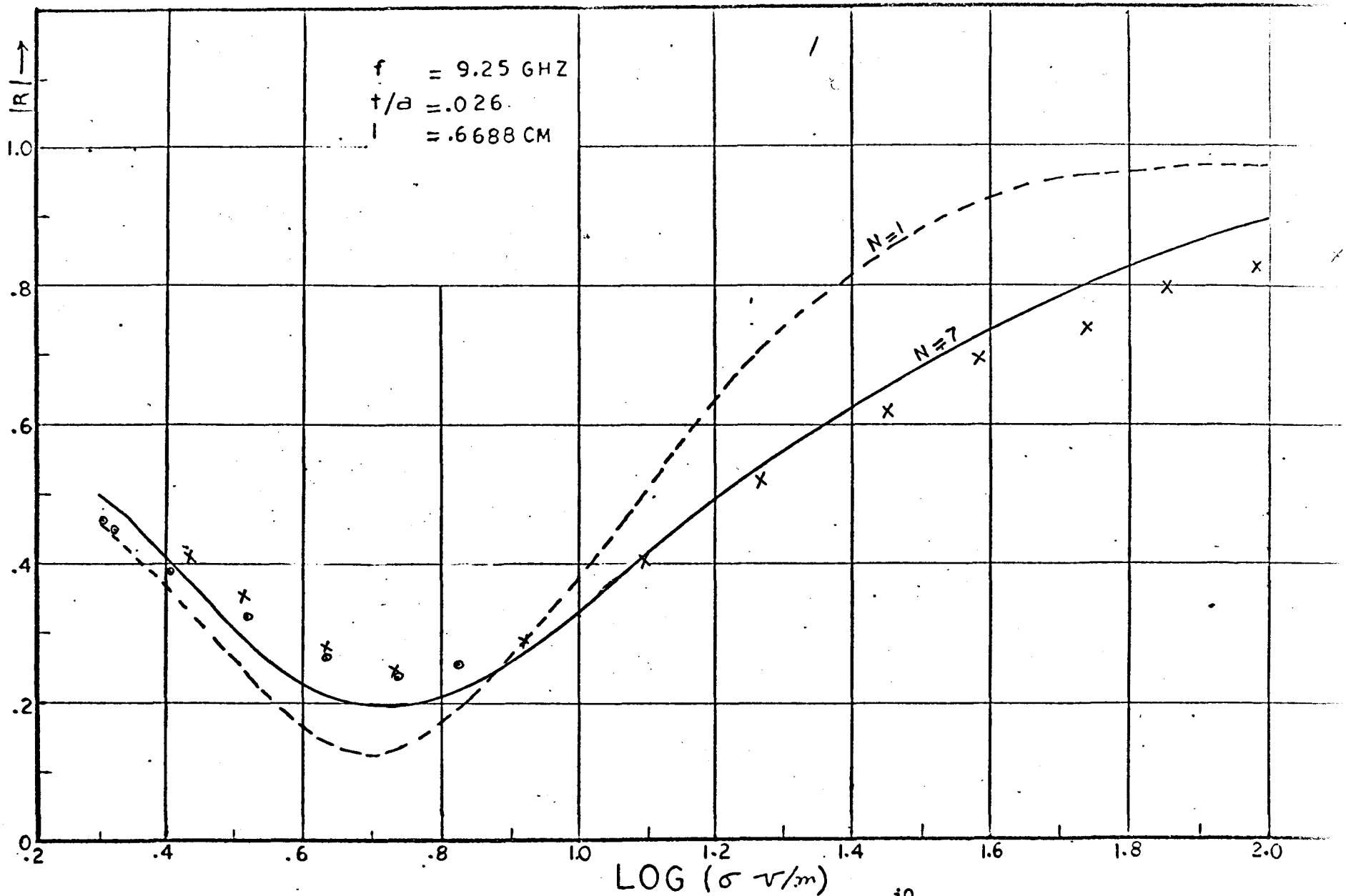

Figure 4.11 a-2 The Practical and Theoretical Values of $|R|$ in $R = |R|e^{j\theta}$ for $t/a = .026$

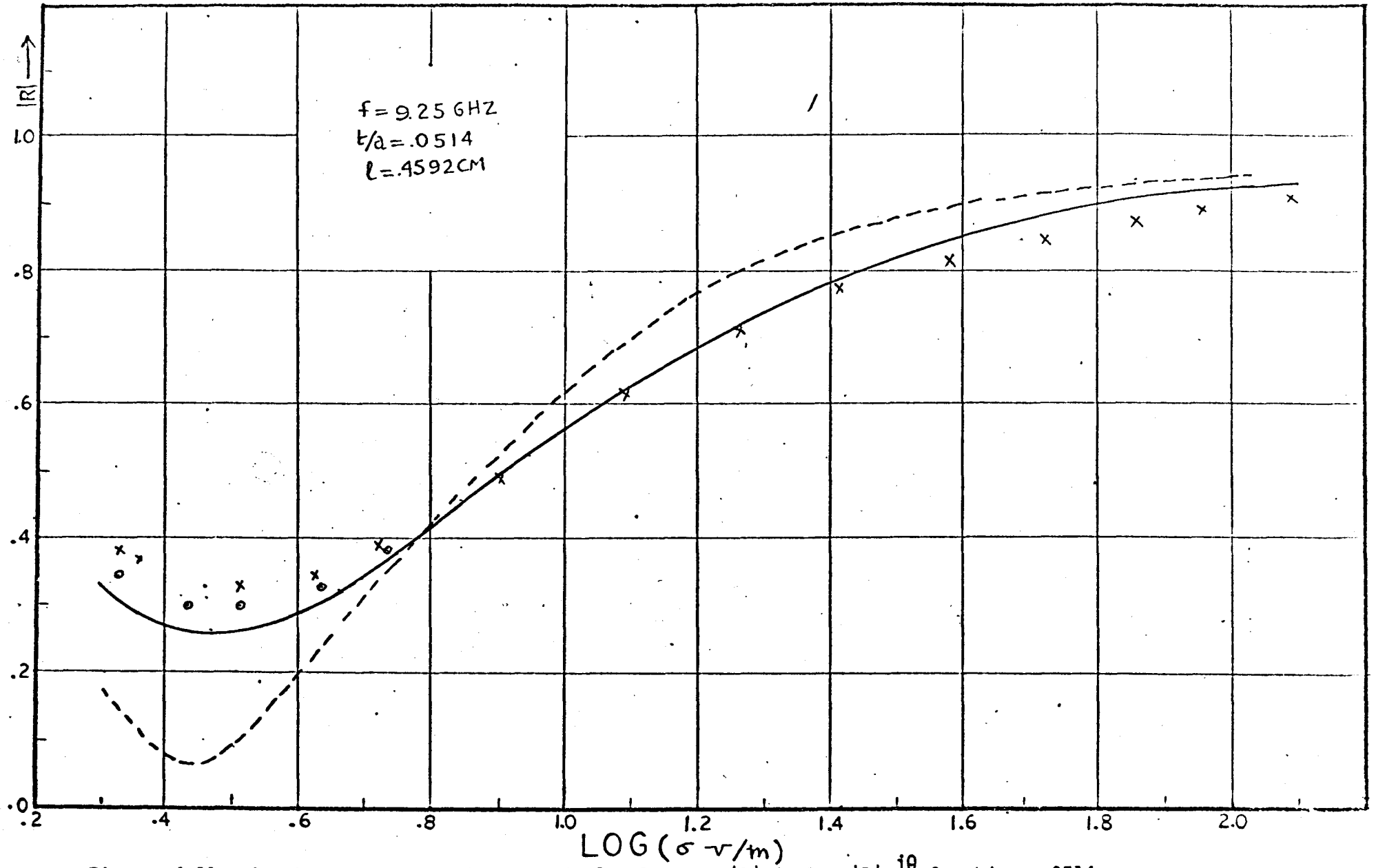

Figure. 4.11 a-3 The Practical and Theoretical Values of $|R|$ in $R = |R|e^{j\theta}$ for t/a = .0514

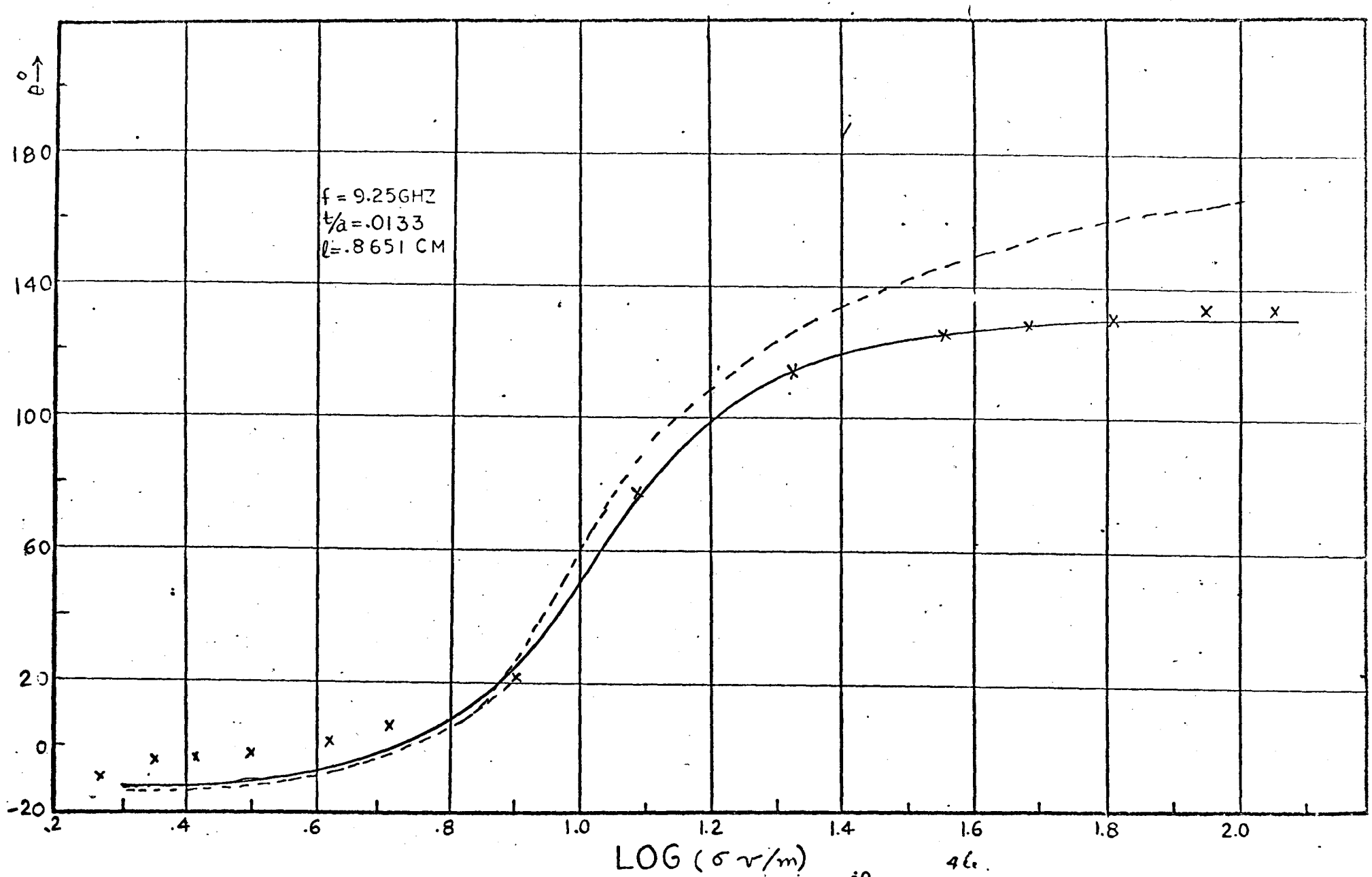

Figure 4.11 b-1 The Practical and Theoretical Values of θ in $R = |R|e^{j\theta}$ for $t/a = .0133$

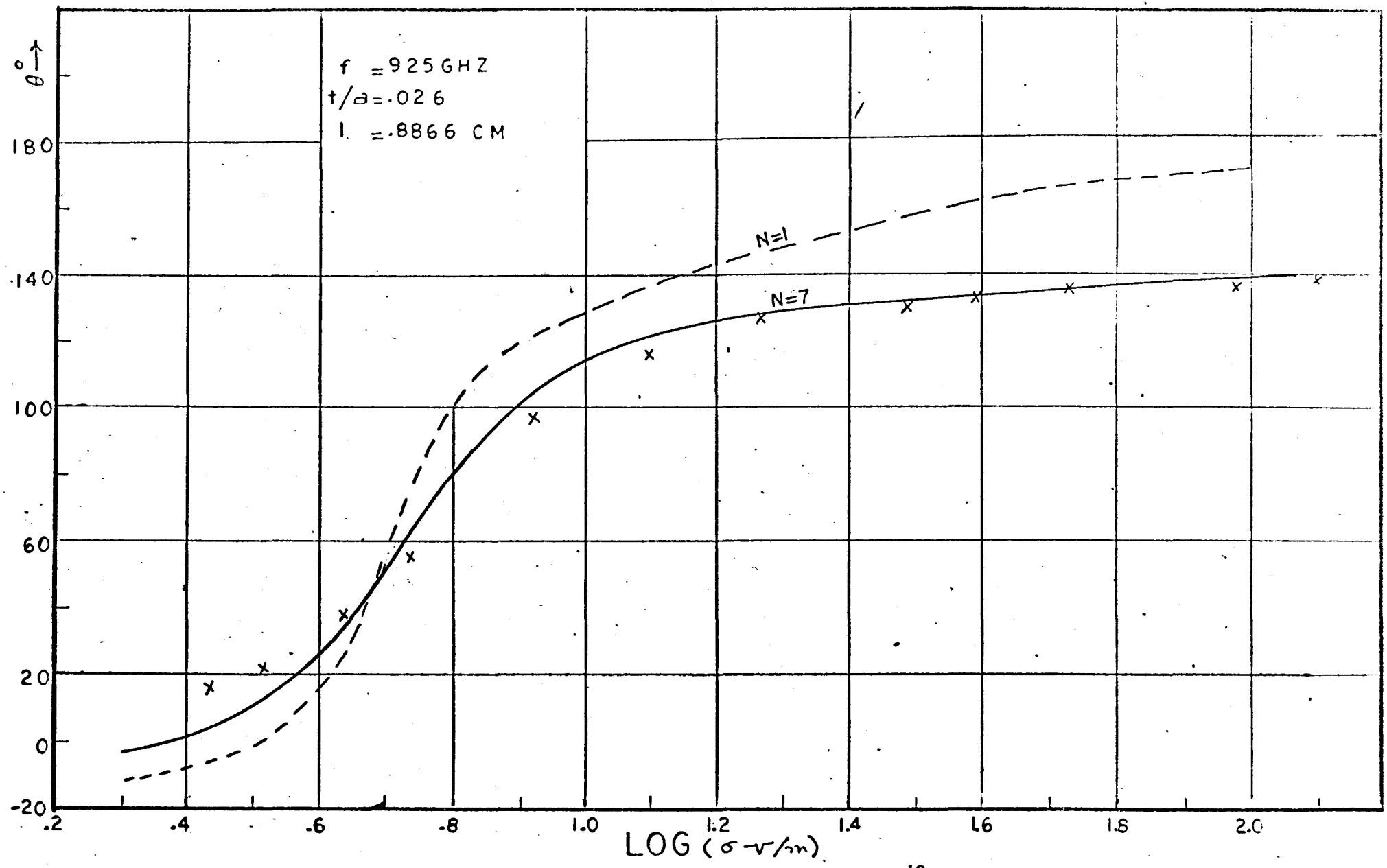

Figure 4.11 b-2 The Practical and Theoretical Values of θ in $R = |R|e^{j\theta}$ for t/a = .026

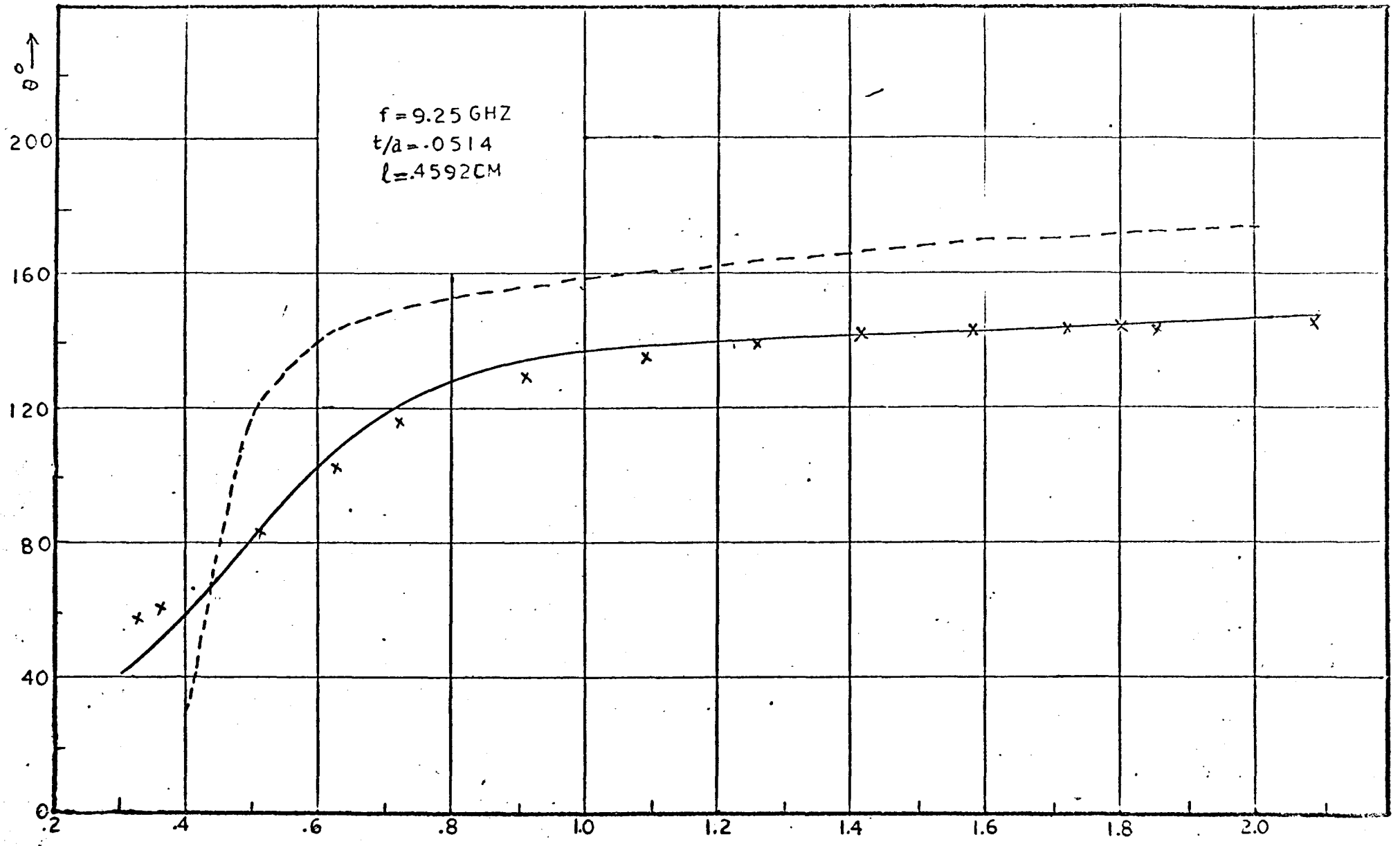

Figure 4.11 b-3 The Practical and Theoretical Values of θ in $R = |R|e^{j\theta}$ for $t/a = .0514$

This discrepancy may be attributed to the effect of the slot in the broad walls of the guide. In the computations the effect of the slot was not taken into account. The slot may have two-fold effect, i) The assumed boundary condition at $y = 0$ and b is not satisfied for $d \leq x \leq d + t$, and ii) Radiation may take place through the small unavoidable air gaps present between the sample and the wave-guide wall. It was shown that this discrepancy was due to the slot by applying silver paint to the top and the bottom of the sample and air gap was also filled with silver paint. The resulting points are shown by circles on the fig. 4.11a and lie nearer the theoretical curve.

Fig. 4.12 gives the computations of $\rho = 1/\sigma$ from these measurements, together with the theoretical curve and the measurements made with $t/a = 1.0$ (i.e. completely filled guide). For a partially filled guide, $\hat{\varepsilon}_r$ was computed by using the approximate relationship 4.2 and assuming N=1. It may be observed that the results are different from either the theoretical values or the practical measurements for the completely filled guide. At higher end of T and hence σ, the discrepancy is due to two reasons, i) use of approximate expression for γ for the deduction of σ and ii) neglect of higher order modes. At lower end of σ, the disagreement may also be due to the slot for reasons similar to those discussed above.

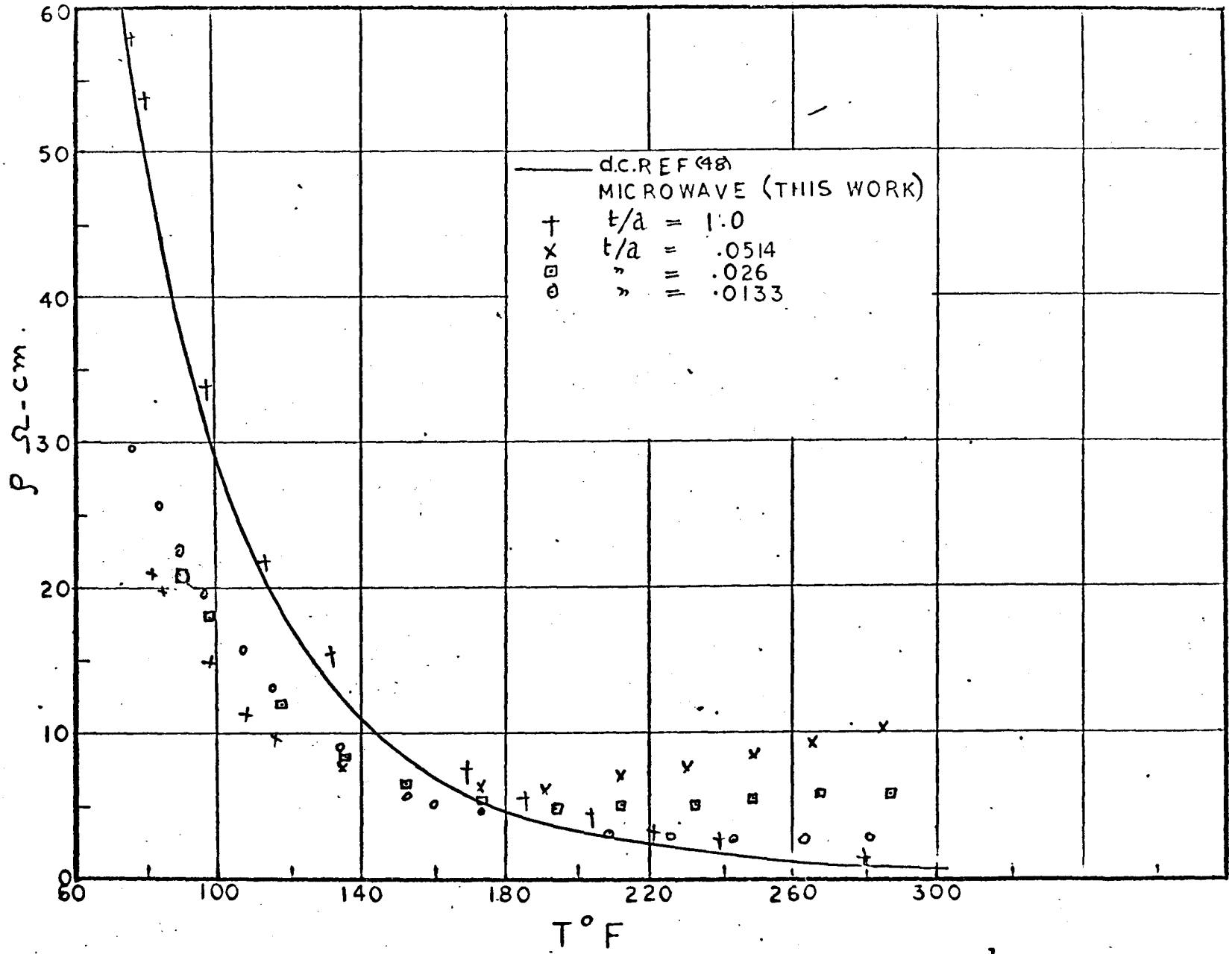

Figure 4.12 The Practical and Theoretical Values of $\rho = 1/\sigma$

CHAPTER V

THE CONDUCTIVITY AND DIELECTRIC CONSTANT OF GERMANIUM AT MICROWAVE FREQUENCIES

5.1 INTRODUCTION

A general treatment of the frequency dependence of the high frequency transport properties of cubic crystals has been reported by Champlin[46] and the high frequency dielectric constant of germanium is given in the references 1, 2 and 7. However, some gross simplifications have been made in these investigations. For example, in the references (1) and (2) relaxation time of charge carriers has been assumed constant and in the reference (7) only scattering by acoustic mode has been considered. These assumptions are not justified. The relaxation time of carriers varies with their energy. Also the consideration of only acoustical phonon scattering leads to the d. c. mobility of carriers varying with temperature as $T^{-3/2}$ [47]. This is in contradiction with the experimentally observed variations of $T^{-1.66}$ for electrons and $T^{-2.33}$ for holes in germanium[48].

A number of theoretical models have been suggested to interpret this observation. These include intra-valley optical phonon scattering[26,48], intervalley scattering by acoustical and optical modes[25] and the variation of the effective mass with temperature[46].

In this chapter, calculations have been made of the microwave mobility and dielectric constant of lightly doped n-type germanium using the following scattering mechanisms.

For electrons

1 - Ionized impurity

2 - Intra-valley ac-oustical and optical phonons

3 - Inter-valley

For holes

1 - Ionized impurity

2 - Acoustical and optical phonons

The computations have been made for $100° \leq T \leq 500°K$, $10^{19} \leq Nd \leq 10^{25}/m^3$ and $10^9 \leq f \leq 10^{12}$ Hz. The effective masses have been assumed constant and scattering by neutral impurities has been neglected.

5.2 THEORETICAL CONSIDERATIONS

5.2.1 Microwave Mobility and Dielectric Constant

The expression for microwave mobility is the same as that for d.c. mobility except that $\langle\tau\rangle$ in the latter is replaced by $\left\langle \frac{\tau}{1+j\omega\tau} \right\rangle$ (49) for the applied electric field varying as $\exp(j\omega t)$. Thus

$$\mu_{ac} = q \left\langle \frac{\tau}{1+j\omega\tau} \right\rangle / m_c^* \qquad (5.1)$$

where m_c^* = conductivity effective mass. The conductivity σ is then a function of frequency

$$\sigma(\omega) = q^2 n \left\langle \frac{\tau}{1+j\omega\tau} \right\rangle / m_c^* \qquad (5.2)$$

n = charge carrier density

and the relaxation time average $\langle\tau\rangle$ is given by (50)

$$\langle\tau\rangle = \int_0^\infty \epsilon^{3/2}\tau(\epsilon)\exp^{-\epsilon}kTd\epsilon / \int_0^\infty \epsilon^{3/2}\exp\frac{-\epsilon}{kT}d_\epsilon \qquad (5.3)$$

To evaluate $\langle\tau\rangle$, one needs to know the variation of τ with energy and that depends on the scattering mechanism. These aspects are considered later.

If in a system both electrons and holes are present, $\sigma(\omega)$ assumes the following form

$$\sigma(\omega) = q^2 \{n \frac{\tau_n}{1+j\omega\tau_n} / m^*_{cn} + p \frac{\tau_p}{1+j\omega\tau_p} / m^*_{cp} \} \qquad (5.4)$$

where n and p are respectively electron and hole concentrations

τ_n and τ_p are their respective relaxation times

m^*_{cn} and m^*_{cp} are their respective conductivity effective masses

Now the current density with alternating fields is given by

$$\vec{J} = \epsilon_o \epsilon_r \frac{\partial\vec{E}}{\partial t} + \sigma\vec{E}$$

$$= (j\omega \epsilon_o \epsilon_r + \sigma)\vec{E}$$

$$= j\omega \epsilon_o \hat{\epsilon}_r \vec{E}$$

where $\hat{\epsilon}_r = \epsilon_r - j\frac{\sigma}{\omega\epsilon_o}$

$\epsilon_r = \epsilon_\ell/\epsilon_o$ lattice contribution to the dielectric constant

Substituting σ from 5.4, gives

$$\epsilon_r = \epsilon_\ell/\epsilon_o - \frac{q^2}{\epsilon_o}\left[\frac{n}{m^*_{cn}}\left\langle\frac{\tau_n^2}{1+\omega^2\tau_n^2}\right\rangle + \frac{p}{m^*_{cp}}\left\langle\frac{\tau_p^2}{1+\omega^2\tau_p^2}\right\rangle\right]$$

cont'd

$$- j \frac{q^2}{\omega \varepsilon_o} \left[\frac{n}{m_{cn}^*} \left\langle \frac{\tau_n}{1+\omega^2 \tau_n^2} \right\rangle + \frac{p}{m_{cp}^*} \left\langle \frac{\tau_p}{1+\omega^2 \tau_p^2} \right\rangle \right]$$

$$\stackrel{\Delta}{=} \varepsilon_{rm}(\omega) - j \frac{\sigma(\omega)}{\omega \varepsilon_o}$$

$$\varepsilon_{rm}(\omega) = \varepsilon_{\ell}/\varepsilon_o - \frac{q^2}{\varepsilon_o} \left[\frac{n}{m_{cn}^*} \left\langle \frac{\tau_n^2}{1+\omega^2 \tau_n^2} \right\rangle + \frac{p}{m_{cp}^*} \left\langle \frac{\tau_p^2}{1+\omega^2 \tau_p^2} \right\rangle \right] \tag{5.5}$$

$$\sigma(\omega) = q^2 \left[\frac{n}{m_{cn}^*} \left\langle \frac{\tau_n}{1+\omega^2 \tau_n^2} \right\rangle + \frac{p}{m_{cp}^*} \left\langle \frac{\tau_p}{1+\omega^2 \tau_p^2} \right\rangle \right] \tag{5.6}$$

Once the form of $\tau(\varepsilon)$ is known, the equations 5.5 and 5.6 are readily evaluated.

The relaxation time $\tau(\varepsilon)$ may be calculated from the scattering or transition probability for a given scattering mechanism. Thus if H' is the perturbing potential and causes a charge carrier to make a transition from state k to k', then the scattering probability per unit time S(k,k') is proportional to the transition matrix element M(k,k') given by[51]

$$M(k,k') = \int \psi_{k'}^* \; H' \; \psi_k \; d\vec{r} \tag{5.7}$$

$\psi_{k'}$ and ψ_k are the wave functions of the charge carriers in the state k' and k respectively. Then

$$S(k,k') = \frac{2\pi}{\hbar} \left| M(k,k') \right|^2 N(\varepsilon) \tag{5.8}$$

where $N(\varepsilon)$ = density of final states

$$\propto \varepsilon^{1/2}$$

If θ is the angle between k and k', then $\tau(k)$ can be written, using Maxwellian statistics, as

$$\tau(k)^{-1} = \int(1-\cos\theta)\, S(k,k')dk'$$

Now if it is assumed that the scattering processes conserve energy, or nearly so, then the above equation can be reduced to simpler form. Thus if k' lies on the same energy surface as k and θ is the angle between k and k', then

$$\tau(k)^{-1} = \int(1-\cos\theta)\, S(k,k')\, d\Omega \qquad (5.9)$$

$$d\Omega = 2\pi \sin\theta d\theta$$

For isotropic scattering S(k,k') is independent of θ.

Thus the evaluation of $\tau(k)$ ($= \tau(|k|) = \tau(\varepsilon)$) reduces to the evaluation of M(k,k'). The expressions for this will be given for various scattering processes in the following sections.

5.2.2 Ionized Impurity Scattering [52,53]

When a semi-conductor is doped, the doping atoms become ionized either by giving up an electron or taking an electron. These charged particles produce coulomb fields and a perturbing potential.

$$V = \frac{ze/4\pi}{\varepsilon_0 \varepsilon_r r} \exp(-qr)$$

where ze = effective charge of the impurity atom

ε_r = dielectric constant

r = distance from the centre of the atom

$1/q$ = screening length

$$q^2 = \frac{e^2}{\epsilon_o \epsilon_v kT} Nd \left(2\frac{n+p}{Nd}\right) \text{ (mks units)}$$

Nd = ionized donors and acceptors density

This leads from (5.7) to

$$S(k,k') = \frac{2\pi}{\hbar} \left[\frac{ze^2}{\epsilon_o \epsilon_v (|k-k'|^2 + q^2)}\right]^2$$

and to impurity relaxation time τ_I

$$\frac{1}{\tau_I(\epsilon)} = A \left[\log_e (1+2b) - \frac{2b}{1+2b}\right]^{-1} \qquad (5.10)$$

$$A = \frac{Nd}{2\pi} \left(\frac{ze^2}{\epsilon_o \epsilon_v}\right)^2 (2\epsilon)^{-3/2} m^{*-1/2}$$

$$2b = \frac{8m^*\epsilon}{q^2\hbar^2}$$

or $$\frac{1}{\tau(\epsilon)} = c_1 \epsilon^{-3/2} / \left(\log_e (1+c_2\epsilon) - \frac{c_2 \epsilon}{1+c_2\epsilon}\right)$$

c_1 and c_2 being constants, independent of energy

5.2.3 Lattice Scattering[47,52]

Due to thermal energy, the atoms in a solid vibrate about their mean position and produce a local variation of potential. This periodic potential causes the electrons (and holes) to make transitions from one state to another state. In the process the electrons either gain or lose energy and momentum to the crystal lattice. If the electrons lose energy, a phonon of equivalent energy is emitted and if it gains energy, a phonon is absorbed. Thus if k and k' are initial and

final wave vectors of an electron and Q is the wave vector of the phonon involved, then the following relations hold.

$$\vec{K} - \vec{K}' = \pm\vec{Q} + \vec{G} \qquad (5.11)$$

$$\varepsilon(k) - \varepsilon(k') = \pm\hbar\omega$$

where + on the R.H.S. of both equations is for phonon emission and -ve for phonon absorption. $\hbar\omega$ is the energy of the phonon and $\vec{G}$ is any reciprocal lattice vector. If $\vec{G} = 0$, the scattering process is normal and if non-zero, then the process is an Umklapp one.

From equation 5.11, it appears that the energy of the carriers is no longer conserved in the scattering process. However, if the fields are small, (which is the case treated here), it may be shown that

$$\hbar\omega \ll \varepsilon$$

and thus $\varepsilon(k') = \varepsilon(k)$

The phonon involved in the scattering process may be of different types. For example, it may be of low energy and low momentum - (acoustical scattering) or it may be of low momentum and high energy (optical scattering). Further, if the semi-conductor has different equivalent conduction band minima (as germanium has), the electrons may be scattering from one valley to the other (intervalley scattering). Again the phonons involved may be acoustical or optical, but momentum and energy now depend on the value of Q involved which in turn depends on the position of the energy minima. These processes will now be considered in a little more detail.

5.2.4 Intra-valley Acoustical Scattering

This has been best treated by Bardeen and Shockley using the concept of deformation potential. The elastic displacements $\mu(\vec{r})$ of the atoms would produce changes in the position of energy band minima and maxima. If $\mathcal{E}_m$ = energy of minimum or maximum with $\mu(\vec{r})$ and ϵ_{mo} is the equilibrium value, then it is shown that [52]

$$\delta\epsilon_m = \epsilon_{mo} - \epsilon_m = E_1 \nabla\mu(\vec{r})$$

(E_1 is being a constant) may be treated effectively as the perturbing potential of the charge carriers near the minimum or maximum. By expanding $\nabla.\vec{\mu}(\vec{r})$ in a Fourier Series, it is shown then that the matrix element M(k,k') is given by [53]

$$|M(k,k')|^2 = \frac{\hbar(2N_Q+1)}{2\rho} |\vec{Q}|^2 \mathcal{E}_{1c}^2$$

$\mathcal{E}_{1c} = \delta\epsilon_m/\Delta$; $\Delta = \frac{\Delta V}{V}$ V = volume of the crystal

ρ = density of material

$$N_Q = \left[\exp\frac{\hbar\omega_Q}{kT} - 1\right]^{-1} \qquad (5.12)$$

if $\hbar\omega_Q \ll kT$, then $(2N_Q+1) \simeq 2\frac{kT}{\hbar\omega_Q}$

Then assuming isotropic scattering, equation 5.9 gives

τ_L = lattice scattering time constant

= constant $x\epsilon^{-\frac{1}{2}}/T$ (5.13)

T = temperature in ^oK

The constant is independent of temperature and energy of the carrier (assuming constant effective masses).

5.2.5 Intervalley Scattering

It is now known that germanium has a conduction band minimum in (111) direction of k-space. Thus there are eight equivalent minima. These different minima are called valleys and an electron in ith valley with wave vector $\vec{k}_i$ may make a transition to another valley j with final wave vector $\vec{k}_j$. In the process the electron either absorbs or emits a phonon. The probability of this process is given by the matrix element M(k,k') which is as follows[25]

$$\left|M(k,k')\right|^2 = \begin{matrix} N_Q \\ N_Q + 1 \end{matrix} \times \frac{C(k,k')}{\omega_Q} \cdot \delta \left[\varepsilon(k) - \varepsilon(k') \pm h\omega_Q\right] \begin{matrix} \text{absorbed} \\ \text{emitted} \end{matrix}$$

where $C(k,k')$ independent of Q and ε or $T.N_Q$ is given by equation 5.12 and $\pm h\omega_Q$ is the energy of the phonon absorbed (+sign) or the phonon emitted (-ve sign). Then the relaxation time due to such scattering is obtained from 5.9 as

$$(\tau_{Iv})^{-1} = \sum_i C_i \left[\frac{(\varepsilon + h\omega_i)^{1/2}}{1 + \exp \frac{h\omega_i}{kT}} + \frac{(\varepsilon - h\omega_i)^{1/2}}{1 - \exp - \frac{h\omega_i}{kT}} \text{ or zero}\right] \qquad (5.14)$$

where i varies over different phonons possible

$h\omega_i$ = energy of ith phonon

C_i = "coupling constants" of ith phonon expressing the scattering strength

The second term on the R.H.S. is zero if $\varepsilon < h\omega_i$ because in that case no phonon can be emitted.

5.2.6 Intravalley Optical Mode Scattering

The electrons or holes may be scattered by optical phonons (electrons remaining in the same valley after scattering). For germanium, which is a nonpolar crystal, the matrix element is essentially the same as for intervalley scattering as $k \to k'$ [25] and hence τ_{opt} is of the same form as 5.14.

5.2.7 Energy Bands and Lattice Vibrations in Germanium

Before one can proceed to compute the mobility, a knowledge of the conduction and valence bands and the lattice vibrational spectrum is necessary for two reasons.

(i) The form of the energy bands gives information about the effective masses and enables the computations of carrier concentrations and the evaluation of the relaxation time integrals.

(ii) The location of the energy bands and the lattice vibrational spectrum give the information on the phonons involved in the scattering and their energies.

It is known that germanium has two valence bands degenerate at $\vec{k}=0$. The form of these energy bands may be approximated near $\vec{k} = 0$ as follows [53].

$$\epsilon = -\frac{\hbar^2}{2m_0}\left\{A\,k^2 \pm \left[B^2k^4 + c^2\,(kx^2\,ky^2 + ky^2\,kz^2 + kz^2\,kx^2)\right]^{1/2}\right\} \qquad (5.15)$$

$A = 13.1$, $B = 8.3$ and $C = 12.5$

m_0 = free electron mass

The holes with + sign in 5.15 are referred to as light mass holes and with - sign as heavy mass holes. These masses are given respectively by the following equations

$$m^*_{hl}/m_o = \frac{1}{A + (B^2+C^2/6)^{1/2}} = .044$$

$$m^*_{hh}/m_o = \frac{1}{A - (B^2+C^2/6)^{1/2}} = 0.30$$

The conduction band in germanium has 8 equivalent minima in the direction (111) located at the zone boundary. Near the minimum the ϵ-k relationship has the form (54)

$$\epsilon = \frac{\hbar^2}{2}\left\{\frac{k_1^2}{m_\ell} + \frac{k_2^2}{m_t} + \frac{k_3^2}{m_t}\right\}$$

$$m_l = 1.64m_o$$

$$m_t = 0.819m_o$$

The phonons involved in the intervalley scattering are given in the table 5.1. It may be observed that all the non-zero phonons involved are in (100) plane and have maximum values in the (100) direction.

The energies of the phonons are given by the lattice vibrational spectrum. This has been determined by Brockhouse (55) from neutron diffraction experiments. In the lattice spectrum, there are six branches, three acoustical and three optical. Energies of the various phonons relative to the present work are given in the table 5.2.

TABLE 5.1

VARIOUS PHONONS INVOLVED IN THE INTERVALLEY SCATTERING IN N-TYPE GERMANIUM

$$\vec{Q} = \vec{K}_i - \vec{K}_j - \vec{G}$$

$$\vec{K}_i = \frac{2\pi}{a} (1,1,1)$$

$\vec{K}_j$ $2\pi/a$ x	$\vec{K}_i - \vec{K}_j$ $2\pi/a$ x	$\vec{Q}$ $2\pi/a$ x
$(1\bar{1}\bar{1})$	(002)	(002)
$(\bar{1}1\bar{1})$	(020)	(020)
$(\bar{1}\bar{1}1)$	(020)	(200)
$(\bar{1}\bar{1}\bar{1})$	(022)	(200)
$(\bar{1}1\bar{1})$	(202)	(020)
$(\bar{1}\bar{1}1)$	(220)	(002)
$(\bar{1}\bar{1}\bar{1})$	(222)	(000)

TABLE 5.2

DIFFERENT PHONONS AND THEIR ENERGIES FOR GERMANIUM AT ZONE EDGE

Phonon		Frequency = $(\epsilon/h) \times 10^{-12}$Hz*
Transverse Optical	TO[100]	8.25 ± 0.3
Longitudinal	L[100]	6.9 ± 0.4
Transverse Acoustic	TA[100]	2.45 ± 0.15
Optical	[Q=0]	9.0 ± 0.30

* Table II of reference (55)

Although the intervalley scattering could involve phonons corresponding to all the branches of the lattice vibrational spectrum, it is shown by Herrig and Vogt[54] that the contribution due to two lowest branches (Transverse acoustic) is very small and can be neglected. This leaves five phonons (1 longitudinal acoustical, 3 optical at Q = [001] and 1 at Q = 0 that is the intravalley optical) which can take part in the scattering of electrons.

For holes there is no intervalley scattering and the only phonons involved are optical and longitudinal acoustical ones. However, for holes, interband transition can take place but these transitions have not been observed in Haynes-Shockley experiments and are assumed to be very rapid.

5.2.8 Variation of ϵ_1

The lattice contribution ϵ_1/ϵ_0 to the dielectric constant has been observed to vary with temperature by Cardona et al [56] and have given the following formula.

$$\frac{1}{n}\frac{dn}{dT} = 6.7 \times 10^{-5}/^{\circ}c$$

where

$$n = \sqrt{\epsilon_1/\epsilon_0}$$

5.4 THEORETICAL RESULTS AND DISCUSSION

The relaxation times given earlier can now be combined to give the total relaxation time constant τ as follows,

$$\frac{1}{\tau(\varepsilon)} = \frac{1}{\tau_I(\varepsilon)} + \frac{1}{\tau_L(\varepsilon)} + \frac{1}{\tau_{ph}(\varepsilon)}$$

where τ_{ph} = relaxation time due to phonon scattering other than low energy acoustical scattering.

Thus

$$[\tau(\varepsilon)]^{-1} = [\tau_I(\varepsilon)]^{-1} + C\left\{\left(\frac{T}{T_o}\right)\left(\frac{\varepsilon}{kT_o}\right)^{1/2} + \sum_i c_i \left(\frac{h\omega_i}{kT_o}\right)^{3/2} \times \left[\frac{(\varepsilon/h\omega_i+1)^{1/2}}{1+\exp\frac{h\omega_i}{kT}} + \frac{(\varepsilon/h\omega_i-1)^{1/2} \text{ or zero}}{1-\exp\frac{-h\omega_i}{kT}}\right]\right\} \qquad (5.15a)$$

The first term on the right hand side of the above equation represents the contribution due to ionized impurity scattering and is given by 5.10. The first term in the curly bracket represents intravalley acoustical scattering relaxation time obtained from 5.13. The terms in the summation are contributions due to intravalley optical and intervalley scattering by phonon of energy $\hbar\omega_i$. The constants c_i measure the strengths of coupling relative to acoustic phonons. T_o is the reference temperature which will be taken as 300°K. The constant C fixes the absolute value of mobility at 300°k.

The values of c_i's are not knownbut these can be left in as adjustable parameters. These can be varied so that the relaxation time obeys the same variation with temperature as has been observed in the

experiments, ie. $T^{-1.66}$ for electrons and $T^{-2.33}$ for holes. These two cases will be treated separately in the following sections.

5.3.1 Electrons Mobility in Germanium

It has been mentioned in art. 5.2.7 that there are five phonons which can take part in the scattering and hence five adjustable constants c_i. It is quite laborious to handle this situation. However, if it is observed that the three phonons (2 optical at Q = 100 and 1 optical at Q = 0) have nearly equal energies and the other two have same energy, then these phonons could be grouped together in two groups without making any serious error. This leaves two constants c_1 and c_2 to be adjusted which is comparatively an easy task. The values of c_1 and c_2 were varied and τ was computed as a function of temperature (between 100° to 300°k). Each time c was adjusted to give

$$\mu_{300} = .3800 = q\langle\tau\rangle/m_c^*$$

The results of computation are plotted in fig. 5.1. The abscissa in the figure represents c_1 and the ordinate -n, the exponent of T. c_2 was taken as a parameter.

It may be observed that there are different sets of c_1 and c_2 which can give the correct value of n = 1.66. No unique combination is possible using only the d.c. mobility data.

Because of this it is convenient to neglect all the scattering by all the intervalley phonons and assume that the scattering is only by optical mode scattering of frequency 9×10^{12} Hz, (or that all phonons are grouped together having one energy). If this is done and c_1

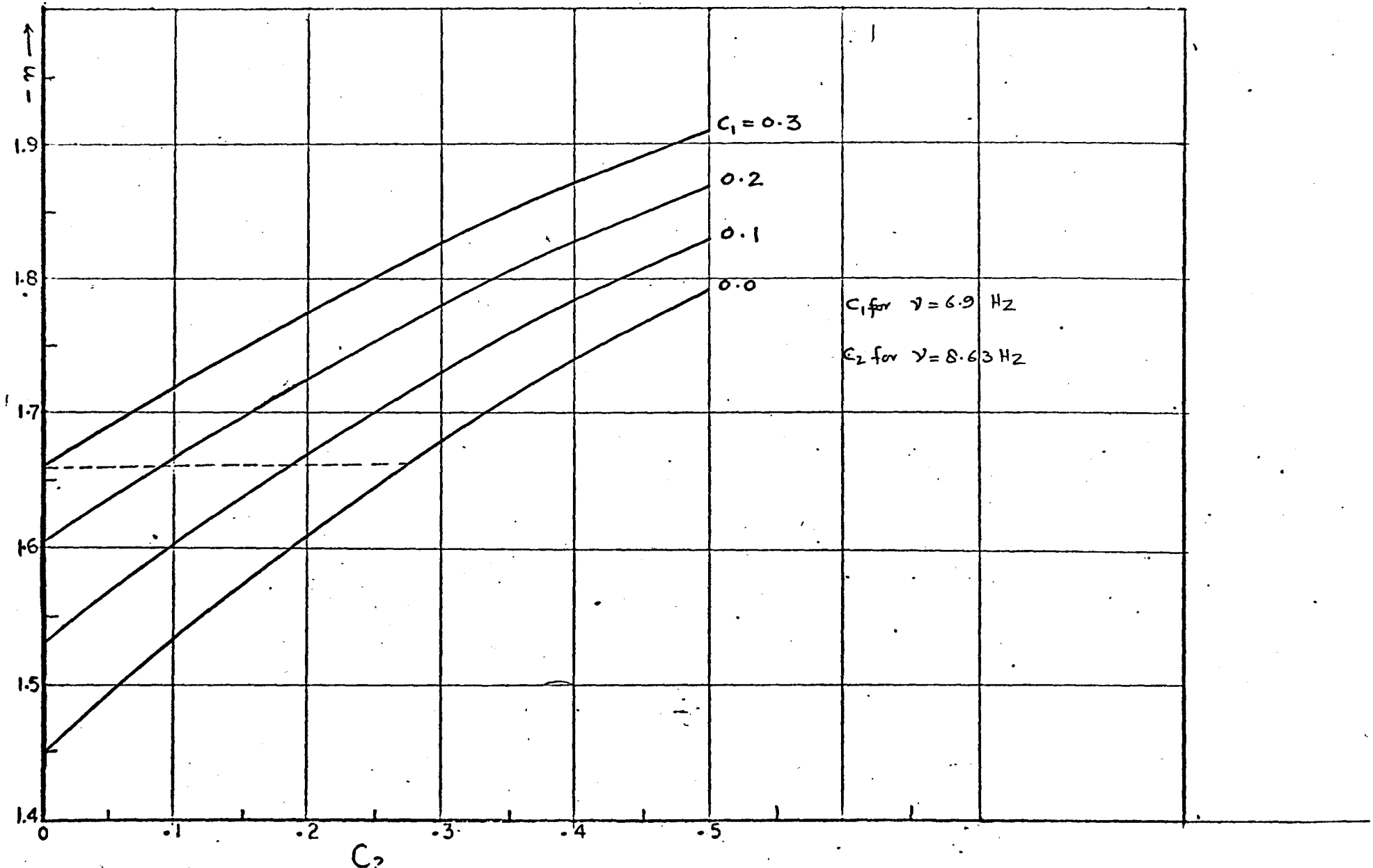

Figure 5.1 Variation of the Index n in T^{-n} for n type Germanium as a function of c_1 and c_2

is varied over values from zero to 1, it may be seen from the figures 5.2a and b that the value of $c_1 = 0.2735$, to give $n = -1.66$. This means that 27.4% of the lattice scattering is due to optical and or inter-valley scattering.

The linearity of the log $\mu \sim$ log T relationship in the ranges of c_1 and c_2 considered, was checked and is shown in the fig. 5.3.

With these values of c_1 and w, one is able to compute $\langle\tau\rangle$ and $\langle\tau/1+j\omega\tau\rangle$ and hence $\sigma(\omega)$. In the actual computations, the use of m_c^* was avoided by using

$$\sigma_n(\omega) = \frac{q^2 n}{m^*_{c_n}} \left\langle \frac{\tau_n}{1+j\omega\tau_n} \right\rangle \frac{\langle\tau_n\rangle}{\langle\tau_n\rangle}$$

$$= q\mu_{no}(T)\, n \left\langle \frac{\tau_n}{1+j\omega\tau_n} \right\rangle / \langle\tau_n\rangle \qquad (5.16)$$

where $\mu_{no}(T)$ = d.c. mobility of electrons

$= 0.3800\ (T/300)^{-1.66}\ m^2/\text{volt sec.}$

n = electron concentration / m^3

For temperatures greater than about 100°k, almost all donors are ionized. Then for $T \gtrsim 100$°k, the carrier concentrations were obtained as follows.

The charge neutrality condition gives

$$n - p = N_d$$

also $np = n_i^2$

whence $$n = \frac{N_d}{2}\left[1 + \sqrt{1+4n_i^2/N_d^2}\right] \qquad (5.17)$$

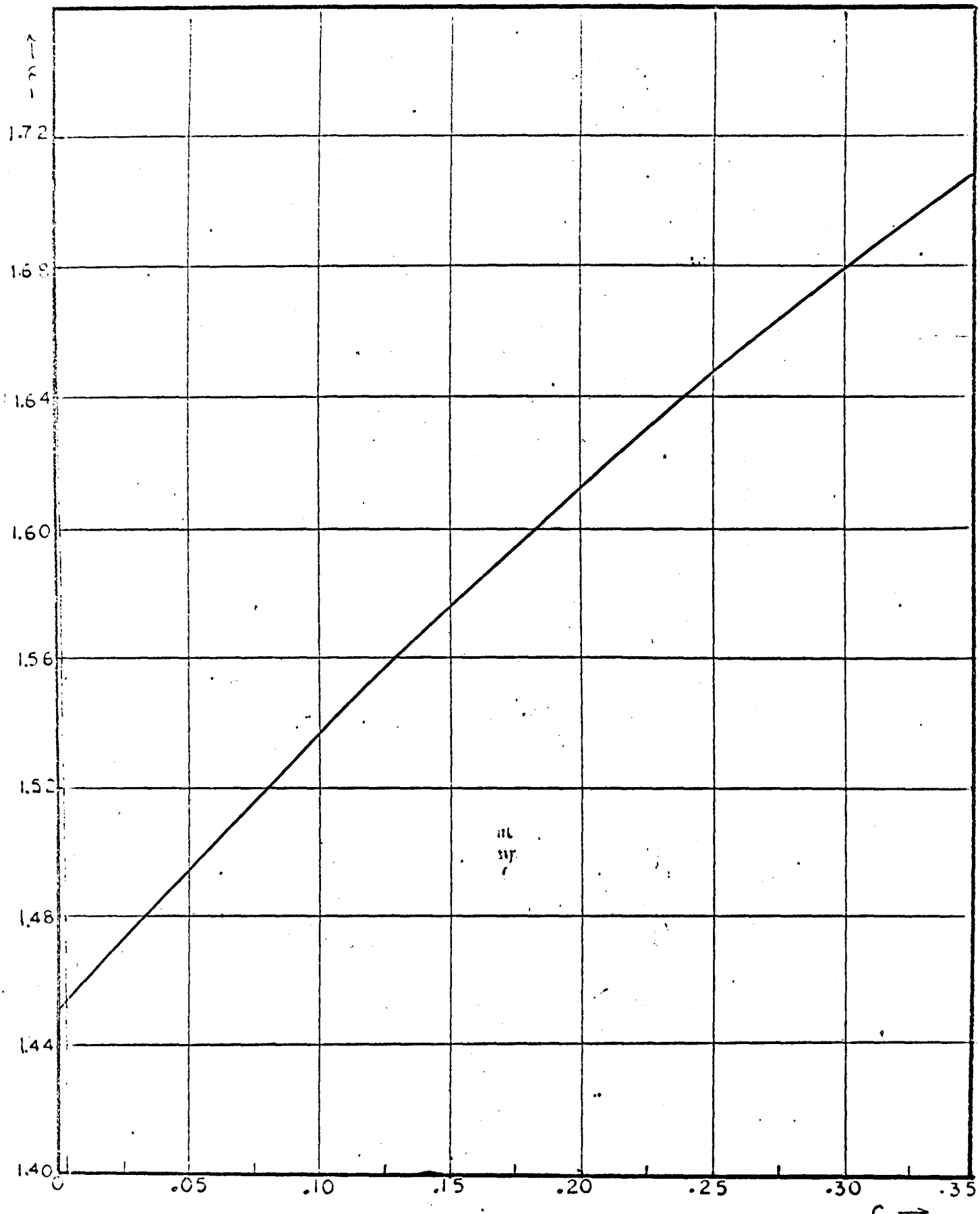

Figure 5.2a Variation of the index n in T^{-n} as a function of c_1

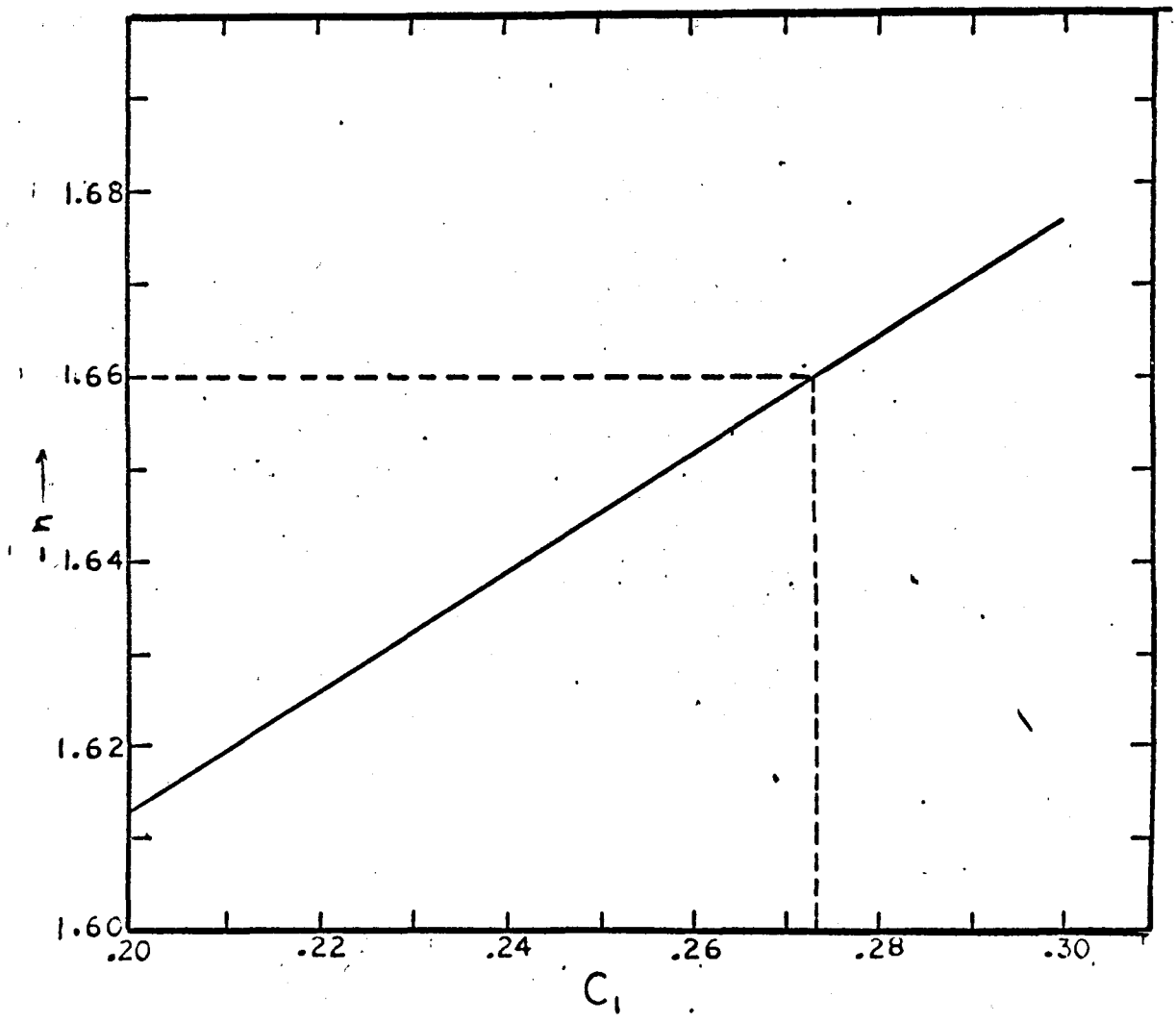

Figure 5.2b $n \sim c_1$ on enlarged scale

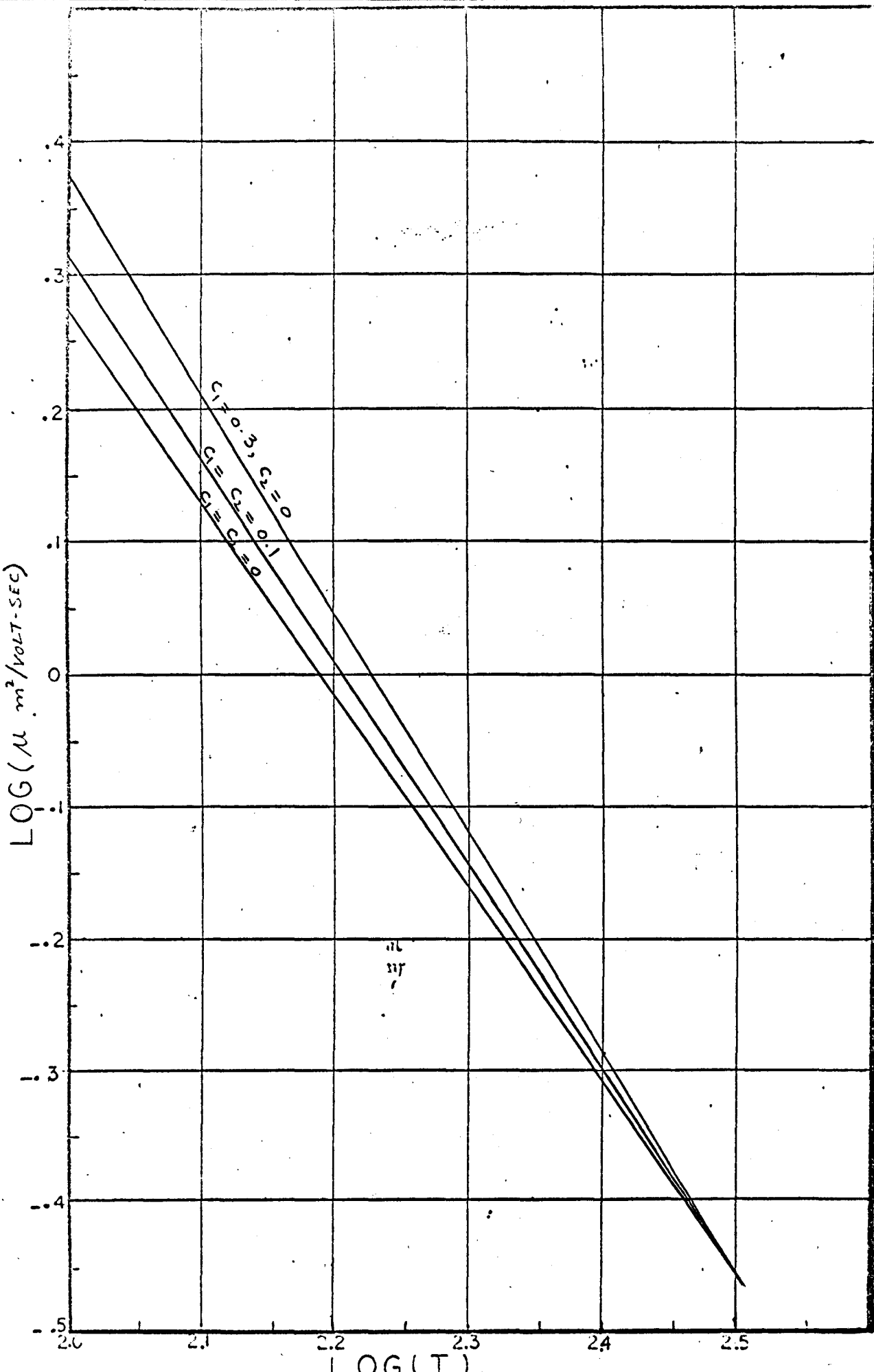

Figure 5.3 Variation of electron mobility in Germanium with Temperature and c_1 and c_2

$$p = \frac{N_d}{2}\left[-1 + \sqrt{1+4n_i^2/N_d^2}\right] \qquad (5.18)$$

For germanium $n_i^2 = 3.1 \times 10^{44} T^3 \exp(-9100/T)/m^3$.

The value of N_d can be computed from the known conductivity and mobilities of carriers at a particular temperature. Thus if a sample has σ_0 d.c. conductivity at 300°k, then

$$\sigma_0 = q\ (n\ \mu_n + p\ \mu_p)$$

$$\mu_n = .38\ m^2/\text{volt-sec.}$$

$$\mu_p = .18\ m^2/\text{volt-sec.}$$

Substituting n and p from 5.17 and 5.18 into the above equation yields a quadratic equation in N_d which is easily solved. Once N_d is known, values of n and p as a function of temperature could be evaluated. In the limiting cases, 5.17 and 5.18 reduce to

(i) when $n_i \ll N_d$

$$n \simeq N_d;\quad p = n_i^2/N_d$$

(ii) when $n_i \gg N_d$

$$n \simeq n_i \simeq p$$

The condition (i) is valid at low temperatures and (ii) at high temperatures.

5.3.2 Hole Mobility in Germanium

In the case of holes, there is no intervalley scattering so that there is only one phonon (i.e. optical one) which can take part in the scattering and hence only one adjustable parameter. The computations were carried out in the same manner as for electrons. The values of the exponent n_h are plotted in the fig. 5.4 for various values of c_1. It is found that for $n = -2.33$ $c_1 = 1.89$. This means that relatively large

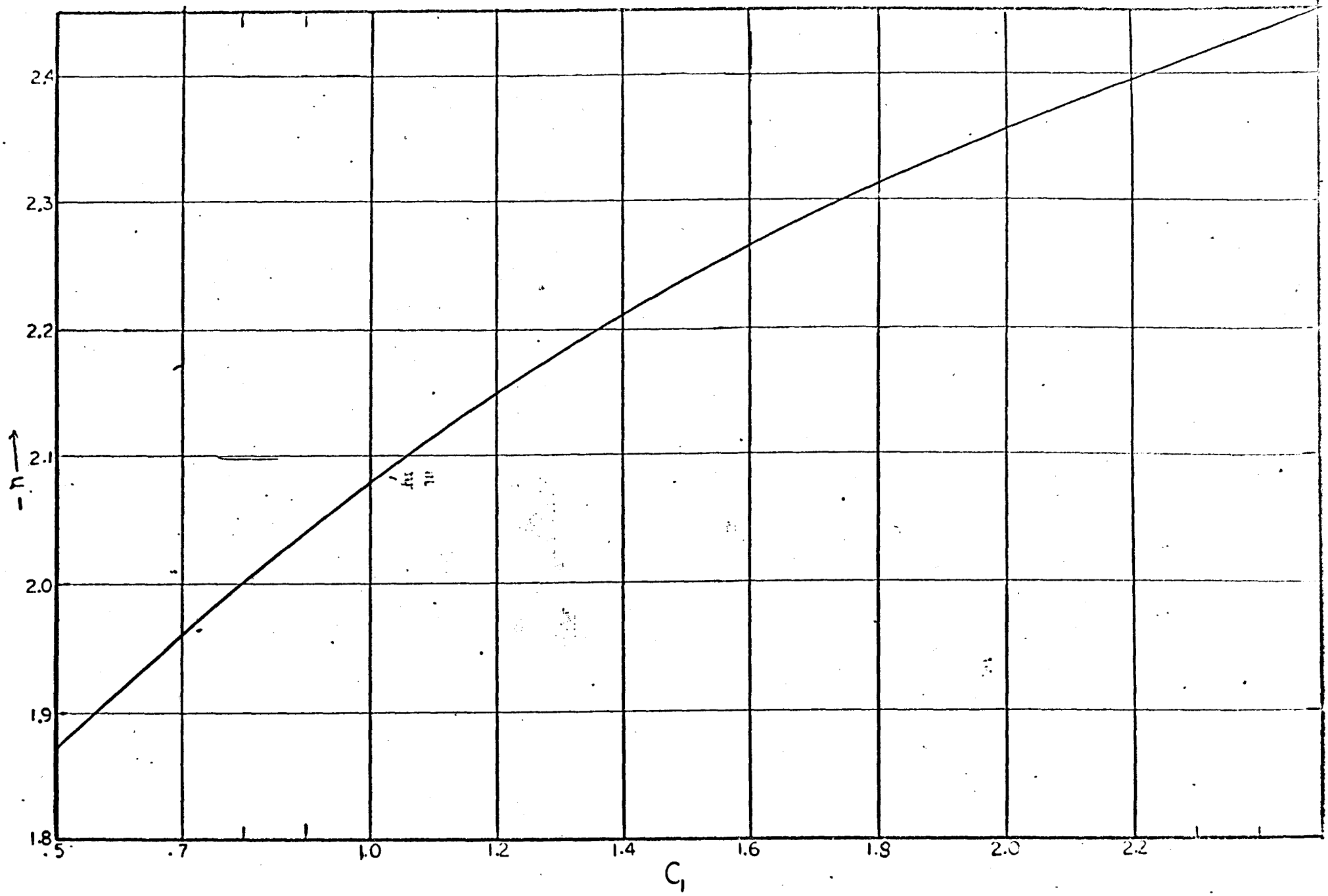

Figure.5.4 Variation of n in T^{-n} for p type Germanium as a Function of c_1

amount of scattering is due to optical mode scattering. This has also been the conclusion of Conwell[26]. With values of $c_l = 1.89$ and $\omega_q/2\pi = 9 \times 10^{12}$ Hz, one can again compute

$$\sigma_p(\omega) = q\, \mu_{po}(T)\, p \left\langle \frac{\tau_p}{1 + j\omega\tau_p} \right\rangle / \langle \tau_p \rangle \qquad (5.20)$$

$$\mu_{po} = .18\ (T/200)^{-2.33}$$

p = hole concentration $/m^3$

p can be calculated from the equation 5.18

5.3.3 Microwave Conductivity and Permittivity of Germanium

The computations of $\sigma(\omega)/\sigma(o)$ and ϵ_{rm} for n type germanium were carried out with the help of a 7040 IBM computer using equations 5.16 and 5.20 as a function of frequency, doping and temperature. The results of the computations are plotted in figures 5.5 through 5.7.

The fig. 5.5 gives $\sigma(\omega)/\sigma(o)$ as a function of temperature and f and doping as parameter. The temperature was varied between 100°k to 500°k and the frequency from 10^9 Hz to 10^{12} Hz. The computations were made with two values of donor densities N_d so as to give the room temperature conductivities of 10 and 100 mhos/m

It may be seen that for all values of T and N_d considered, the microwave conductivity is essentially equal to d.c. conductivity for frequencies less than about 10 GHz. The effect of increasing frequency becomes evident above about 10 GHz and the effect increases at lower temperatures because of the increase in τ and hence $\omega\tau$. As the frequency goes higher, $\sigma(\omega)/\sigma(o)$ decreases even at room temperature.

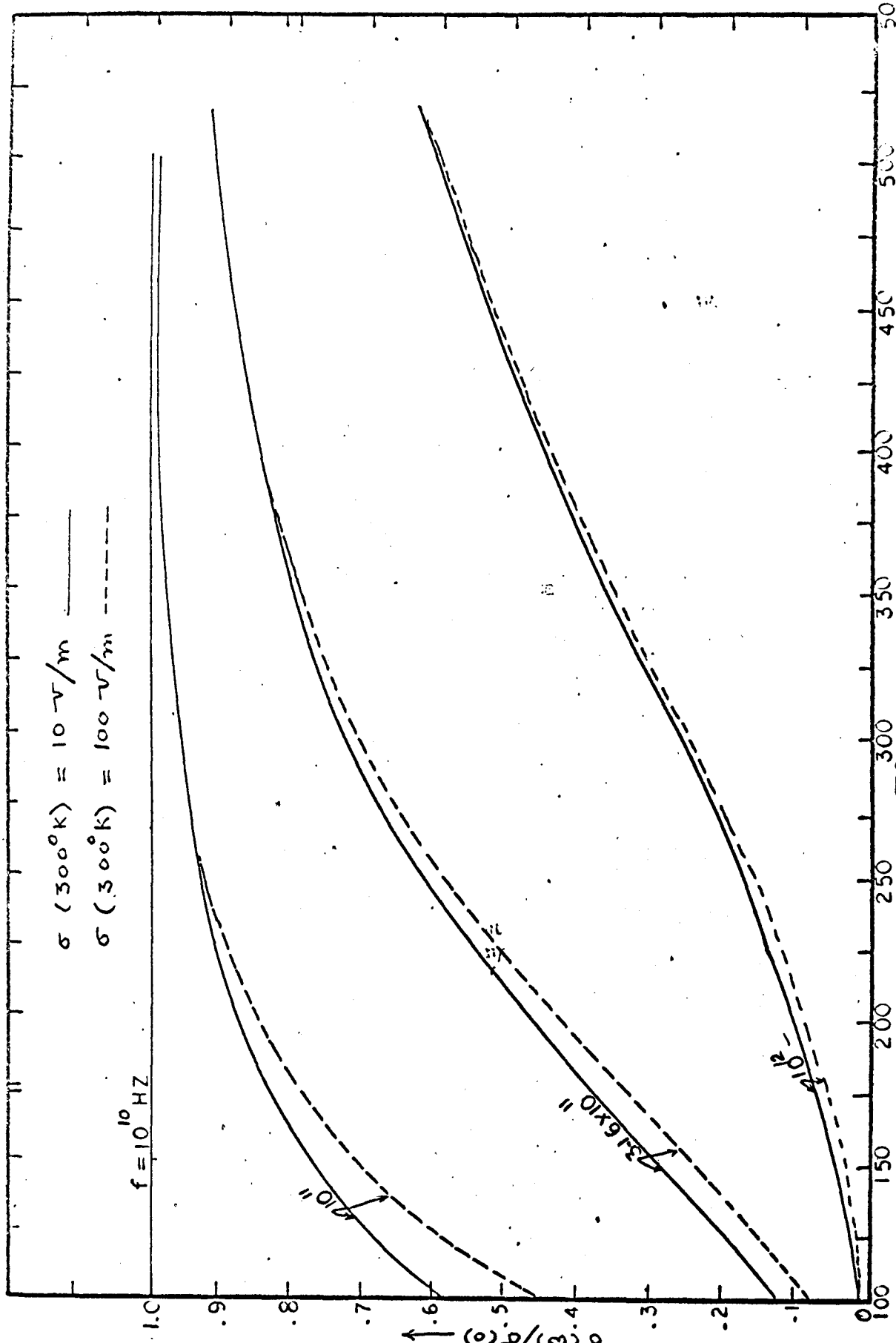

Figure 5.5 Ratio of High Frequency Conductivity to d.c. Conductivity as a Function of T and f.

The effect of the doping is seen to be more significant at lower temperatures.

The effect of frequency on the dielectric constant of germanium is shown in fig. 5.6, in which the abscissa represents the log f, the ordinate the ε_{rm}, with T as a parameter. The doping was kept low so that the doping effect on ε_{rm} is negligible. It may be observed that again the effect of the frequency becomes significant for $f \gtrsim 10^{10}$ Hz for $T \lesssim 200^{o}k$. For high temperatures, the dielectric constant begins to change at higher frequencies than 10^{10} Hz. This is to be expected because both τ_n and τ_p decrease with temperature. It may be further observed that at higher frequencies, the values of ε_{rm} for all values of $T \lesssim 200^{o}k$ approach a limiting value.

This condition applies when $\omega\tau >> 1$ so that

$$\left\langle \frac{\tau^2}{1+\omega^2\tau^2} \right\rangle \rightarrow \frac{1}{\omega^2}$$

The changes in ε_r with temperature are due to two reasons

(i) The value of $\langle\tau\rangle$ and hence $\langle\tau/1+\omega^2\tau^2\rangle$ changes with temperature

(ii) At high temperature, the carrier concentration also changes.

The effect of doping on ε_r is shown in the fig. 5.7. The frequency in these computations was taken to be 9.25 GHz so as to minimize the frequency effect. The effect of doping is seen to be more pronounced at lower temperatures.

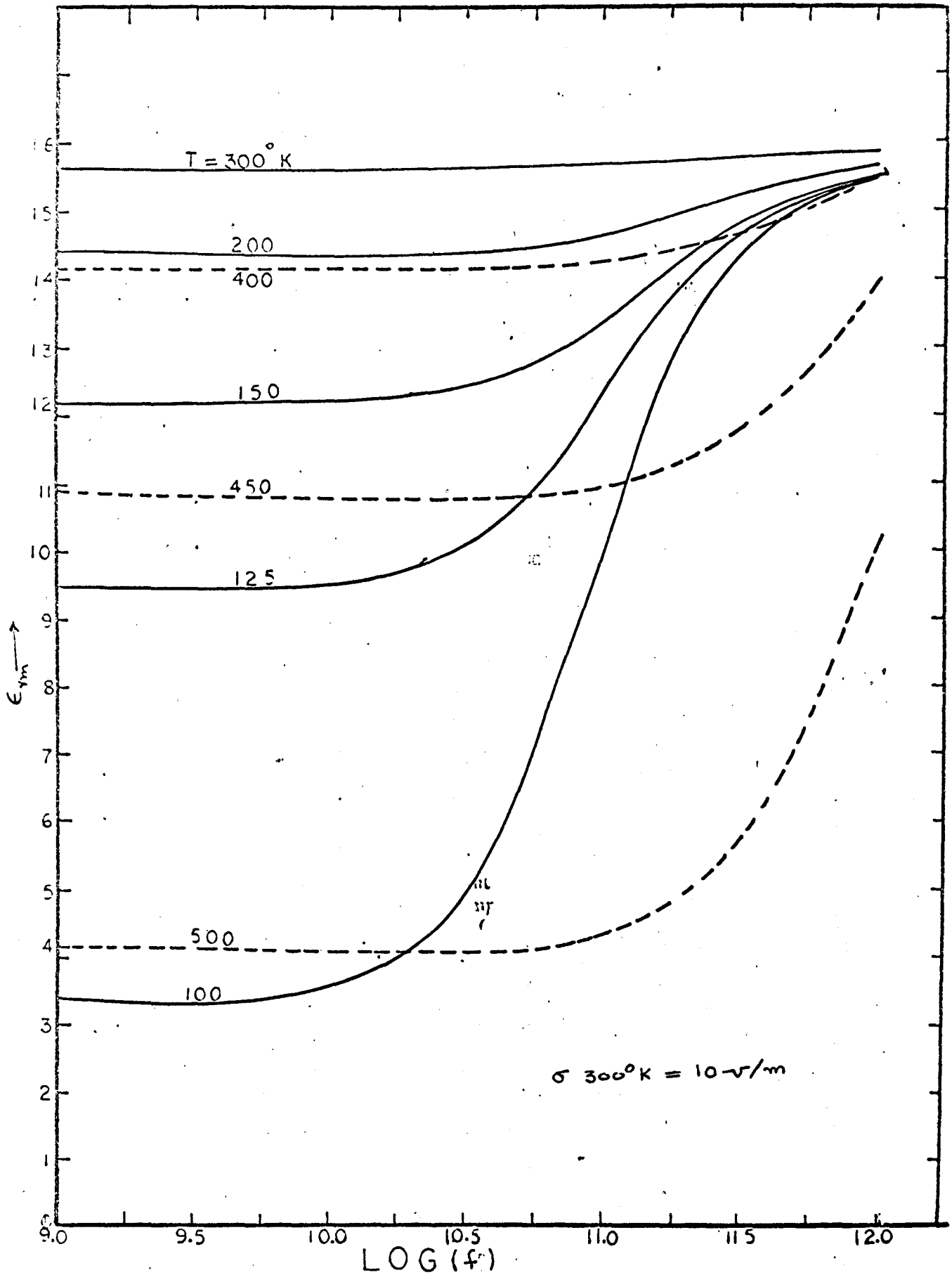

Figure 5.6 Variation of Dielectric Constant of n type Germanium as a Function of f and T

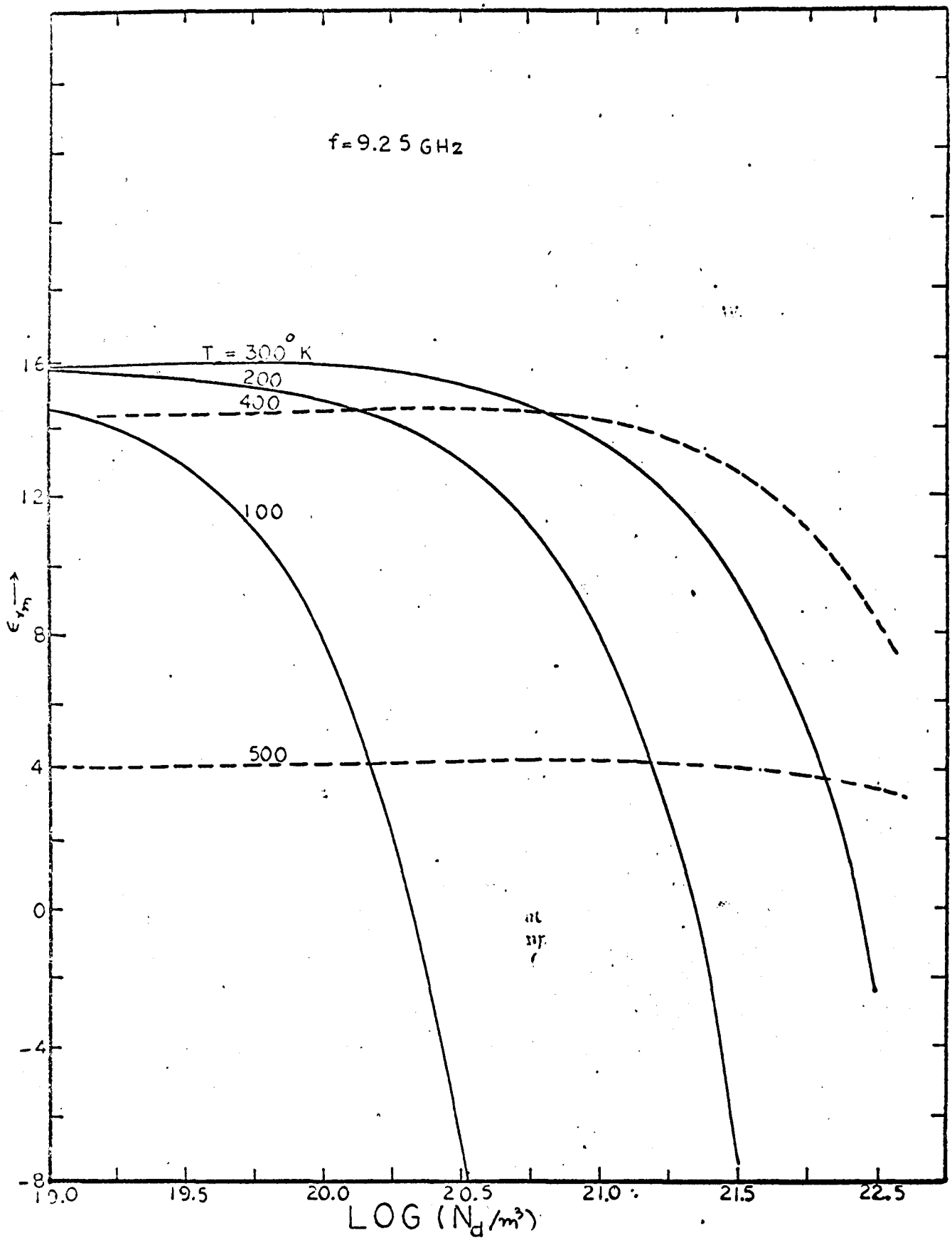

Figure 5.7 Variation of ϵ_{r_m} of n type Germanium with Doping.

5.4 THE MEASUREMENT OF $\sigma(\omega)$ and ε_{rm}

The measurement of the microwave conductivity and dielectric constant was carried out on samples of n type Ge of resistivities of 22Ω-cm and 10 Ωcm at 9.25 and 34.5 GHz. The wave-guide configuration used for these measurements is shown in fig. 1.1. This configuration has the advantage that the material properties can be expressed explicitly in terms of propagation constants and no transcendental equation has to be solved after the propagation constant has been computed.

If γ is the propagation constant in the section of the wave-guide filled with semi-conductor in fig. 1.1 and Γ is the propagation constant in the empty guide, then $\hat{\varepsilon}_r$ is given by

$$\hat{\varepsilon}_{rm} - 1 = \frac{\gamma^2 - \Gamma^2}{k_o^2} = \frac{\gamma^2 - \Gamma^2}{\omega^2 \mu_o \varepsilon_o}$$

so that

$$\varepsilon_r - 1 = \frac{\beta^2 - \beta_o^2 - \alpha^2}{\omega^2 \mu_o \varepsilon_o} \qquad (5.21a)$$

$$\sigma = \frac{2\alpha\beta}{\omega\mu_o} \qquad (5.21b)$$

$$\alpha + j\beta = \gamma$$

$$j\beta_o = \Gamma$$

For a given system γ was computed from the measured value of the reflection coefficient at the interface of an empty guide and the semi-conductor loaded guide at $z = o$ with a short at $z = \ell$, (fig. 5.8).

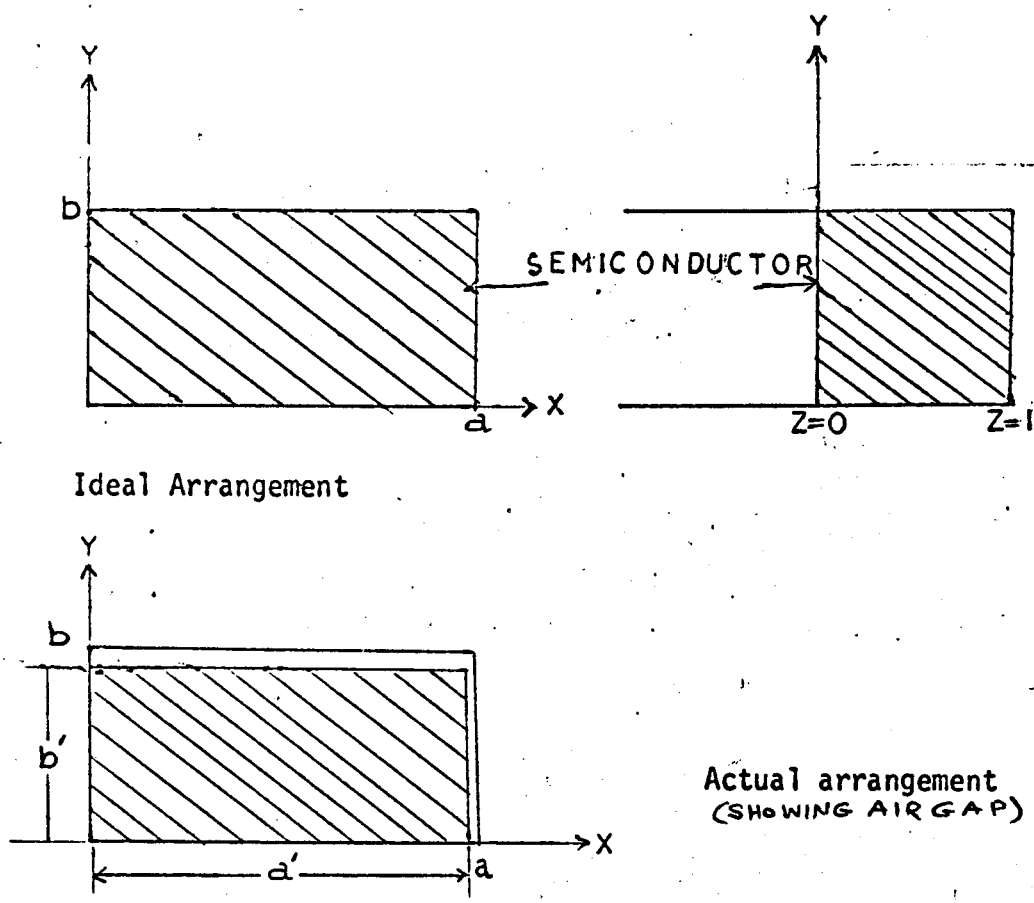

Figure 5.8 Completely Filled Wave-Guide Configuration used in the Experiments on n type Germanium

The propagation constant γ in terms of reflection coefficient R at z=o is given by the solution of the following equation

$$\frac{\tanh \gamma \ell}{\gamma \ell} = z_n / j\beta_0 \ell = \frac{1}{j\beta_0 \ell} \quad \frac{1+R}{1-R}$$

From this equation γ can be computed numerically or graphically using the graphs of Von Hippel[57]. In the present work, however, numerical solution was preferred to obtain a higher accuracy.

The reflection coefficient R was measured by means of the reflection bridge described in the appendix A. For optimum accuracy, the sample length ℓ was chosen to be a quarter wave length approximately.

The measurement of the reflection coefficient at different temperatures was carried out by placing the section of the wave-guide containing the semi-conductor sample in a "Delta Design Chamber" (fig. 4.10) in which the temperature could be caried from -300°F to +600°F by the application of liquid nitrogen or electric heaters. The measurements were carried out between the temperatures of about 100°k to 500°k and the temperature was measured with a copper constantan thermo-couple and an H.P. meter, type 425A, giving an accuracy of about $\pm 2^{\circ}$K.

5.5 EXPERIMENTAL RESULTS AND DISCUSSION

The results of measurement of microwave conductivity and dielectric constant at 9.25 and 34.5 GHz are presented in the figures 5.9 through 5.12. The solid lines represent the theoretical curves of σ and ϵ_{rm} as computed from equations given in previous sections.* The crosses or the circles represent the experimental points. The probable

* The behaviour of σ with temperature as shown in figures 5.9 and 5.10 may be explained as followed. As the temperature is decreased from the/CONTD

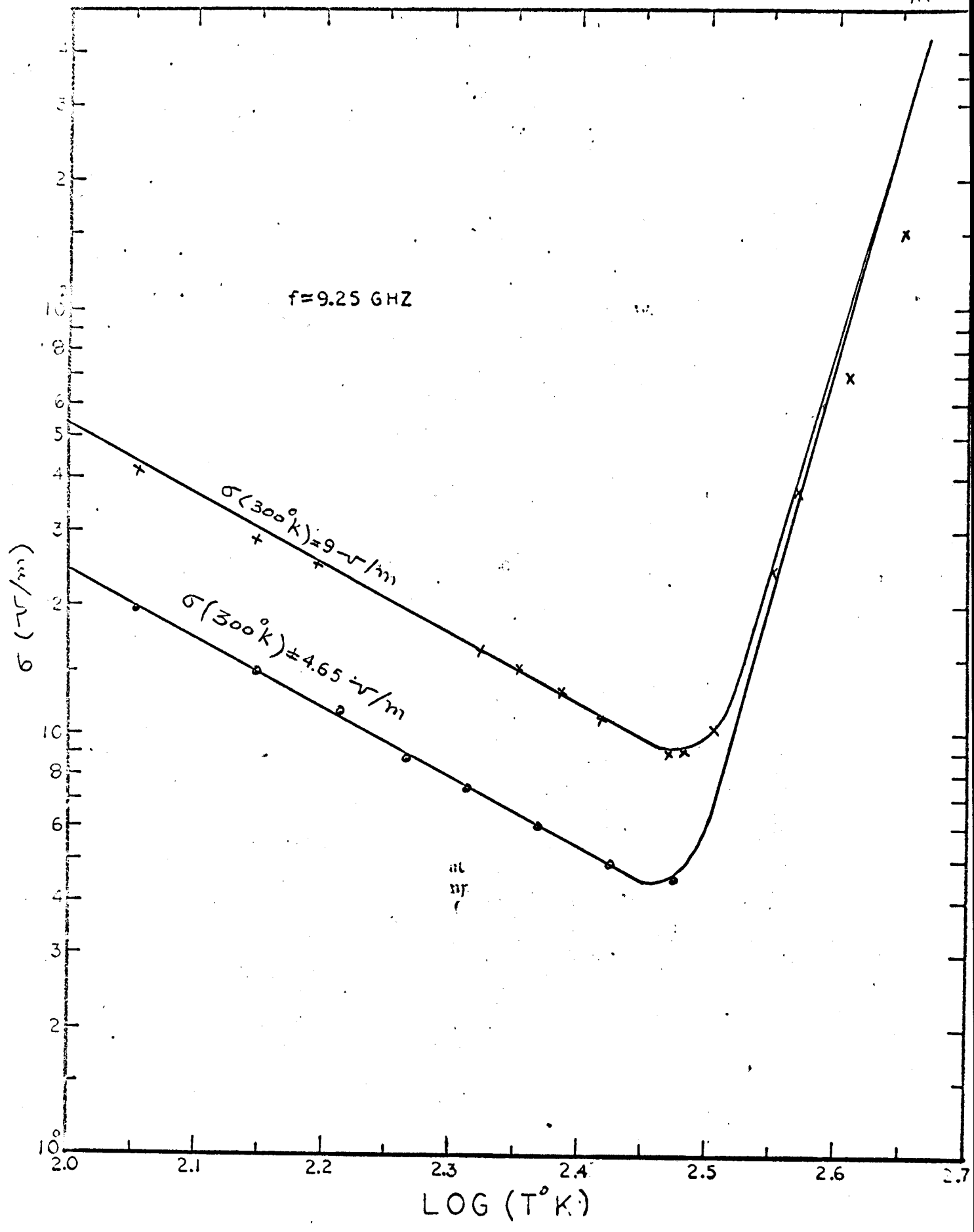

Figure 5.9 The Theoretical (Solid Curves) and Practical (Circles and Crosses) Values of $\sigma^{(\omega)}$ as a Function of Temperature

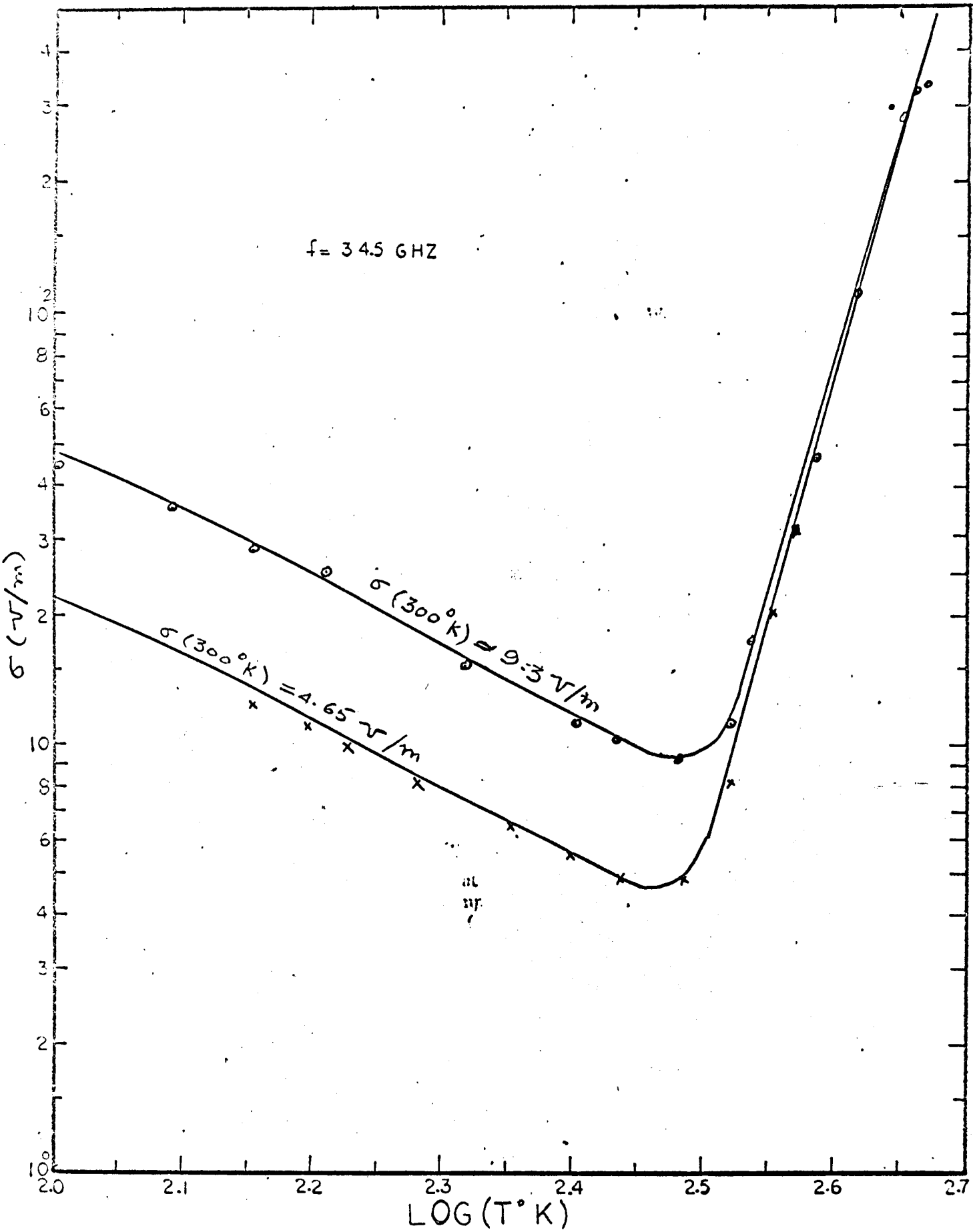

Figure 5.10 The Theoretical (Solid Curves) and Practical (Circles and Crosses) Values of $\sigma^{(\omega)}$ as a Function of Temperature

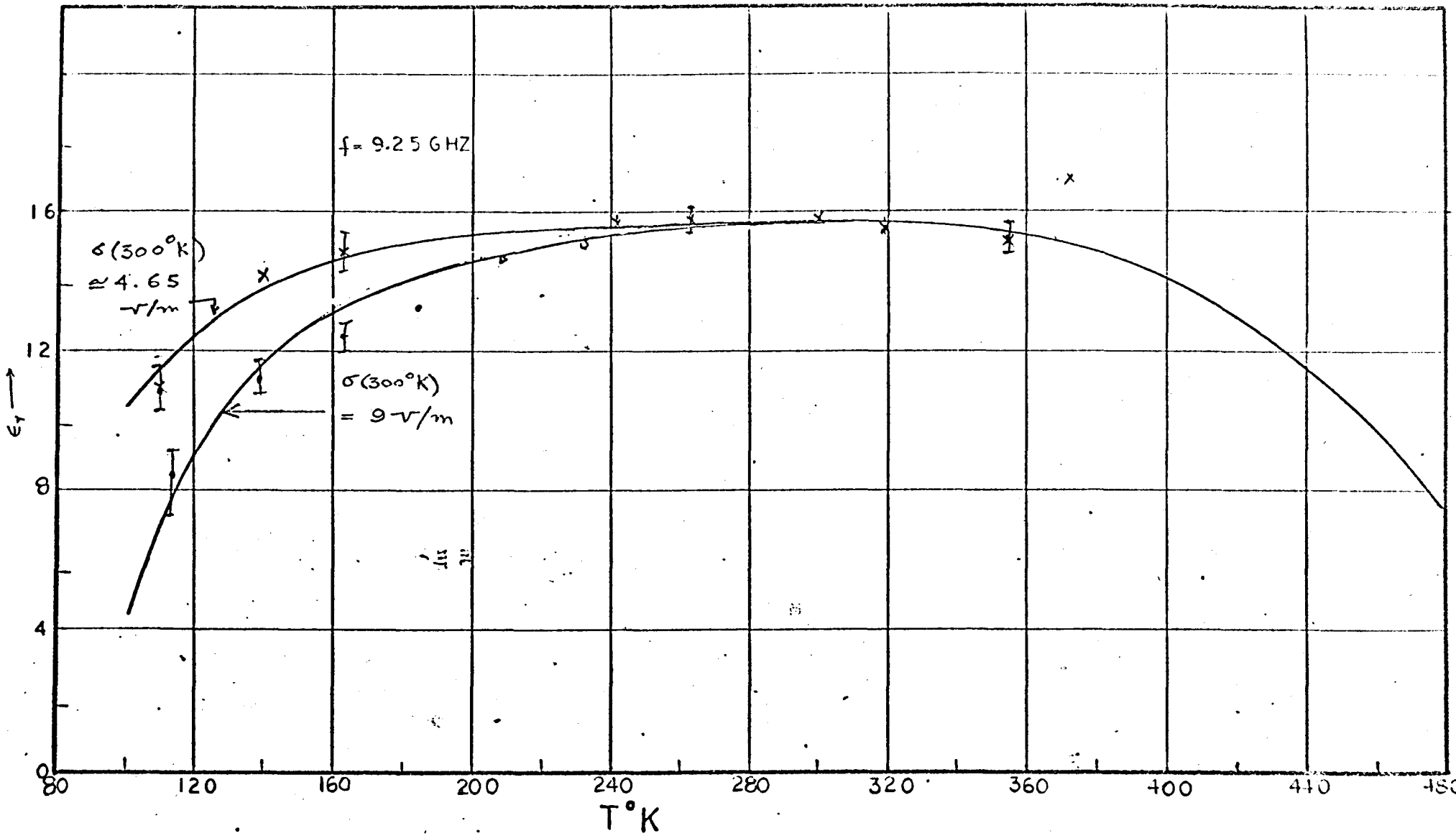

Figure 5.11 The Theoretical (Solid Curves) and Practical (Circles and Crosses) Values of ϵ_r as a Function of Temperature

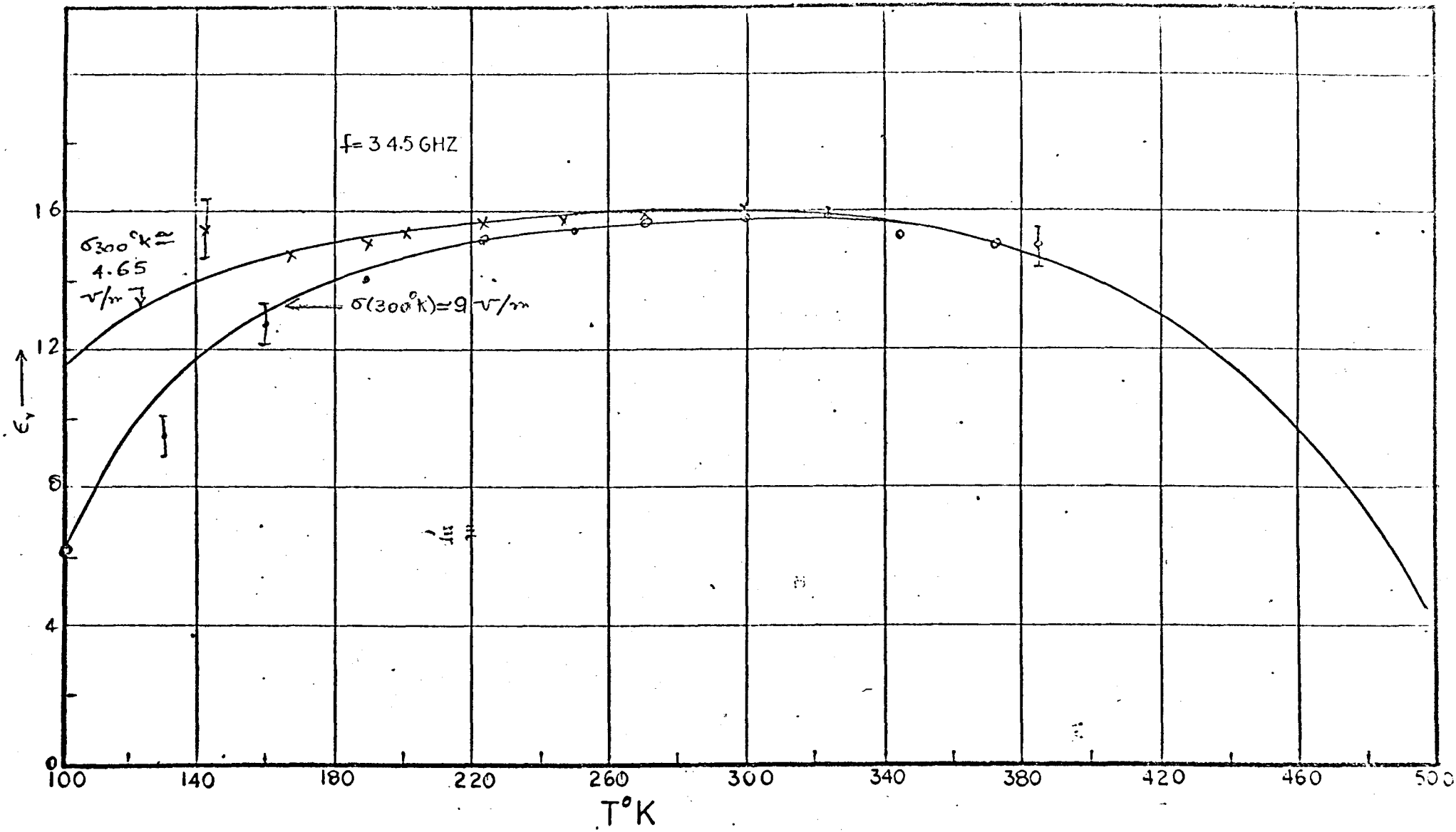

Figure 5.12 The Theoretical (Solid Curves) and Practical (Circles and Crosses) Values of ϵ_r as a Function of Temperature

errors were computed from the estimated errors in the reflection coefficient and the uncertainty in the b dimension of the sample.

To interpret the data, the gap effect was taken into account. This was necessary because the sample dimensions were not exactly equal to the waveguide dimensions. The gap between the sample and the broad walls has been found to have a considerable effect on the measurement of $\hat{\varepsilon}_r$ [16,17]. In the present work, the following two equations were considered,

$$\hat{\varepsilon}_r(m) = (\hat{\varepsilon}_r - 1)\, b'/b \tag{5.22}$$

$$\hat{\varepsilon}_r(m) = \hat{\varepsilon}_r / \left[1 + (\hat{\varepsilon}_r - 1)\, \frac{b-b'}{b}\right] \tag{5.23}$$

where $\hat{\varepsilon}_r$ is the actual permittivity, $\hat{\varepsilon}_r(m)$ the measured value of permittivity and b' is the actual narrow dimension of the sample.

While applying the correction for the gap effect, it was found that for low values of conductivities, equation (5.22) gives adequate results. The equation (5.23) however, was found to be valid only at higher conductivities, say greater than about 25 mhos/m. At lower values of conductivities, (5.23) was found to overcorrect the measured values. For example, at room temperature, and for $\frac{b-b'}{b} = 1/160$ and measured values of $\varepsilon_r = 15.7$ and $\rho = 10.4$ ohms-cm, the equation (5.22) and (5.23) gave the values of $\varepsilon_r = 15.8$, $\rho = 10.3$ and $\varepsilon_r = 14.4$ $\rho = 8.6$ ohm-cm respectively. The former values are closer to the theoretical values.

room temperature, the mobility of the carriers increases while the number of carriers in a doped material remains practically constant - about 100°K. Thus the conductivity increases with the decrease in temperature. The rise in the conductivity above room temperature is due to the rapid increase in the numbers of intrinsic carriers.

It may be seen from figures 5.9 through 5.12 that the agreement between the measured values and theoretical values of σ is quite good. There seems to be some discrepancy between the measured values of σ and the theoretical curve at 9.25 GHz at higher end of the temperatures. This is possibly due to the gap effect. The equation 5.23 which is obtained from the first order perturbation theory [16] probably fails at high values of $\frac{\sigma}{\omega\epsilon_0}$ that occur at higher temperatures.

There is seen to be a fair agreement of ϵ_r between theory and experiment. The discrepancy at lower end of temperature is again attributed to the gap effect. At higher end of temperature, it is found that it is not possible to get accurate values of ϵ_r even after applying the correction due to the gap effect. The reason for this is that as T and hence σ goes high, the contribution of ϵ_r to the propagation constant becomes negligible, $\hat{\epsilon}_r \rightarrow -j\frac{\sigma}{\omega\epsilon_0}$ and $\alpha \rightarrow \beta$. When this happens, it may be seen from the equation (5.21a) that even a small measuring error of α or β would cause a large error in the measurement of ϵ_r. A very high accuracy, indeed, would be required to measure ϵ_r in this situation.

CHAPTER VI

CONCLUSIONS

6.1 GENERAL

A variety of microwave measuring techniques are required to measure the complex permittivity ($\hat{\epsilon} = \epsilon_0\epsilon_r - j\frac{\sigma}{\omega}$) of semi-conductors because of large possible variation in the conductivity. The accuracy of measurement depends on the choice of a particular technique for a given conductivity value. A number of methods of measurement have been investigated to determine the range of conductivities to which they are best suited.

Particular attention has been given to systems which involve the measurement of the reflection coefficient. A fully filled wave-guide configuration has been used to investigate the dependence of the complex permittivity of n type germanium on temperature, frequency and doping. An investigation of the exact and the approximate expressions used for computations of the dominant mode propagation constant in a partially filled wave-guide configuration has been carried out together with the effects of the higher order modes which are excited at the junction of such a guide and an empty one. During the investigations a new method of measurement involving the replacement of one narrow wall of a rectangular wave-guide was developed. This method has been termed the "lossy wall measuring technique".

6.2 LOSSY WALL MEASURING TECHNIQUE

The theory of the wave propagation in such a system and the exact and the approximate expressions for the propagation constants of H_{no} modes are developed in the Chapter III. Numerical computations of the dominant mode propagation constant are presented for $1 \leq \sigma \leq 1000$ mhos/m and $0 \leq \varepsilon_r \leq 16$. The calculations were done for three frequencies 9.25, 34.5 and 70.5 GHz. Experiments to confirm the theory were performed at 9.25 GHz with germanium samples of conductivity in the range $2 < \sigma < 400$ mhos/m and the measurements were made with a microwave transmission bridge.

The computations show that the approximate expressions for the propagation constant give adequate results at the higher end of the range of ε_r considered and over the whole range of conductivity considered. The computations further show that this method of measurement is most useful when $\sigma \simeq \omega\varepsilon_0\varepsilon_r$ and becomes more accurate with the increasing frequency.

The experimental results at 9.25 GHz give accurate results for both ε_r and σ in the conductivity range $4 \gtrsim \sigma \gtrsim 20$ mhos/m. However, for lower values of σ, the conductivity measurement is not accurate but the dielectric constant term is in good agreement with the expected value. This disagreement is attributed to errors in the measurement of the small phase change produced in such a system and the inadequacy of the theoretical model which assumes only the TE_{10} mode propagating in the system. Also, the experimental results show that for $\sigma \gtrsim 20$ mhos/m the measurement of ε_r is not accurate. This is attributed to

the fact that in this range of σ, small errors in the measurement of the transmission coefficient can cause large errors in the calculated values of ε_r.

6.3 PARTIALLY FILLED WAVE-GUIDE

6.3.1 Exact and Approximate Solution of the Dominant Mode Propagation Constant

A wave-guide configuration commonly used in the measurement of various electrical properties of semi-conductors is the one shown in the fig. 1.3. In the measurements previously reported in literature, the propagation constant has been computed from approximate expressions, the accuracy of which has been doubtful. Computations of the dominant mode propagation constant for $0.1 \leq \sigma \leq 10$ mhos/m, $.001 \leq t/a \leq 0.25$ and $\varepsilon_r = 16, 12$ have been carried out at three different frequencies 10, 34.5 and 70.5 GHz using the exact and approximate expressions. The computations show that for all values of σ and t/a considered at 34.5 and 70.5 GHz and $t/a < .05$ and $\sigma \leq 10$ mhos/m, at 10 GHz the attenuation constant varies linearly with σ so that α = constant x σ. The variations of γ with ε_r are found to be significant only at higher end of the ranges of t/a and σ.

The comparison of the exact and the approximate values of the propagation constant shows that unless t/a is very small (<.0025), the approximate expressions do not give adequate results for the ranges of t/a, σ and ε_r considered.

These calculations, which have not been previously reported, show

that approximate methods of solution for the propagation constant of a wave-guide partially filled with a semi-conductor should be used with due caution.

6.3.2 Higher Order Modes Effect

In a practical experimental arrangement, this partially filled structure forms a junction with an empty guide. At such a junction higher order modes are excited. The effect of H_{no} higher order modes has been studied and the expression for the input impedance at the junction (z=o) is obtained for such a structure terminated with a short circuit. Calculationsof the reflection coefficient at the junction z = o are obtained for $1 \leq \sigma \leq 10$ mhos/m, $0.01 \leq t/a \leq 0.25$ and $\varepsilon_r = 16$, at 9.25 GHz. The mode number n was varied from 1 to 7 (1, 3, 5, 7). The calculations show that unless $t/a \gtrsim .08$ and $\sigma \gtrsim 2.5$ mhos/m, the effect of the higher order modes becomes significant.

Experiments were also performed to measure the reflection coefficient at such a junction at 9.25 GHz for t/a values of .0133, .026 and .0515 and $2 \leq \sigma \gtrsim 100$ mhos/m. The measurement results were found to confirm the above observations about the higher order modes. The best fit between theory and experiment is obtained with N=7 (the order the higher mode) for higher values of σ and t/a.

This wave-guide system with semi-conductor has possible application to microwave modulating devices and this study was undertaken to determine characteristics of such a structure which have not been previously reported.

6.4 EFFECT OF FREQUENCY, DOPING AND TEMPERATURE ON THE COMPLEX PERMITTIVITY OF N-TYPE GERMANIUM

Theoretical computations have been made of microwave dielectric constant and conductivity of n type germanium as a function of temperature ($100^{0} \leq T \leq 500^{0}K$), frequency ($10^{9} \leq f \leq 10^{12}$ Hz) and doping ($10^{19} \leq Nd \leq 10^{22}/m^{3}$). The theoretical model used to evaluate the average relaxation time constant includes the scattering by ionized impurities, acoustical and optical mode scattering of charge carriers.

These calculations show that the effect of the frequency for $f \lesssim 10^{10}$ Hz on both σ and ε_r is negligible. At higher frequencies the conductivity decreases and the dielectric constant increases from its low frequency value. The effect is more pronounced at lower temperatures due to the increase in $\langle\tau\rangle$ and hence $\langle\omega^{2}\tau^{2}\rangle$. The effect of the doping is also found to be significant at high impurity concentration and low temperature.

The effect of temperature is such that at a given frequency, the dielectric constant decreases and conductivity increases with a decrease in temperature. This is due to the increase in the value of $\langle\tau\rangle$. Above room temperature and with light doping, the thermally excited carriers have a considerable effect on the dielectric constant.

The associated experiments for measuring the dielectric constant and the conductivity of n type germanium samples of $\sigma \simeq 9$ and 4.7 mhos/m at 9.25 and 34.5 GHz were carried out with the microwave reflection bridge. The completely filled wave-guide configuration was used and the temperature range was $100^{0} \leq T \leq 500^{0}K$. Such measurements for n type germanium

have not been reported previously.

It was found necessary to apply a correction factor for the effect of the unavoidable air gap between the sample and the wave-guide walls. The investigations showed that the first order perturbation theory was valid for $\sigma/\omega\varepsilon_0 \lesssim 4$. With such corrections good agreement between theory and experiment was found between $100^0 \leq T \lesssim 400^0$K at 9.25 GHz and $100^0 \leq T \lesssim 450^0$K at 34.5 GHz and the validity of the theoretical model was confirmed.

APPENDIX A

MICROWAVE REFLECTION BRIDGE

A1 BRIDGE DESCRIPTION

The schematic diagram of the reflection bridge used for the experiments described in the chapters 4 and 5 is given in the fig. A1. The microwave power source feeds the H-arm of a magic tee. Arm I of the tee has coupled to it a reflection coefficient reference which consists of a precision type variable calibrated attenuator followed by a precision type variable short circuit. The second arm is coupled to the network under test and a matched detector is connected to the E-arm.

The measurement of the reflection coefficient under test is carried out in two steps, as follows.

(a) First a fixed short is coupled to the arm II of the tee and the attenuator and the short in arm I are varied to obtain minimum power output in the detector in the E-arm. Let $A_o^{(nep)}$ and $l_o^{(meters)}$ be the readings of the attenuator and the short respectively, for this condition.

(b) Now the test assembly with a reflection coefficient R is placed in arm II, at the same plane as the short in the step I. Again the attenuator and short in the arm I are varied to obtain minimum output in the E-arm. Let these readings be

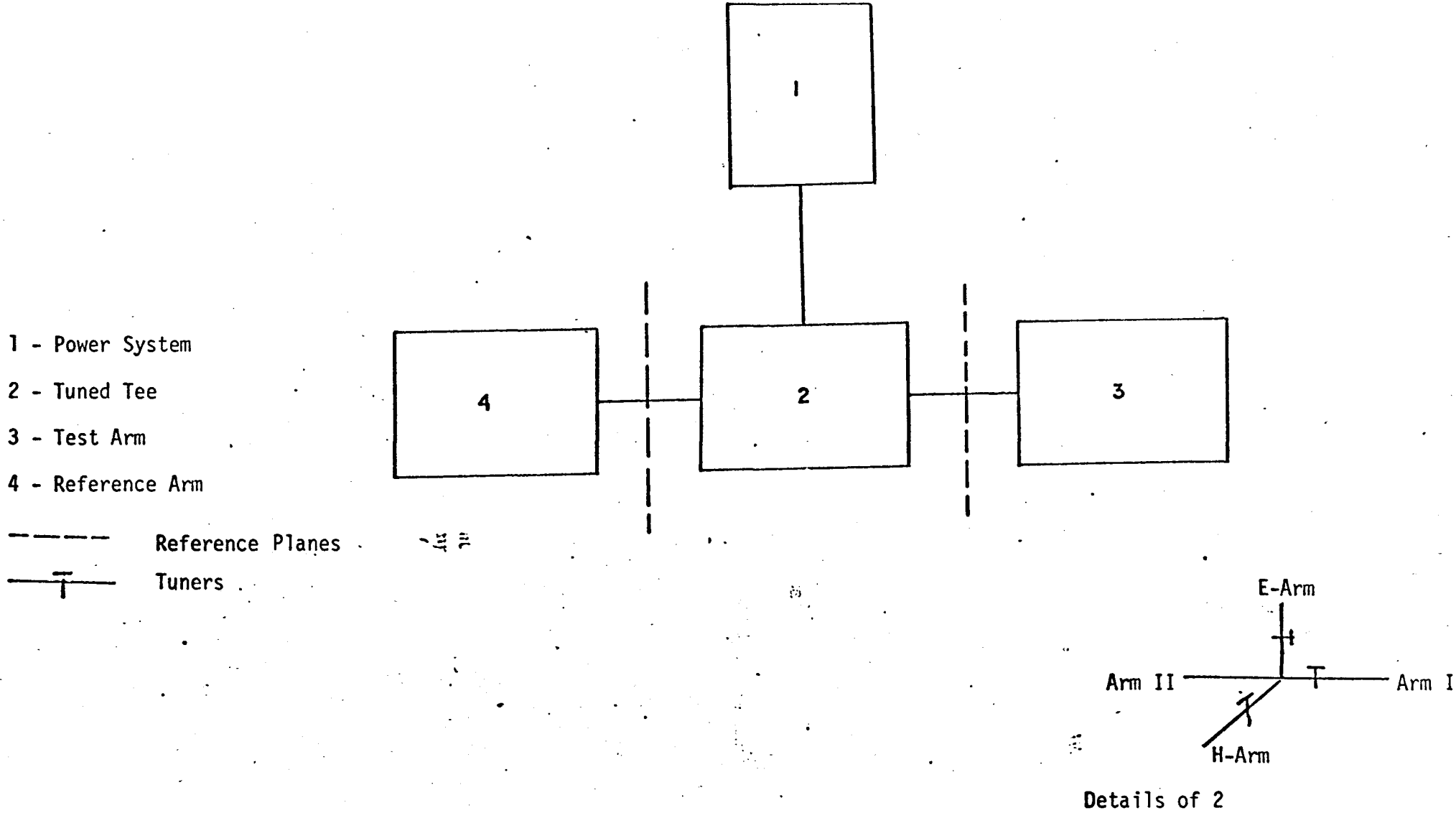

Figure A1 Schematic Diagram of the Microwave Reflection Bridge Used in the Experiments.

A_1 neps and ℓ_1 meters respectively. Then, as shown later, R is given by

$$R = - \exp - 2(A+j\phi) \qquad (A1)$$

where $A = A_1 - A_0$ nepers

$\phi = \beta_0(\ell_1 - l_0)$ radians

β_0 = phase constant in the variable short

A2 SCATTERING MATRIX OF TEE

Equation A_1 may be proved by considering the scattering matrix of a hybrid tee. This is as follows for the tee shown in the fig. A2.

$$S = \begin{bmatrix} S_{11} & S_{12} & S_{13} & S_{14} \\ S_{21} & S_{22} & S_{23} & S_{24} \\ S_{31} & S_{32} & S_{33} & S_{34} \\ S_{41} & S_{42} & S_{43} & S_{44} \end{bmatrix} \qquad (A2)$$

If the system is lossless and isotropic, then the reciprocity theorem gives

$$S_{ij} = S_{ji} \quad i \neq j$$

Now if it is assumed that the tee has been tuned so that

$$S_{33} = 0 = S_{44}$$

$$S_{34} = 0 = S_{43}$$

then the scattering matrix reduces to

$$S = \begin{bmatrix} S_{11} & S_{12} & S_{13} & S_{14} \\ S_{12} & S_{22} & S_{23} & S_{24} \\ S_{13} & S_{23} & 0 & 0 \\ S_{14} & S_{24} & 0 & 0 \end{bmatrix} \qquad (A3)$$

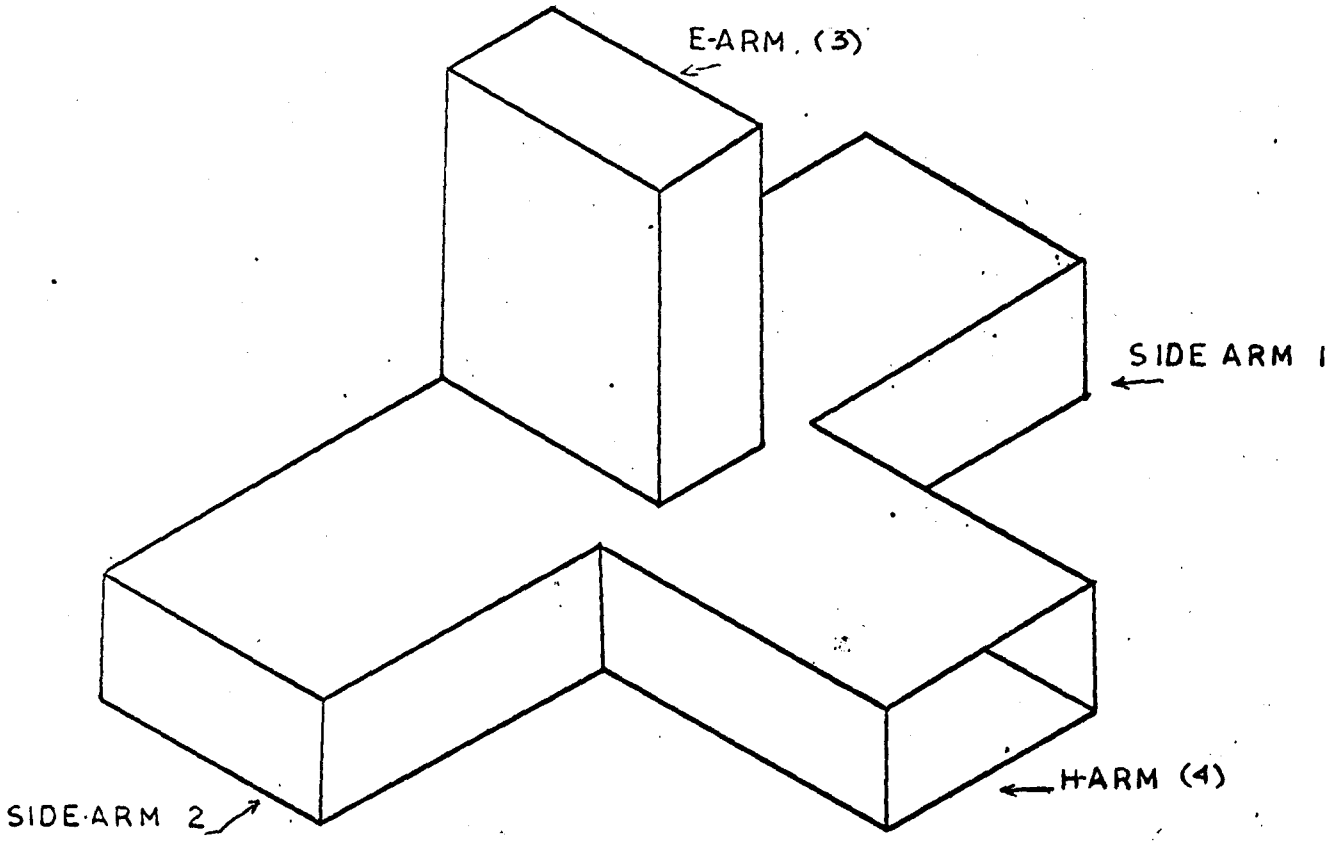

Figure A2 Three Dimensional View of a Hybrid Tee

The scattering matrix is a unitary one[31] and the following theorem applies.

"The sum of the squares of the absolute magnitudes of elements in any row (or column) is unity". This theorem gives from equation (A3)

$$|S_{11}|^2 + |S_{12}|^2 + |S_{13}|^2 + |S_{14}|^2 = 1 \qquad \text{(A4a)}$$

$$|S_{12}|^2 + |S_{22}|^2 + |S_{23}|^2 + |S_{24}|^2 = 1 \qquad \text{(A4b)}$$

$$|S_{13}|^2 + |S_{23}|^2 = 1 \qquad \text{(A4c)}$$

$$|S_{14}|^2 + |S_{24}|^2 = 1 \qquad \text{(A4d)}$$

Adding (A4a) and (A4b) and using (A4c) and (A4d) gives

$$|S_{11}|^2 + |S_{22}|^2 + 2|S_{12}|^2 = 0$$

$$\therefore S_{11} = S_{22} = S_{12} = 0$$

Thus (A3) reduces to

$$S = \begin{bmatrix} 0 & 0 & S_{13} & S_{14} \\ 0 & 0 & S_{23} & S_{24} \\ S_{13} & S_{23} & 0 & 0 \\ S_{14} & S_{24} & 0 & 0 \end{bmatrix} \qquad \text{(A5)}$$

Now if a_i is the incident waves at the port i and b_i is the reflected wave at that port, then

$$b_1 = a_3 S_{13} + a_4 S_{14}$$

$$b_2 = a_3 S_{23} + a_4 S_{24}$$

$$b_3 = a_1 S_{13} + a_2 S_{23}$$

$$b_4 = a_1 S_{14} + a_2 S_{24}$$

Assuming that the detector, which is coupled to arm 3 is matched so that $a_3 = 0$, the above equations give

$$\frac{b_1}{b_2} = \frac{S_{14}}{S_{24}}$$

If R_1 and R_2 are the reflection coefficients at the arms I and II respectively so that

$$a_1 = R_1 b_1 \text{ and } a_2 = R_2 b_2,$$

then
$$b_3 = R_1 S_{13} b_1 + R_2 S_{23} b_2$$

$$= R_1 S_{13} \frac{S_{14}}{S_{24}} b_2 + R_2 S_{23} b_2$$

$$= b_2 R_1 \frac{S_{13} S14}{S_{24}} + S_{23} R_2 \qquad \text{(A6)}$$

Now if

(a) $R_2 = -1$ (short circuit plate), and $R_1 = R_{10}$ so that $b_3 = 0$, (balanced condition), then

$$10 \quad \frac{S_{13} S_{14}}{S_{24}} = + S_{23}$$

and (b) $R_2 = R$ (under test) and $R_1 = R_{11}$ so that again $b_3 = 0$, then

$$R_{11} \quad \frac{S_{13} S_{14}}{S_{24}} = - R S_{23}$$

The above two equations give

$$R = \frac{R_{11}}{R_{10}} \qquad \text{(A7)}$$

A3 REFLECTION COEFFICIENT OF THE REFERENCE ARM

The reference arm consists of a precision variable attenuator and a precision variable short connected in cascade as shown in fig. A3. The scattering matrix of the attenuator is for an isotropic system

$$S = \begin{bmatrix} S_{11} & S_{12} \\ S_{12} & S_{22} \end{bmatrix}$$

and the incident and reflected waves at the ports are given by

$$\begin{bmatrix} b_1 \\ b_2 \end{bmatrix} = \begin{bmatrix} S_{11} & S_{12} \\ S_{12} & S_{22} \end{bmatrix} \begin{bmatrix} a_1 \\ a_2 \end{bmatrix}$$

When a calibrated sliding short is connected at the port 2, then

$$a_2 = - [\exp (-2j\beta_o x)] b_2$$

where β_o = phase constant in the sliding short system

x = distance of the short from the reference plane

$$\therefore \quad b_1 = S_{11} a_1 - S_{12} e^{-2j\beta_o x} b_2$$

$$b_2 = S_{12} a_1 - S_{22} e^{-2j\beta_o x} b_2$$

$$\text{or} \quad b_2 \left\{ 1 + S_{22} e^{-2j\beta_o x} \right\} = S_{12} a_1$$

$$\therefore \quad b_1 = S_{11} a_1 - S_{12} e^{-2j\beta_o x} \left[\frac{S_{12} a_1}{1 + S_{22} e^{-2j\beta_o x}} \right]$$

$$\text{or} \quad \frac{b_1}{a_1} = \left[S_{11} - \frac{S_{12}^2 e^{-2j\beta_o x}}{1 + S_{22} e^{-2j\beta_o x}} \right]$$

If S_{11} and S_{22} are small as compared to unity, the above equation

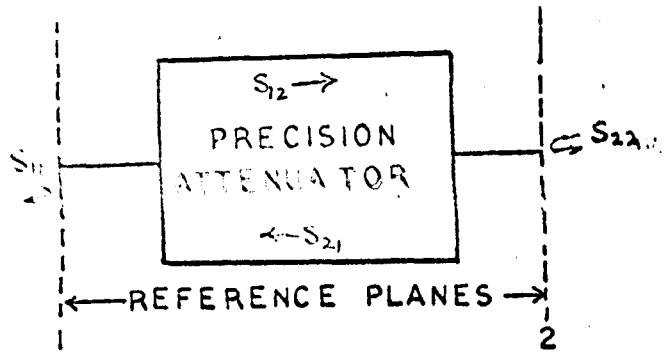

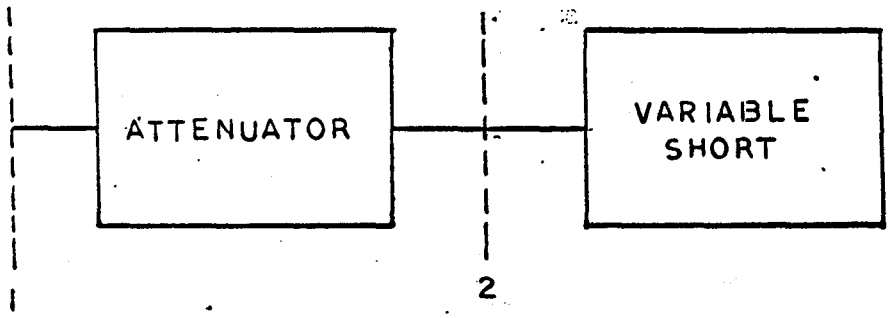

Figure A3 The Details of the Reference Arm

reduces to

$$\frac{b_1}{a_1} = - S_{12}^2 \, e^{-2j\beta_0 x}$$

Now if the wave suffers an attenuation of y nepers while travelling in the attenuator, then

$$S_{12} = e^{-y}$$

$$\therefore \quad \frac{b_1}{a_1} = - e^{-2(y+j\beta_0 x)} = 0$$

$$\therefore \quad \frac{R_{10}}{R_{11}} = - e^{-2(A_1-A_0)-2j\beta_0(\ell_1-\ell_0)}$$

$$= -e^{-(A+j\phi)} \qquad \text{(A8)}$$

A4 TUNING OF A HYBRID TEE

In the above analysis it is assumed that $S_{33} = S_{44} = S_{34} = 0$ and in a commercial grade tee it is seldom so. In order to meet this condition it is necessary to place lossless tuners in the E and H arms and make the VSWR looking into these arms unity with arms I and II terminated with matched loads. In practice it is very difficult to get a VSWR less than 1.02 to 1.03. After this adjustment S_{34} is checked by measuring the output in the E-arm while feeding the H-arm with terminations placed on arms I and II. If S_{34} is not zero, it can be reduced to a minimum by placing a tuner in one of the side arms. This adjustment will usually disturb the tuning of E- and H- arms so these must again be tuned and the process repeated till the effect the side arm tuner on

E and H arms tuning becomes negligible. If the tee is of good quality S_{34} will normally be very small and need only very small amount of tuning to make S_{34} negligible.

APPENDIX B

COMPUTER PROGRAMMES

FLOW CHART
FOR
LOSSY WALL GUIDE

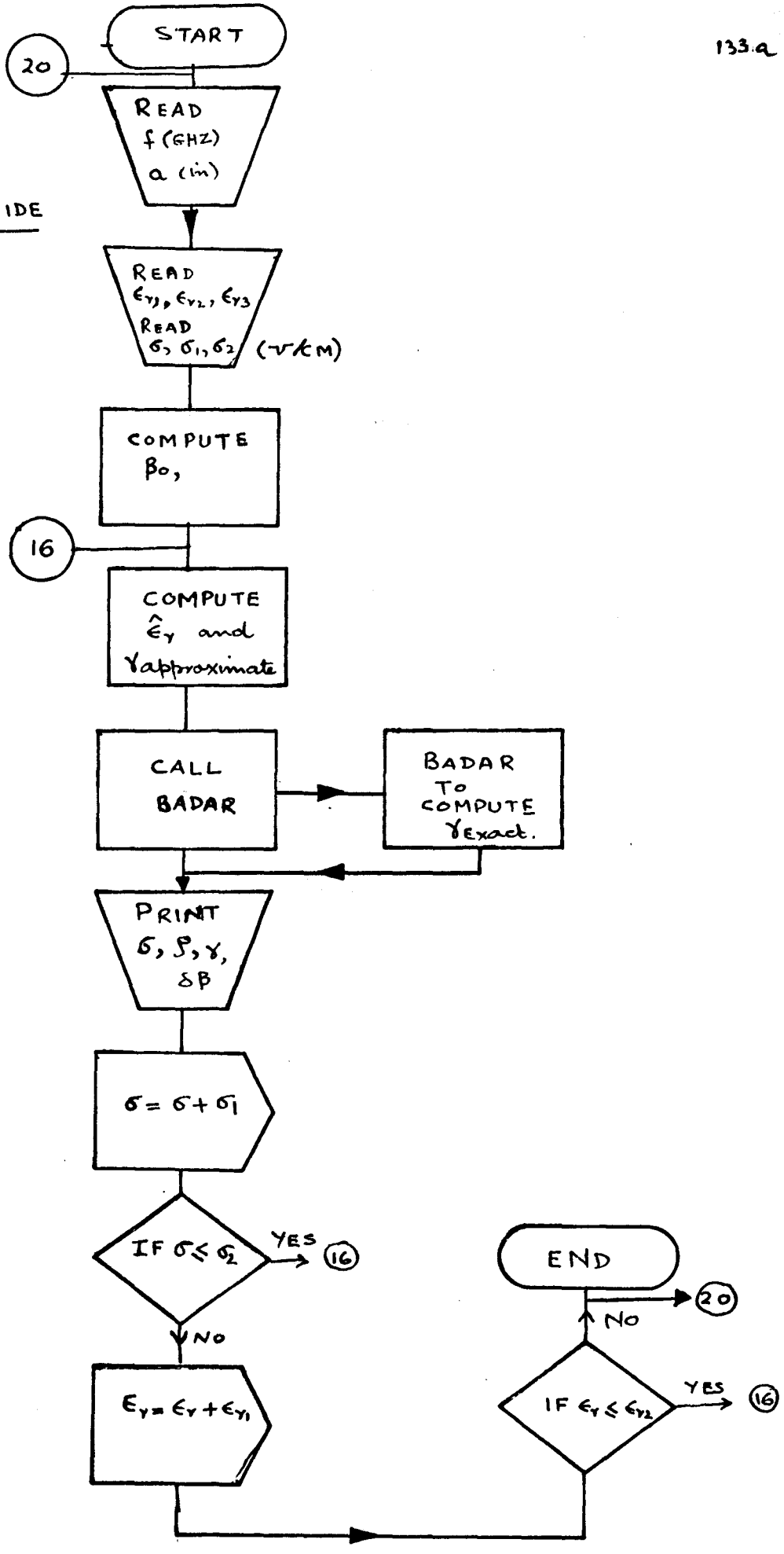

```
$JOB   WATFOR  0005053SHEIKH          015    004
$IBJOB         NODECK
$IBFTC WALLOS
C LOSSY WALL WAVE GUIDE
C SOLUTION OF DOMINANT MODE PROPAGATION CONSTANT AS A FUNCTION OF ε_r and σ
C
      COMPLEX C, CP, CD, Y, FY, DFY, U, AKC, DY, GAME, GAMA
      DIMENSION  VER (3), VSIO(3)
   20 CONTINUE
      READ (5,1) A,F
    1 FORMAT (2F10.5)
      READ(5,2) (VER(I),I=1,3),(VSIO(I),I=1,3)
    2 FORMAT (3F10.5)
      ER = VER(1)
      SI = VSIO(1)
      V = 2.998E10
      PI = 3.141593
      AMU = 4.*PI*1.E-9
      EPSO = 1./(AMU*V*V)
      F = F*1.E9
      A = A*2.54
      OMEGA = 2.*PI*F
      OMEGS = OMEGA*OMEGA
      BETAO = SQRT(OMEGS/V/V - PI*PI/A/A)
      XX = OMEGS/V/V
    3 CONTINUE
      WRITE (6,8) ER
    8 FORMAT (4H ER=,F10.2/)
   16 CONTINUE
      CP = CMPLX(ER , -SI/OMEGA/EPSO)
      CD = XX*A*A*CP
      C = CSQRT(-1./CD)
      GAMA = CSQRT(PI*PI/(A*A*(1. + C)*(1.+ C))-XX)
      DB = AIMAG(GAMA) - BETAO
      WRITE (6,4) GAMA,DB
    4 FORMAT (30X, 3E15.5)
      RO = 1./SI
      CALL BADAR( A,XX, GAMA, BETAO, CP)
      DB = AIMAG(GAMA) - BETAO
      WRITE(6,5) SI, RO, GAMA, DB
    5 FORMAT (1X, 2E12.3, 5X,3E15.5)
      ZZ = ALOG10(SI)
      ZZ = ZZ + VSIO(2)
      SI  = 10.**ZZ
      IF(SI .LE.VSIO(3)) GO TO 16
      SI  = VSIO(1)
      ER = ER - VER(2)
      IF(ER.GE.VER(3)) GO TO 3
      WRITE (6,19)
   19 FORMAT (1H0)
      GO TO 20
   21 STOP
      END
$IBFTC BADAR
      SUBROUTINE BADAR (A, XX, GAMA, BETAO, CP)
      COMPLEX  GAMA, GAME, AKI, AKJ, FK, DFK, CP, Y, YY, DK
      N = 0
    2 CONTINUE
      IF (N.GT.  10) GO TO 3
```

```
      GAME = GAMA
      AKI = CSQRT(GAME*GAME + XX)
      Y =-AKI*AKI - XX*(CP - 1.)
      AKJ = CSQRT( Y)
      Y = AKI*A
      YY = CSIN(Y)/CCOS(Y)
      FK = AKI + AKJ*YY
      DFK = 1. + AKJ*A*(1.+YY*YY) + AKI*YY/AKJ
      DK = -FK/DFK
      AKI = AKI+ DK
      GAMA = CSQRT(AKI*AKI -XX)
      P = ABS(REAL(GAME - GAMA))
      Q = ABS(AIMAG(GAME - GAMA))
      IF (P.LT.1.E-6.AND.Q.LT.1.E-6) GO TO 1
      N = N + 1
        GO TO 2
    3 WRITE (6,4)
    4 FORMAT (26H NO CONVERGENCE IN THE SUB)
    1 DB = AIMAG(GAMA) - BETAO
      RETURN
      END
$ENTRY
.122        70.5
16.          4.          0.
.01         .2          10.2
.122        70.5
3.          1.           1.
.01         .2          10.2
$IBSYS
```

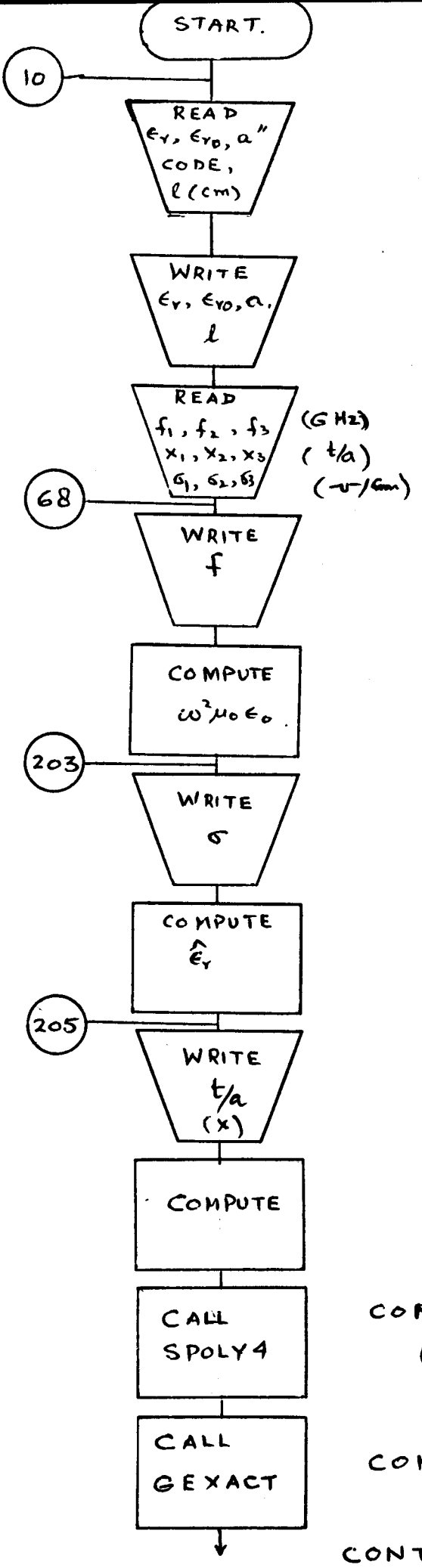

FLOW CHART FOR PARTIALLY FILLED WAVEGUIDE

CONTD./

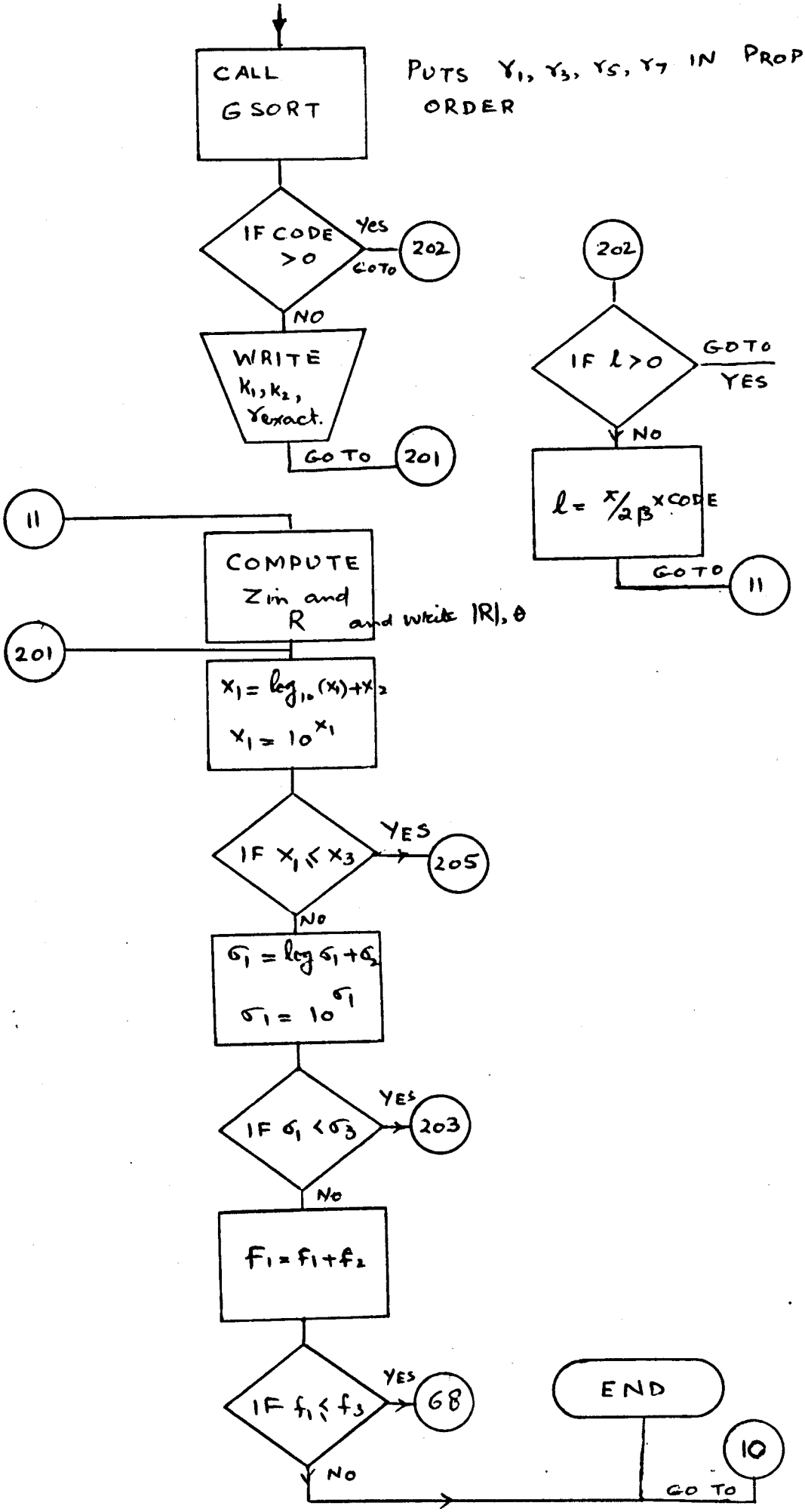
CALL GSORT
PUTS Y_1, Y_3, Y_5, Y_7 IN PROPER ORDER
IF CODE >0
Yes
GOTO
202
NO
WRITE K_1, K_2, Yexact.
GO TO
201
202
IF $\ell > 0$
GOTO YES
NO
$\ell = \pi/2\beta \times$ CODE
GOTO
11
11
COMPUTE Zin and R and write |R|, θ
201
$x_1 = \log_{10}(x_1) + x_2$
$x_1 = 10^{x_1}$
IF $X_1 \leq X_3$
YES
205
NO
$\sigma_1 = \log \sigma_1 + \sigma_2$
$\sigma_1 = 10^{\sigma_1}$
IF $\sigma_1 < \sigma_3$
YES
203
NO
$F_1 = f_1 + f_2$
IF $f_1 \leq f_3$
YES
68
NO
END
10
GO TO

```
$JOB            003505SHEIKH            015   004
$IBJOB          DECK
$IBFTC
C       SOLUTION FOR CENTRALLY LOADED WAVEGUIDE                          0//
        COMPLEX  T, CP, TI, TJ, GAS, GA , GAP, GAM, AKI, AKJ             0SS
        COMPLEX FK, DFK, U, V,TAA, CO, RF                                0TT
        COMPLEX AA(6), YY(9)                                             0UU
        DIMENSION AKI(9), AKJ(9) , GA(9) ,T(9,9)                         0VV
        DIMENSION  VF(5), VX(5), VER(5), VSI(5)                          0WW
        DIMENSION AKIAB(9), AKJAB(9), AKIAR(9), AKJAR(9)                 0XX
   10   READ(5,1) ER, ER1, A, CODE, AL                                   0YY
    1   FORMAT (5F10.5)                                                  0ZZ
        WRITE (6,2) ER,ER1,A, AL                                         0//
    2   FORMAT (4H ER=,2F10.3,F10.2, F12.5/)
        READ (5,62) (VF(I), I=1,3),(VX(I), I=1,3), (VSI(I), I=1,3)       055
   62   FORMAT (3F20.10)                                                 044
        F = VF(1)                                                        044
        SI = VSI(1)                                                      055
        X = VX(1)                                                        077
   65   A = A*2.54                                                       077
        PI = 3.1415928                                                   088
        S = PI/A                                                         099
   68   WRITE (6,200) F                                                  0SS
        XX = .043929*F*F                                                 055
  203   WRITE (6,204) SI                                                 022
        CP = CMPLX( ER, -1800.*SI/F)                                     066
  205   WRITE (6,206) X                                                  077
   69   Y = PI*X                                                         055
        TS = A*X                                                         066
        D = (A - TS)/2.                                                  077
        BETO = SQRT(XX - S*S)                                            099
        DO 3 N=1,7,2                                                     099
        DO 3 M=1,7,2                                                     0TT
        AN = FLOAT(N)                                                    044
        IF (N.NE.M) GO TO 4                                              066
        T(N,M)= AN*AN*S*S - XX*ER1 - XX*(CP-ER1)*(X+SIN(AN*Y)/(AN*PI))   033
        GO TO 3                                                          044
    4   L = (N + M)/2                                                    077
        K = (N - M)/2                                                    066
        ALL= FLOAT(L)                                                    077
        AK = FLOAT(K)                                                    0==
        T(N,N)= XX*(CP -ER1)/PI*(SIN(Y*ALL)/ALL*((-1.)**L) +             0==
       1  SIN(Y*AK)/AK*(-1.)**(K+3))                                     0UU
    3   CONTINUE                                                         044
        AA(5) = CMPLX(1.,0.0)                                            077
        AA(4) = -T(1,1) - T(3,3) - T(5,5) - T(7,7)                       044
        AA(3) =  T(1,1)*(T(3,3) + T(5,5) + T(7,7)) + T(3,3)*(            044
       1 T(5,5) + T(7,7)) + T(5,5)*T(7,7) - T(3,1)*T(1,3) - T(1,5)*T(5,1) 077
       2 - T(1,7)*T(7,1) - T(3,5)*T(5,3) - T(3,7)*T(7,3) -T(5,7)*T(7,5)  077
        AA (2) = -T(1,1)*(T(3,3)*(T(5,5) + T(7,7)) + T(5,5)*T(7,7))      077
       1 -T(3,3)*T(5,5)*T(7,7)                                           0''
       2  + T(1,1)*(T(3,5)*T(5,3) + T(3,7)*T(7,3) + T(5,7)*T(7,5))       0''
       3  +T(3,3)*(T(1,5)*T(5,1) + T(1,7)*T(7,1) + T(5,7)*T(7,5))       0VV
       4 + T(5,5)*(T(3,7)*T(7,3) + T(1,3)*T(3,1) + T(1,7)*T(7,1))       055
       5 + T(7,7)*(T(1,5)*T(5,1) + T(3,5) *T(5,3) + T(1,3)*T(3,1))      055
       6-T(1,3)*T(3,5)*T(5,1) - T(1,3)*T(3,7)*T(7,1)-T(1,5)*T(5,3)*T(3,1) 077
       7-T(1,5)*T(5,7)*T(7,1)-T(1,7)*T(7,5)*T(5,1)-T(1,7)*T(7,3)*T(3,1)  077
       8-T(3,7)*T(7,5)*T(5,3) - T(5,7)*T(7,3)*T(3,5)                     055
        AA(1) = T(1,1)*(T(3,3)*T(5,5)*T(7,7) + T(3,5)*T(5,7)*T(7,3) +    077
```

```
     1 T(3,7)*T(7,5)*T(5,3)) +                                          077
     2 T(3,3)*(T(1,5)*T(5,7)*T(7,1) + T(1,7)*T(7,5)*T(5,1))             0''
     3 + T(5,5)*(T(1,3)*T(3,7)*T(7,1) + T(1,7)*T(7,3)*T(3,1 ))          0''
     4 + T(7,7)*(T(1,3)*T(3,5)* T(5,1) + T(1,5)*T(5,3)*T(3,1))+         0WW
     5 T(1,5)*T(5,1)*T(7,3)*T(3,7) + T(1,7)*T(7,1)*T(3,5)*T(5,3) -      077
     6 (T(1,1)*(T(3,3)*T(5,7)*T(7,5) + T(5,5)*T(7,3)*T(3,7) +           066
     7 T(7,7)*T(3,5)*T(5,3))+                                           066
     8 T(3,3)*(T(5,5)*T(7,1)*T(1,7) + T(7,7)*T(1,5)*T(5,1))             077
     9+ T(5,5)*T(1,3)*T(3,1)*T(7,7)+T(1,3)*T(3,5)*T(5,7)*T(7,1) )       077
      AA(1) = AA(1) - (T(1,3)*T(3,7)*T(7,5)*T(5,1) + T(1,5)*T(5,7)*     077
     1 T(7,3)*T(3,1) + T(1,7)*T(7,5)*T(5,3)*T(3,1) + T(3,5)*T(5,1)*     066
     2 T(1,7)*T(7,3) + T(3,7)*T(7,1)*T(1,5)*T(5,3))                     077
     3 + T(1,3)*T(3,1)*T(5,7)*T(7,5)                                    0==
      TI = T(1,1)*T(3,3) -T(3,1)*T(1,3)                                 0==
      TJ = (T(1,1) +T(3,3))/2.                                          0XX
      YY(1) = TJ - CSQRT(TJ*TJ -TI)                                     077
      YY(3) = TJ + CSQRT(TJ*TJ -TI)                                     077
      CALL SPOLY4(AA,YY)                                                077
      COMPLEX ZO, Z, G, P, TN, NF, CS, CC                               077
      DIMENSION ZO(9), Z(9), G(9,9), P(9,9), DEL(9,9),TN(9)             077
      DO 5 N=1,7,2                                                      077
      AKI(N)= CSQRT(YY(N)*YY(N) + XX*ER1)                               077
      AKJ(N) = CSQRT(YY(N)*YY(N) + XX*CP )                              0''
      DO 5 M= 1,7,2                                                     0''
      IF (N.NE.M) GO TO 8                                               0YY
      DEL(N,N)= 1.                                                      088
      GO TO 5                                                           099
    8 DEL(N,M)= 0.0                                                     0==
    5 CONTINUE                                                          0''
      COMMON /ANE/AKI, AKJ, D, TS, XX, CP, GA , ER1                     0''
      CALL EXACTG                                                       0==
      CALL GSORT(GA)
      IF(CODE.GT.0.0) GO TO 202                                         0''
      DO 207 M = 1,7,2                                                  088
      AKIAB(M) = CABS(AKI(M))                                           099
      AKJAB(M) = CABS(AKJ(M))                                           0ZZ
      AKIAR(M) = ATAN2(AIMAG(AKI(M)), REAL(AKI(M)))*57.296              099
      AKJAR(M) = ATAN2(AIMAG(AKJ(M)), REAL(AKJ(M)))*57.296              099
  207 WRITE (6,208) AKIAB(M), AKIAR(M), AKJAB(M), AKJAR(M), GA(M)       0==
      GO TO 201                                                         0''
  202 UO = 4.*PI*1.E-9                                                  0''
      OMG =2.*PI*F*1.E9                                                 0==
      TI = CMPLX(0.0,1.0)*OMG*UO                                        0''
      DO 9 N=1,7,2                                                      099
      AN = FLOAT (N)                                                    099
      Z(N)= TI/GA(N)                                                    100
      TJ = CSQRT(CMPLX(AN*AN*S*S - XX, 0.0))                            1//
      ZO(N)= TI/TJ                                                      1SS
      IF(AL.GT.0.0) GO TO 11                                            1TT
      AL = PI/2./AIMAG(GA(1)) *CODE                                     1UU
   11 U = GA(N)*AL                                                      1UU
      V = CEXP(U)                                                       1VV
      TN(N)= (V - 1./V)/(V + 1./V)                                      1WW
      TN(N)= TN(N)*Z(N)                                                 1XX
    9 CONTINUE                                                          1YY
      DO 14 M=1,7,2                                                     1ZZ
      AKI(M) = CSQRT(GA(M)*GA(M) + XX*ER1)                              1//
      AKJ(M) = CSQRT(GA(M)*GA(M) + XX*CP)                               111
```

```
      U = AKI(M)*D                                                        155
      V = AKJ(M)*TS                                                       144
      CO = CCOS(V)                                                        144
      TAA = CSIN(U)                                                       155
      CS = CSIN(V)                                                        177
      CC = CCOS(U)                                                        177
      NF= 1./CSQRT(D- TAA*CC/AKI(M) + TAA*TAA/(CS*CS)*(1.-CO)*            188
     1  (TS + CS/AKJ(  M)))                                              199
      GAP = AKJ(M)*AKJ(M)                                                 155
      GAM= AKI(M)*AKI(M)                                                  155
      DO 14 N=1,7,2                                                       122
      AN = FLOAT(N)                                                       166
      ANT = AN*TS*S/2.                                                    177
      P(N,M)= SQRT(2./A)*NF*2.*SIN(AN*PI/2.)*(AN*S*SIN(ANT)*TAA           177
     1  - AKI(M)*CC*COS(ANT ))*                                           155
     2 (GAP - GAM)/(GAP - AN*AN*S*S)/(GAM - AN*AN*S*S)                    166
   14 CONTINUE                                                            177
      DO 15 I=1,7,2                                                       199
      DO 15 J=1,7,2                                                       199
      G(I,J)= CMPLX(0.0,0.0)                                              177
      DO 16 M=1,7,2                                                       144
   16 G(I,J)= G(I,J) + ZO(M)*DEL(M,I)*DEL(M,J) + TN(M)*P(I,M)*P(J,M)      166
      G(I,J) = G(I,J) - ZO(1) *DEL(I,1)*DEL(J,1)                          133
   15 CONTINUE                                                            144
      COMPLEX ZN, REC, DET, DETT, DET37                                   177
      DIMENSION ZN(9), REC(9), RECAB(9), RECAR(9)                         166
      ZN(1) = TN(1)/ZO(1)                                                 177
      ZN(2)= G(1,1)/ZO(1)                                                 1==
      ZN(3)= (G(1,1)*G(3,3) - G(1,3)*G(3,1))/G(3,3)/ZO(1)                 1==
      CALL DET3 (G, DET)                                                  100
      ZN(4) = DET/ZO(1)/(G(3,3)*G(5,5) - G(3,5) *G(5,3))                  144
      CALL DET7(G, DETT, DET37)                                           177
      ZN(5) = DETT/ZO(1)/DET37                                            144
      DO 17 N= 1,5                                                        477
      REC(N)= (ZN(N) - 1.)/(ZN(N) + 1.)                                   177
      RECAB(N)= CABS(REC(N))                                              177
   17 RECAR(N)= ATAN2(AIMAG(REC(N)), REAL(REC(N)))*57.296                 1''
      WRITE (6,18) (RECAB(I), I= 1,5), (RECAR(J), J= 1,5)                 1''
  201 IF(VX(2).LE.0.0)GO TO 71                                            1VV
      ZZ = ALOG10(X)                                                      155
      ZZ = ZZ + VX(2)                                                     155
      X = 10.**ZZ                                                         177
      IF (X.LE.VX(3)) GO TO 205                                           177
      X = VX(1)                                                           155
   71 IF( VSI(2).LE.0.0) GO TO 72                                         177
      ZS = ALOG10(SI)                                                     177
      ZS = ZS + VSI(2)                                                    1''
      SI = 10.**ZS                                                        1''
      IF (SI.LE.VSI(3)) GO TO 203                                         1WW
      SI =VSI(1)                                                          177
   72 IF(VF(2).LE.0.0) GO TO 74                                           166
      F = F + VF(2)                                                       166
      IF(F.LE.VF(3)) GO TO 68                                             166
   74 CONTINUE                                                            177
      WRITE (6,51)                                                        1''
   18 FORMAT (31X, 5E12.4/31X, 5E12.4)                                    1''
   51 FORMAT (1H0)                                                        177
  200 FORMAT (1X, F10.3)                                                  1==
```

```
  204 FORMAT (11X, E10.4)                                                1==
  206 FORMAT (21X, E10.4)                                                1XX
  208 FORMAT (31X, 6E12.4)                                               177
  209 FORMAT (F10.4, F10.2)                                              177
  210 FORMAT (F10.3)                                                     177
  211 FORMAT (E10.3)                                                     177
  212 FORMAT (3E15.5)                                                    177
      GO TO 10                                                           177
   13 STOP                                                               177
      END                                                                1''
$IBFTC EXACTG
      SUBROUTINE EXACTG                                                  1YY
      COMPLEX  AKI, AKJ, CP, GA, U, V, CO, TAA, FK, DFK, RF, GAS         188
      DIMENSION GA(9), AKI(9), AKJ(9)                                    199
      COMMON /ANE/ AKI, AKJ, D, TS, XX, CP, GA , ER1                     1==
      DO 60 M=1,7,2
   60 GA(M)= CSQRT(AKI(M)*AKI(M) - XX*ER1)                               1''
      DO 36 M= 1,7,2                                                     1==
      N = 0                                                              1==
      GO TO 31                                                           1''
   32 AKJ(M)= CSQRT(AKI(M)*AKI(M) + XX*(CP -ER1))                        188
   31 U = AKI(M)*D                                                       199
      V = AKJ(M)*TS/2.                                                   1ZZ
      TAA= CSIN(U)/CCOS(U)                                               199
      CO = CCOS(V)/CSIN(V)
      FK = AKJ(M)*TAA- AKI(M)*CO
      DFK = AKI(M)/AKJ(M)*(TAA+ AKI(M)*TS/2.*(1. + CO*CO)) +
     1 AKJ(M)*D*(1. + TAA*TAA) - CO
      RF = -FK/DFK
      AKI(M)= AKI(M) + RF
      GAS = CSQRT( AKI(M)*AKI(M) - XX*ER1)
      PP = ABS(REAL(GAS-GA(M)))
      Q = ABS(AIMAG(GAS-GA(M)))
      IF (N.GT.15)GO TO 33
      IF(PP.LT.1.E-6.AND.Q.LT.1.E-6) GO TO 54
      N = N + 1
      GA(M) = CSQRT(AKI (M)*AKI(M) - XX*ER1)
      GO TO 32
   54 GA(M)= CSQRT(AKI(M)*AKI(M) - XX*ER1)
      AKJ(M)= CSQRT(AKI(M)*AKI(M) + XX*(CP -ER1))
      GO TO 36
   33 WRITE (6,34)
   34 FORMAT (15H NO CONVERGENCE)
   36 CONTINUE
      RETURN
      END
$IBFTC DET3
      SUBROUTINE DET3  (G, DET)
      COMPLEX G, DET
      DIMENSION G(9,9)
      DET =  G(1,1)*(G(3,3)*G(5,5) - G(3,5)*G(5,3))
     1 -G(1,3)*(G(3,1)*G(5,5) - G(3,5)*G(5,1))
     2 + G(1,5)*(G(3,1)*G(5,3) - G(3,3)*G(5,1))
      RETURN
      END
$IBFTC SPOLY4
      SUBROUTINE SPOLY4(AA,YY)
      COMPLEX AA,YY, FF, DFF, RF, YX, BB, YYU, YYUN, CC,DY,T(9,9)
```

```
      DIMENSION AA(6), YY(9), BB(6), CC(6),YX(9), D(9), YXR(9),YXI(9)
      DO 1 N = 1,3,2
      NN = 0
    5 IF(NN.GT.15) GO TO 2
      YYU = CSQRT(YY(N) )
      FF = CMPLX(0.,0.)
      DFF = CMPLX(0.,0.)
      DO 3 M=1,5
      MM = M - 1
      LL = M - 2
      FF = FF + AA(M)*YY(N )**MM
      AM = FLOAT(MM)
      DFF = DFF + AM*AA(M)*YY(N )**LL
    3 CONTINUE
      RF = -FF/DFF
      YY(N) = YY(N) + RF
      YYUN= CSQRT(YY(N))
      DY = YYU - YYUN
      PP = ABS(REAL(DY))
      QQ = ABS(AIMAG(DY))
      IF (PP. LT.1.E-6.AND.QQ.LT.1.E-6) GO TO 1
      NN = NN + 1
       GO TO 5
    2 WRITE(6,6)
    6 FORMAT(25H NO CONVERGENCE IN SPOLY,4)
    1 CONTINUE
      CC(2) = AA(4) + YY(1) + YY(3)
      CC(1) = AA(3) - YY(1)*YY(3) + (YY(1) + YY(3))*CC(2)
      YY(5) = -CC(2)/2. - CSQRT(CC(2)*CC(2)/4. - CC(1))
      YY(7) = -CC(2)/2. + CSQRT(CC(2)*CC(2)/4. - CC(1))
      DO 4 M = 5,7,2
      YX(M) = CSQRT(YY(M))
    4 YXR(M) = REAL(YY(M))
      IF (YXR(5).LT.YXR(7)) YY(5) = YX(5)
      IF (YXR(5).LT.YXR(7)) YY(7) = YX(7)
      IF (YXR(5).GT.YXR(7)) YY(5) = YX(7)
      IF (YXR(5).GT.YXR(7)) YY(7) = YX(5)
      DO 9 N= 1,3,2
    9 YY(N)= CSQRT(YY(N))
      RETURN
      END
$IBFTC DET7
      SUBROUTINE DET7(G, DETT, DET37)
      COMPLEX G(9,9), DETT, DET37
      DETT = G(1,1)*(G(3,3)*(G(5,5)*G(7,7) - G(5,7)*G(7,5))-
     1 G(3,5)*(G(5,3)*G(7,7) - G(7,3)*G(5,7))+G(3,7)*(G(5,3)*G(7,5)-
     2 G(5,5)*G(7,3))) -G(1,3)*(G(3,1)*(G(5,5)*G(7,7)-G(5,7)*G(7,5))-
     3 G(3,5)*(G(5,1)*G(7,7) -G(5,7)*G(7,1))+G(3,7)*(G(5,1)*G(7,5) -
     4 G(5,5)*G(7,1))) + G(1,5)*(G(3,1)*(G(5,3)*G(7,7)-G(5,7)*G(7,3)) -
     5 G(3,3)*(G(5,1)*G(7,7)-G(5,7)*G(7,1)) + G(3,7)*(G(5,1)*G(7,3)-
     6 G(5,3)*  G(7,1)))-G(1,7)*(G(3,1)*(G(5,3)*G(7,5)-G(5,5)*G(7,3))-
     7  G(3,3)*(G(5,1)*G(7,5)-G(5,5)*G(7,1))+ G(3,5)*(G(5,1)*G(7,3)-
     8 G(5,3)*G(7,1)))
      DET37 = G(3,3)*(G(5,5)*G(7,7)-G(5,7)*G(7,5))-G(3,5)*(G(5,3)*
     1 G(7,7)-G(5,7)*G(7,3))+  G(3,7)*(G(5,3)*G(7,5)-G(5,5)*G(7,3))
      RETURN
      END
$IBFTC CSQRT
```

```
      SUBROUTINE GSORT  (GA)
      DIMENSION DA (9), GAR(9), GAI(9)
      COMPLEX GA(9), GAX(9)
      DO 1 M=1,7,2
      GAX(M)= GA(M)
      GAR(M) = REAL(GA(M))
    1 GAI(M) = AIMAG(GA(M))
      GAMX =AMAX1(GAI(1), GAI(3), GAI(5), GAI(7))
      DO 2 M= 1,7,2
    2 DA(M)= GAMX - GAI(M)
      IF(DA(3).EQ.0.0) GO TO 3
      IF(DA(5).EQ.0.0) GO TO 4
      IF(DA(7).EQ.0.0) GO TO 5
      GA(1) = GAX(1)
      GAMM = AMIN1 (GAR(3), GAR(5), GAR(7))
      DO 6 M=3,7,2
    6 DA(M)= GAMM - GAR(M)
      IF(DA(7).EQ.0.0) GO TO 7
      IF(DA(5).EQ.0.0) GO TO 8
      GA(3) = GAX(3)
      IF (GAR(5).LT.GAR(7)) GA(5) = GAX(5)
      IF (GAR(5).LT.GAR(7)) GA(7) = GAX(7)
      IF (GAR(5).GT.GAR(7)) GA(5) = GAX(7)
      IF (GAR(5).GT.GAR(7)) GA(7) = GAX(5)
      GO TO 9
    8 GA(3) = GAX(5)
      IF (GAR(3).LT.GAR(7)) GA(5) = GAX(3)
      IF (GAR(3).LT.GAR(7)) GA(7) = GAX(7)
      IF (GAR(3).GT.GAR(7)) GA(5) = GAX(7)
      IF (GAR(3).GT.GAR(7)) GA(7) = GAX(3)
      GO TO 9
    7 GA(3) = GAX(7)
      IF (GAR(3).LT.GAR(5)) GA(5) = GAX(3)
      IF (GAR(3).LT.GAR(5)) GA(7) = GAX(5)
      IF (GAR(3).GT.GAR(5)) GA(5) = GAX(5)
      IF (GAR(3).GT.GAR(5)) GA(7) = GAX(3)
      GO TO 9
    3 GA(1) = GAX(3)
      GRMM = AMIN1(GAR(1), GAR(5), GAR(7))
      DO 10 M= 1,7,2
   10 DA(M) = GRMM -GAR(M)
      IF(DA(7).EQ.0.0) GO TO 11
      IF(DA(5).EQ.0.0) GO TO 12
      GA (3) = GAX(1)
      IF (GAR(5).LT.GAR(7)) GA(5) = GAX(5)
      IF (GAR(5).LT.GAR(7)) GA(7) = GAX(7)
      IF (GAR(5).GT.GAR(7)) GA(5) = GAX(7)
      IF (GAR(5).GT.GAR(7)) GA(7) = GAX(5)
      GO TO 9
   11 GA(3) = GAX(7)
      IF (GAR(1).LT.GAR(5)) GA(5) = GAX(1)
      IF (GAR(1).LT.GAR(5)) GA(7) = GAX(5)
      IF (GAR(1).GT.GAR(5)) GA(5) = GAX(5)
      IF (GAR(1).GT.GAR(5)) GA(7) = GAX(1)
      GO TO 9
   12 GA(3) = GAX(5)
      IF (GAR(1).LT.GAR(7)) GA(5) = GAX(1)
      IF (GAR(1).LT.GAR(7)) GA(7) = GAX(7)
```

```
      IF (GAR(1).GT.GAR(7)) GA(5) = GAX(7)
      IF (GAR(1).GT.GAR(7)) GA(7) = GAX(1)
      GO TO 9
    4 GA(1) = GAX(5)
      GRMM = AMIN1(GAR(1), GAR(3), GAR(7))
      DO 13 M= 1,7,2
   13 DA(M) = GRMM - GAR(M)
      IF(DA(3).EQ.0.0) GO TO 14
      IF(DA(7).EQ.0.0) GO TO 15
      GA(3) = GAX(1)
      IF (GAR(3).LT.GAR(7)) GA(5) = GAX(3)
      IF (GAR(3).LT.GAR(7)) GA(7) = GAX(7)
      IF (GAR(3).GT.GAR(7)) GA(5) = GAX(7)
      IF (GAR(3).GT.GAR(7)) GA(7) = GAX(5)
      GO TO 9
   14 GA(3) = GAX(3)
      IF (GAR(1).LT.GAR(7)) GA(5) = GAX(1)
      IF (GAR(1).LT.GAR(7)) GA(7) = GAX(7)
      IF (GAR(1).GT.GAR(7)) GA(5) = GAX(7)
      IF (GAR(1).GT.GAR(7)) GA(7) = GAX(1)
      GO TO 9
   15 GA(3) = GAX(7)
      IF (GAR(1).LT.GAR(3)) GA(5) = GAX(1)
      IF (GAR(1).LT.GAR(3)) GA(7) = GAX(3)
      IF (GAR(1).GT.GAR(3)) GA(5) = GAX(3)
      IF (GAR(1).GT.GAR(3)) GA(7) = GAX(1)
      GO TO 9
    5 GA(1) = GAX(7)
      GRMM = AMIN1(GAR(1), GAR(3), GAR(5))
      DO 16 M= 1,7,2
   16 DA(M) = GRMM - GAR(M)
      IF(DA(3).EQ.0.0) GO TO 17
      IF(DA(5).EQ.0.0) GO TO 18
      GA(3) = GAX(1)
      IF (GAR(3).LT.GAR(5)) GA(5) = GAX(3)
      IF (GAR(3).LT.GAR(5)) GA(7) = GAX(5)
      IF (GAR(3).GT.GAR(5)) GA(5) = GAX(5)
      IF (GAR(3).GT.GAR(5)) GA(7) = GAX(3)
      GO TO 9
   17 GA(3) = GAX(3)
      IF (GAR(1).LT.GAR(5)) GA(5) = GAX(1)
      IF (GAR(1).LT.GAR(5)) GA(7) = GAX(5)
      IF (GAR(1).GT.GAR(5)) GA(5) = GAX(5)
      IF (GAR(1).GT.GAR(5)) GA(7) = GAX(1)
      GO TO 9
   18 GA(3) = GAX(5)
      IF (GAR(1).LT.GAR(3)) GA(5) = GAX(1)
      IF (GAR(1).LT.GAR(3)) GA(7) = GAX(3)
      IF (GAR(1).GT.GAR(5)) GA(5) = GAX(3)
      IF (GAR(1).GT.GAR(3)) GA(7) = GAX(1)
    9 CONTINUE
      RETURN
      END
$ENTRY
16.       1.          .9
9.25
.01333
.02                   .1                    1.1
```

FLOW CHART FOR MICROWAVE CONDUCTIVITY OF GERMANIUM

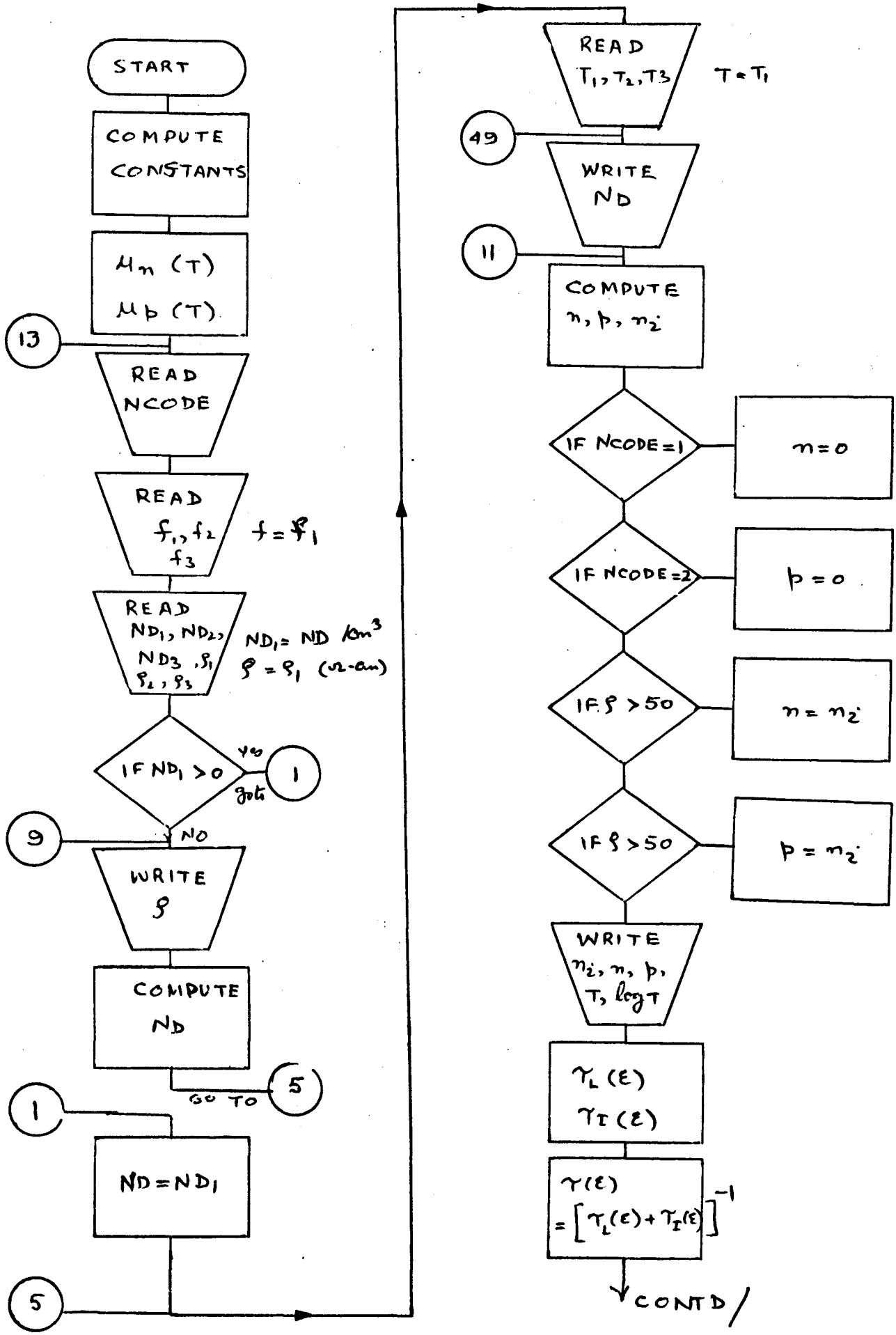

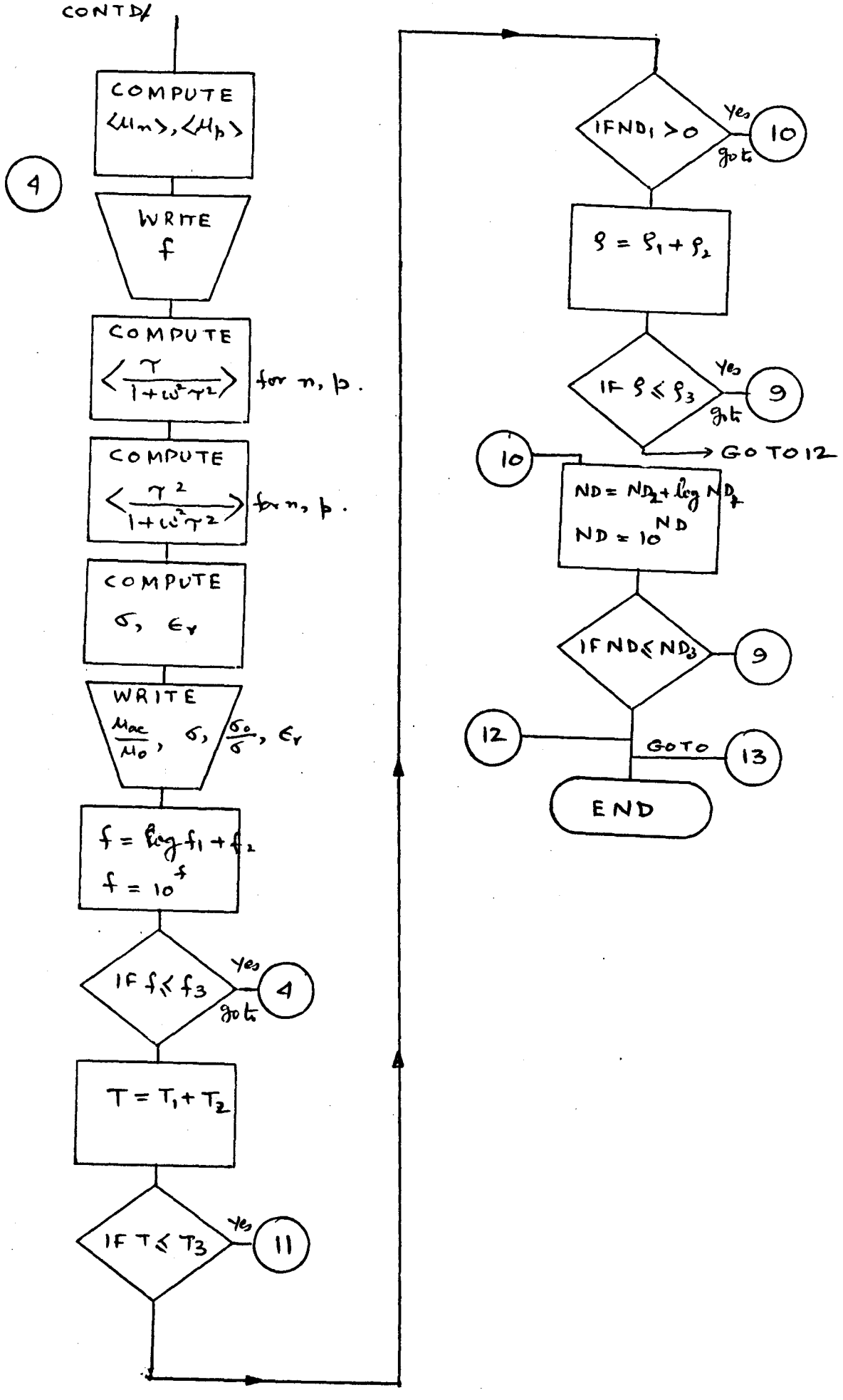
CONTD/
COMPUTE
⟨μn⟩, ⟨μp⟩
4
WRITE
f
COMPUTE
⟨τ / (1+ω²τ²)⟩ for n, p.
COMPUTE
⟨τ² / (1+ω²τ²)⟩ for n, p.
COMPUTE
σ, εr
WRITE
μac/μ0, σ, σ0/σ, εr
f = log f1 + f2
f = 10^f
IF f ≤ f3
yes
goto
4
T = T1 + T2
IF T ≤ T3
yes
11
IF ND1 > 0
yes
goto
10
ρ = ρ1 + ρ2
IF ρ ≤ ρ3
yes
goto
9
10
GO TO 12
ND = ND2 + log ND
ND = 10^ND
IF ND ≤ ND3
9
12
GOTO
13
END

```
C     MICROWAVE CONDUCTIVITY OF GERMANIUM
      REAL ML, MT, MC, MD, MCH, MDH, M1, M2, MIS, MISH, ND
      DIMENSION VND(3), VT(3), VCI(3), VCJ(3),VRO(3), VF(3)
      PI = 3.1415928
      Q = 1.601E-19
      FEM = 9.108E-31
      MT = .0819
      ML = 1.64
      EPSO = 8.854E-12
      BK = 1.38026E-23
      H = 6.62377E-34
      HB = H/2./PI
      EVBK = BK/Q
      M1 = .35
      M2 = .044
      MC = 3.*FEM/(2./MT + 1./ML)
      MD = FEM*(ML*MT*MT)**(1./3.)
      MCH = (M1**1.5 + M2**1.5)/(M1**.5 + M2**.5)*FEM
      MDH = (M1**1.5 + M2**1.5)**(2./3.)*FEM
      MIS = 3./(1./SQRT(ML) + 2./(SQRT(MT)))
     1 *SQRT(FEM)
      MISH=(M1**.5 + M2**.5)*SQRT(FEM)
      WRITE (6,21) MC, MD, MIS, MCH,MDH,MISH
      VI = 9.E12
      CI = .2735
      CIH = 1.89
      AMOB(T)=.385*(300./T)**1.66
      AMOBH(TT) = .18*(300./TT)**2.33
      ANI(TT) = (1.76E16)*(TT**1.5*EXP(-2275./TT))/EXP (2275./TT)
      W = .2123E13
      WH = .8430E12
      EPS = 16.*EPSO
   13 CONTINUE
      READ (5,6) NCODE
      READ (5,2) (VF (I), I= 1,3)
      F = VF(1)
      READ (5,15)(VND(I), I= 1,3)
      READ (5,2) (VRO(I), I= 1,3)
      IF (VND(1).GT.0.0) GO TO 1
      RO = VRO(1)
   19 WRITE (6,3) RO
      SIO = 1./RO
      ALPHA = 6.84E6
      BET = 2000.*SIO/Q
      GAMA = 5.6*5.6E6*ANI(300.)*ANI(300.) - (SIO/Q)**2
      X = BET /2./ALPHA
      ND = SQRT(X**2 - GAMA/ALPHA) - X
      ND = ND*1.E6
      GO TO 5
    1 CONTINUE
      ND = VND(1)
    5 CONTINUE
      READ (5,2) (VT(I), I=1,3)
      T = VT(1)
    9 CONTINUE
      WRITE (6,3) ND
   11 CONTINUE
```

```
      TL = ALOG10(T)
      XX = 2.*ANI(T)*1.E6/ND
      XX = XX*XX
      CDE = ND/2.*( 1. + SQRT(1. + XX))
      CDH = ND/2.*(-1. + SQRT(1. + XX))
      ANII = ANI(T)*1.E6
      IF (NCODE.EQ.1) CDH = 0.
      IF (NCODE.EQ.2) CDE = 0.
      IF (RO.GE.50.) CDE = ANII
      IF (RO.GE.50.) CDH = ANII
      WRITE (6,7) ANII, CDE, CDH, T, TL
      BETA = T*EVBK
      BETAI = 1./BETA
      DN = 3.*SQRT(PI)/4.*BETA**2.5
      XI = VI*H/BK/T
      DII = EXP(XI) - 1.
      DIJ = 1. - EXP(-XI)
      XI = H*VI/Q
      AA = (T/300.)/SQRT(300.*EVBK)
      BB = (XI/300./EVBK)**1.5
      TAL1(E) = AA*SQRT(E) + CI*BB*SQRT(E/XI + 1.)/DII
      TAL2(E) = TAL1(E) + CI*BB*SQRT(E/XI -1.)/DIJ
      TALH1(E) = AA*SQRT(E) + CIH*BB*SQRT(E/XI + 1.)/DII
      TALH2(E) = TALH1(E) + CIH*BB*SQRT(E/XI - 1.)/DIJ
      FF(E) = EXP(-E/BETA)*(E**1.5)
      A =(8.*SQRT(2.)/ND*EPS/Q*EPS/Q)*(MIS/Q)/Q *2.*PI*Q**1.5
      AH=(8.*SQRT(2.)/ND*EPS/Q*EPS/Q)*(MISH/Q)/Q*2.*PI*Q**1.5
      B = (8.*MD/HB)*(EPS/HB)*(BK/Q)*(T/CDE/Q)*Q
      BH= (8.*MD/HB)*(EPS/HB)*(BK/Q)*(T/CDH/Q)*Q
      TAI (E) = (ALOG(1.+B *E) - B *E/(1. + B *E))/A /E**1.5
      TAIH(E) = (ALOG(1.+BH*E) - BH*E/(1. + BH*E))/AH/E**1.5
      TA1(E) = 1./(W *TAL1(E) + TAI(E))
      TA2(E) = 1./(W *TAL2(E) + TAI(E))
      TAH1 (E) = 1./(WH*TALH1(E) + TAIH(E))
      TAH2 (E) = 1./(WH*TALH2(E) + TAIH(E))
      FF1(E) = TA1(E)*FF(E)
      FF2(E) = TA2(E)*E**1.5
      FFH1(E) = TAH1(E)*FF(E)
      FFH2(E) = TAH2(E)*E**1.5
      TAL = (FINT14(FF1,0.0,XI) + FLIN14(FF2,XI,BETAI))/DN
      TALH = (FINT14(FFH1,0.0,XI)+ FLIN14(FFH2,XI,BETAI))/DN
      SIO = Q*(CDE*AMOB(T) + CDH *AMOBH(T))
    4 CONTINUE
      WRITE (6,3) F
      OMEGA = 2.E+09*PI*F
      OMEGS = OMEGA*OMEGA
      TAM1(E) = TA1(E)/(1. + OMEGS*TA1(E)**2)
      TAM2(E) = TA2(E)/(1. + OMEGS*TA2(E)**2)
      TAMH1(E) = TAH1(E)/(1. + OMEGS*TAH1(E)**2)
      TAMH2(E) = TAH2(E)/(1. + OMEGS*TAH2(E)**2)
      TAM1(E) = TA1(E)*TAM1(E)*FF(E)
      TAM2(E) = TA2(E)*TAM2(E)*E**1.5
      TAMH1(E) = TAH1(E)*TAMH1(E)*FF(E)
      TAMH2(E) = TAH2(E)*TAMH2(E)*E**1.5
      FFM1(E) = TAM1(E)*FF(E)
      FFM2(E) = TAM2(E)*E**1.5
      FFMH1(E) = TAMH1(E)*FF(E)
      FFMH2(E) = TAMH2(E)*E**1.5
```

```
      TAM = (FINT14(FFM1,0.0,XI) + FLIN14(FFM2 ,XI,BETAI))/DN
      TAMH = (FINT14(FFMH1,0.0,XI) + FLIN14(FFMH2,XI,BETAI))/DN
      TAMM = (FINT14(TAMM1,0.0,XI) + FLIN14(TAMM2,XI,BETAI))/DN
      TAMMH = (FINT14(TAMMH1,0.0,XI) + FLIN14(TAMMH2,XI,BETAI))/DN
      RE = TAM/TAL
      RH = TAMH/TALH
      SI = Q*(CDE*AMOB(T)*RE  +  CDH*AMOBH(T)*RH)
      RS = SI/SIO
      DER = Q*(CDE*AMOB(T)*TAMM/TAL + CDH*AMOBH(T)*TAMMH/TALH)/EPSO
      ER = 16.*EXP(1.34E-04*(T-300.)) - DER
      RM = TAMM/TAL/TAL
      RMH = TAMMH/TALH/TALH
      WRITE (6,8) RE, RH, SI, RS, ER,RM,RMH
      ZF = ALOG10(F)
      ZF = ZF + VF(2)
      F = 10.**ZF
      IF(F.LE.VF(3)) GO TO 4
      F = VF(1)
      T = T + VT(2)
      IF (T.LE.VT(3)) GO TO 11
      T = VT(1)
      IF (VND(1).GT.0.0) GO TO 10
      RO = RO + VRO(2)
      IF(RO.LE.VRO(3)) GO TO 19
      RO = VRO(1)
      GO TO 12
   10 ZN = ALOG10(ND)
      ZN = ZN + VND(2)
      ND = 10.**ZN
      IF (ND.LE.VND(3)) GO TO 9
    2 FORMAT (3F10.5)
    3 FORMAT (1X,  E12.4)
    6 FORMAT (I1)
   15 FORMAT (3E10.5)
    7 FORMAT (1X, 5E12.4)
    8 FORMAT (1X, 39X, 7E12.4)
   21 FORMAT (1X, 3E12.4)
   12 CONTINUE
      GO TO 13
   14 STOP
      END
```

REFERENCES

(1) T. S. Benedict and W. Shockley, "Microwave Observation of Collision Frequency of Electrons in Germanium", Phy. Rev. Vol. 89 pp. 1152-1153, 1953.

(2) T. S. Benedict, "Microwave Observation of Collision Frequency of Holes in Germanium", Phy. Rev. Vol 91, pp. 1565-1566, 1953.

(3) J. M. Goldley and S. C. Brown, "Microwave Determination of Average Masses of electrons and holes in Germanium", Phy. Rev. Vol. 98, pp. 1761-1763, 1955.

(4) F. D'Altroy and H. Y Fan, "Microwave Transmission in p-type Germanium", Phy. Rev. Vol. 94, pp. 1415, 1954.

(5) J. Lindmayer and M. Kutsko, "Reflection of Microwaves from Semi-Conductors", Solid State Electronics, Vol. 6, No. 4, pp. 377-381, 1963.

(6) K. S. Champlin, "Frequency Dependence of High Frequency Transport Properties of Cubic Crystals", Phy. Rev. Vol. 130, pp. 1374-1377, 1963.

(7) K. S. Champlin, D. B. Armstrong and P. D. Gunderson, "Charge Carrier Inertia in Semi-Conductors", Proc. IEEE, Vol. 52, pp. 677-685, 1964.

(8) C. R. Haden and T. D. Shockley, Jr., "Nuclear Radiation Perturbation of a Semi-Conductor filled Microwave Cavity", IEEE, Tran. MTT, Vol. 14, pp. 347-349, 1966.

(9) R. A. Smith, "Semi-Conductors", Cambridge University Press, 1964, pp. 216-218.

(10) H. Jacobs, F. A. Brand, M. Benanti, R. Benjamin and J. Meindl, "A New Microwave Semi-Conductor Modulator", IRE Transc. Vol. MTT-8, pp. 553-559, 1960.

(11) H. Jacobs, R. Benjamin and D. A. Holmes, "Semi-Conductor Reflection type Modulator", Solid State Electronics, Vol. 8, pp. 699-708, 1965.

(12) M. W. Gunn and H. Rahman, "The hot Electron Microwave Rotator", Proc. IEEE (Correspondence), Vol. 55, pp. 1082-1084, 1967.

(13) B. R. Nag and S. K. Roy, "Microwave Measurement of Conductivity and Dielectric Constant of Semi-Conductors", Proc. IEEE (Correspondence), Vol. 50, pp. 2515, 1962.

(14) K. S. Champlin and J. D. Holm, "Analysis and Calibration of a Reflection Coefficient Bridge for use with any Wave-guide Mode", IEEE TRANS MTT, Vol. MTT-15, pp. 447-448, 1967.

(15) M. W. Gunn and J. B. Brown, "Measurement of Wave-Guide Properties in a Slotted Wave-Guide Structure." Proc. IEE, Vol. 112 (3) pp. 463-468, 1965

(16) K. S. Champlin and G. H. Glover, "Influence of Wave-Guide Contact on Measured Complex Permittivity of Semi-Conductors", J. Appl. Phys. Vol. 37, pp. 2355-2360, 1966.

(17) K. S. Champlin and G. H. Glover, "Gap Effect in the Measurement of Large Permittivities", IEEE Trans. MTT (Correspondence), Vol. 14, pp. 397-398, 1966.

(18) K. S. Champlin and R. R. Krongard, "The Measurement of Conductivity and Permittivity of Semi-Conductor Spheres by an Extension of Cavity Perturbation Technique". IRE TRANS, Vol. MTT-9, pp 545, 1961

(19) M. E. Brodwin and Pao-Sun Lu, "A Precise Cavity Technique for Measuring Low Resistivity of Semi-Conductors", Proc. IEEE (Corr.) Vol. 53, pp. 1742, 1965.

(20) H. Jacobs, A. F. Brand, J. D. Meindl, M. Benanti and R. Benjamin, "Electrodless Measurement of Semi-Conductor Resistivity at Microwave Frequencies", Proc. IRE, Vol. 49, pp. 928-932, 1961.

(21) B. R. Nag and S. K. Roy, "Microwave Measurement of Conductivity and Dielectric Constant of Semi-Conductors", Proc. IRE (Correspondence), Vol. 51, pp. 962, 1963.

(22) R. Lilja and T. Stubb, "A Study on the Dielectric Constant and Resistivity of Amorphous, Polycrystalline and Mono-Crystalline Selenium at 24 GHz", Acta Polytechnica, Scandinavica, Series PH 28, 1964.

(23) M. W. Gunn, "Hot Electron Effect in n Type Germanium at 9.392 GHz", J. Electronics and Control, Vol. 16, pp. 481, 1964.

(24) M. A. Druesne, "Dielectric Constant of Germanium as a Function of Frequency, Temperature and Resistivity", U. S. Army Elect. Lab Report No. ECOM-2553, Jan. 1965.

(25) C. Herring, "Transport Properties of Many Valley Semi-Conductors", Bell Syst. Tech. J., Vol. 34, No. 2, pp. 237-290, 1955.

(26) E. Conwell, "Lattice Mobility of Hot Carriers", J. Phy. & Chem. Solids, Vol. 8, pp. 234-239, 1959.

(27) R. E. Collin, "Field Theory of Guided Waves", McGraw-Hill, Inc., New York, 1960, Chapter I.

(28) R. E. Collin, "Field Theory of Guided Waves", McGraw-Hill, Inc., New York, 1960, Chapter 5.

(29) R. E. Collin, "Field Theory of Guided Waves", McGraw-Hill, Inc., New York, 1960, Chapter 6.

(30) R. F. Harrington, "Time Harmonic Electromagnetic Fields", McGraw-Hill, Inc., New York, 1961, Chapter 7.

(31) C. G. Montgomery, "Techniques of Microwave Measurements", Boston Tech. Publishers, Inc., Mass., 1964, Chap. 9 and 10.

(32) B. R. Nag, et al, "Microwave Measurement of Conductivity and Dielectric Constant of Semi-Conductors", Proc. IEEE, (Correspondence) Vol. 51, pp. 962, 1963.

(33) R. Koike and H. E. M. Barlow, "Microwave Measurements on the Magneto-Resistance Effects in Semi-Conductors", Proc. IEEE, Vol. 109B, pp. 137, 1962.

(34) N. Marcuvitz, "Waveguide Handbook", M.I.T. Radiation Lab., Series No. 10, McGraw-Hill, Chapter 8, 1951.

(35) R. Lilja and T. Stubb, ibid

(36) A. D. Berk, "Variational Principles for Electromagnetic Resonators and Waveguides", IRE Trans. Vol. AP-4, pp. 104-111, 1956.

(37) D. A. Holmes, and D. L. Feucht, "Microwave Measurement of Conductivity and Dielectric Constant of Semi-Conductors", Proc. IEEE (Correspondence), 52, pp. 100, 1964

(38) K. S. Champlin,and D. B. Armstrong, "Explicit Forms for the Conductivity and Permittivity of Bulk Semi-Conductors in Waveguides", Proc. IEEE, (Correspondence), Vol. 50, pp. 232, 1962.

(39) G. J. Gabriel and M. E. Brodwin, "The Solution of the Guided Waves in Inhomogeneous Anistropic Media by Perturbation and Variational Methods", Trans. IEEE, Vol. MTT-13, pp. 364-370, 1965.

(40) M. W. Gunn, "The Microwave Measurement of Complex Permittivity of Semi-Conductors", Proc. IEEE, (Correspondence), 52, pp. 185, 1964.

(41) K. S. Champlin, "Comment on Microwave Measurement of Conductivity and Dielectric Constant of Semi-Conductors", Proc. IEEE, (Correspondence), Vol. 52, pp. 1061. 1964.

(42) R. A. Buckingham, "Numerical Methods", Sir Isaac Pitman and Sons, Ltd., London, 1957.

(43) R. E. Collin , ibid Chapter 8

(44) M. W. Gunn, "Wave Propagation in a Rectangular Waveguide Containing a Semiconducting Film", Proc. IEE , Vol. 114, pp. 207-210, 1967

(45) R. A. Smith, ibid Chapter 10

(46) K. S. Champlin, D. B. Armstrong, J. D. Holm and N. A. Patrin, "Temperature Dependence of Conductivity Effective Mass of Holes in Germanium" Phy. Rev. (Letters), Vol. 14, pp. 547-548, 1965.

(47) W. Shockley, "Electrons and Holes in Semi-Conductors", D. Van Nostrand Co., 1950, Chapters 11 and 17.

(48) F. J. Morin and J. P. Maita, "Conductivity and Hall Effect in the Intrinsic Range of Germanium", Phy. Rev., Vol. 94, pp. 1525, 1954.

(49) C. Herring op cit Equation 46

(50) R. A. Smith op cit

(51) J. M. Ziman, "Electrons and Phonons", Oxford University Press, 1960.

(52) H. Brooks, "Advances in Electronics and Electron Physics", Vol. 7, Academic Press, pp. 156, 1955.

(53) S. Wang, "Solid State Electronics", McGraw-Hill, Inc., New York, pp. 215, 1966.

(54) C. Herring and E. Vogt, "Transport and Deformation Potential Theory for Many Valley Semi-Conductors with Anistropic Scattering", Phy. Rev., Vol. 101, pp. 944-961, 1956.

(55) B. N. Brockhouse and P. K. Iyengar, "Normal Modes of Germanium by Neutron Spectroscopy", Phy. Rev. Vol. 111, pp. 747-754, 1958.

(56) M. Cardona and W. Paul, "Dielectric Constant Measurements in Germanium and Silicon at Radio Frequencies as a Function of Temperature and Pressure", Solid State Physics in Electronics and Telecommunications, Academic Press, London, (1960), Vol. I, pp. 206-214.

(57) A. R. Von Hippel (Edit), "Dielectric Materials and Applications", John Wiley & Sons, 1954, pp. 88-101.